Norwegian Meteorological Institute
met.no

met.no report

Report no. 15/2010
Air Pollution
ISSN: 0332-9879
Oslo, October 31, 2010

Volcano Version of the SNAP Model

Jerzy Bartnicki, Hilde Haakenstad and Øystein Hov

Norwegian Meteorological Institute
met.no

report

Number	Subject	Date	Classification	ISSN
15/2010	Air Pollution	October 31, 2010	☒ Open ☐ Restricted ☐ Confidential	0332-9879

Title

Volcano Version of the SNAP Model

Authors

Jerzy Bartnicki, Hilde Haakenstad and Øystein Hov

Client(s)	Client reference
Norwegian Meteorological Institute	

Abstract

Volcano eruptions can lead to series economic losses due to disrupted air traffic in large parts of Europe. The latest example of such a disruption was the Eyjafjallajökull eruption in April 2010. Atmospheric dispersion of ash particles from Eyjafjallajökull eruption in Iceland was quickly simulated at met.no with the SNAP model. The results of the SNAP computations in the form of maps with the locations of model particles were made public from the beginning of the event. The main goal of the present report is a description of the volcano version of the SNAP model used as operational for the Eyjafjallajökull eruption and which will be operational at met.no for the potential future volcano eruptions. The SNAP results are shown for the first 10 days of the eruption, the period which includes the highest concentration of volcanic ash over Europe. They were compared with the results of the official VAAC forecasts showing many similarities despite of different source terms used by both models. The event of Ejafjallajökull eruption in April 2010 confirms that, in emergency situation, met.no is ready and prepared for modeling atmospheric dispersion of volcanic ash at present.

Keywords

Volcano eruption, atmospheric dispersion, long-range transport, modelling

Disiplinary signature	Responsible signature
Knut Helge Midtbø	Øystein Hov

Postal address PO Box 43 Blindern, N-0313 Oslo, Norway
Office Niels Henrik Abels vei 40
Telephone +47 2296 3000
Telefax +47 2296 3050
e-mail: met.inst@met.no **Web:** met.no
Bank account 7695 05 00601
Swift code DNBANOKK

Contents

1 Introduction

In the morning of 15 April 2010 most of the flights from Oslo Gardermoen airport were canceled. Later on this day and in several following days, the Oslo airport, as well as majority of other European airports were closed completely because of the cloud of volcanic ash form Eyjafjallajökull eruption arriving to Europe. The volcanic ash erupted into the air consists of small pieces of rocks, minerals and volcanic glass of the size smaller than 2 mm in diameter. It is hard, not hygroscopic and extremely abrasive. The smaller ash particles, with diameter below 10 μm, can stay in the atmosphere for a period of one week or longer. Very small volcanic ash particles coming into the jet engine melt and fuse onto the turbine blades. They can destroy fun blades leading to the engine stop. They can also damage the windscreen of the plane forcing an instrument landing.

The eruption of Eyjafjallajökull in April 2010 was not the first case when air traffic in Europe was troubled by the eruption of volcano located in Iceland. In the last ten years there were at least two eruptions that also disrupted air traffic. On 26 February 2000, the eruption of Hekla started with prominent explosive phase resulting in stratospheric venting of tephra and initial eruption column reaching 11-12 km asl. The Hekla 2000 eruption not only disturbed European air traffic, but also proved that even very low ash concentrations can cause damage to the aircraft [25]. Four years later, on 1 November 2004, the Grimsvötn volcano erupted trough the ice cap of Vatnajokull. The initial eruption column reached 12-14 km asl and the elevation of volcanic plum top was not lower than 9 km until the 3 November [42]. This eruption caused many cancellations and diversions of European flights.

Atmospheric dispersion of ash particles from Eyjafjallajökull volcano eruption in Iceland has been quickly simulated at met.no, first with the SNAP model and then with the EMEP model. The first results of the SNAP run were available on 15 of April and operational calculations with the SNAP model were performed until the end of the emergency period (15.05.2010) and then even longer until 21.05.2010. The results of the SNAP computations in the form of maps with the locations of model particles have been made public from the beginning of the event. The results of the EMEP model have been also available on the internal met.no web pages and continuously updated during the emergency period.

At the beginning of the eruption, the volcano version of SNAP did not exist and a modified bomb version of SNAP had to be used. For running the SNAP model in the emergency volcano mode, some changes in the model structure, parameters and input were necessary, especially at the beginning of the emergency period. Among others, these changes included, new source term with different particle classes and distribution, new structure of the model layers with focus on the vertical layers and additional space and time averaging procedures of interest to the aviation community. The model modifications and development were also continued after the emergency period resulting in a new version of SNAP, which can be called a volcano version.

The main purpose of running the volcano version of SNAP in the operational mode was an updated information about the dispersion of volcanic ash range and pattern which was provided to the public. This information was available in the form of animations and pictures which included the model particles plotted on the map with the model domain. The air concentrations of ash in the air have been also calculated, but not shown externally for

two reasons. Firstly, the information about the source strength and to less extent height was rather uncertain leading to uncertain concentration fields. Secondly, the aviation in Norway was obliged to follow the official 24-hour forecast from the Volcanic Ash Advisory Centre (VAAC) in London and additional concentration field from the SNAP runs could be confusing, because of different source terms used by SNAP and VAAC. However, the concentration fields calculated by SNAP were shown to the Norwegian Aviation Authority at the meeting in Bodø in April 2010.

SNAP was one of many dispersion models which were run during the Eyjafjallajökull eruption. Some of these models were not originally developed for volcano eruption and had to be modified "ad hock". However, the models which were especially designed to simulate volcanic ash dispersion were also in use from the beginning of eruption. These were, first of all, the models from the 9 VAAC Centres located across the world and established by International Civil Aviation Organization (ICAO) in close cooperation with World Meteorological Organization (WMO) and the International Union of Geodesy and Geophysics (IUGG). The responsibility areas for the VAAC Centres are shown in Fig. 1. These Centres are part of an international system set up by ICAO called the International Airways Volcano Watch (IAVW). The IAVW comprises observations of volcanic ash from volcano observatories and other organizations, satellites and aircraft in flight, the issue of warnings in the form of NOTAM and SIGMET messages and, since the mid 1990s, the issue of volcanic ash advisory messages from the VAAC identifying areas of volcanic ash and their predicted movement.

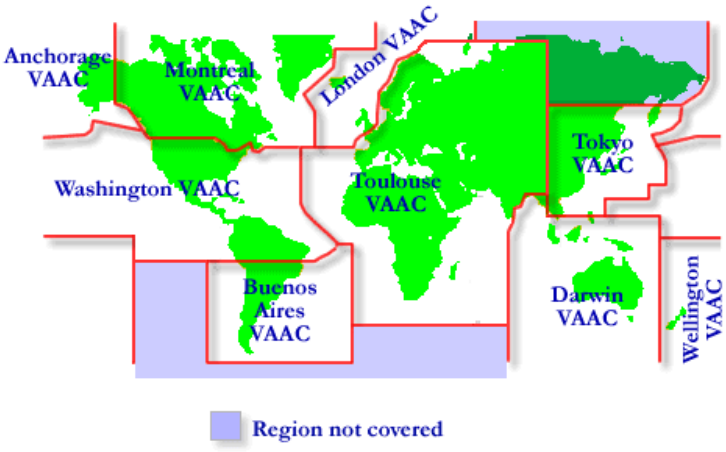

Figure 1: The responsibility areas for the VAAC Centres in case of volcano eruption.

In case of eruption, The VAAC responsible for the area where the eruption took place issues a Volcanic Ash advisory based on observations, meteorological data and forecasts of ash transport and dispersion. For the Eyjafjallajökull eruption VAAC London was, so called lead VAAC for issuing Volcanic Ash Advisory. Different dispersion models are used in different VAACs. For example, the NAME model [27] in London, MEDIA [39] in Toulouze, CENAREM [9] in Montreal and HYSPLIT [10] in Washington and Darwin. The results of the

NAME model were used by VAAC London for forecasting the areas dangerous for the air traffic. The maps produced by VAAC London were closely followed by the Aviation Authorities in Europe with very serious consequences, like disruptions in European air traffic and many cases with closing major European airports.

Different dispersion models were in operational use in the Scandinavian countries from the beginning of eruption. The MATCH model [24] was run operationally in Sweden and DERMA model [46] in Denmark. However, the outputs from both these models were not made public, because as in Norway, the national aviation authorities in these countries used the official VAAC London maps for ash dispersion forecast. The situation was different in Finland, were full results of the SILAM model [43], as well as a description of the source term had been available on the web [44] for the entire period of eruption. In Norway, in addition to SNAP and EMEP models, there was the third one used during the eruption period, namely the FLEXPART model [47], which was run at the Norwegian Institute for Air Protection (NILU).

One of the major problem for verification of all models used for the simulation of Eyjafjallajökull eruption is the lack of direct measurements of volcanic ash concentrations in the air in the emergency period. Since, these concentrations should be available very quickly after eruption start in three-dimensional space, there were many technical difficulties related to such measurements. Nevertheless, they are very important, because of serious consequences of volcano eruptions, especially for the aviation. We can only hope that such measurements will be available in the future, in case another serious volcano eruption takes place. At present, a practical way to verify the models is a comparison of model results with available satellite images and lidar measurements.

What can also help in the model evaluation task is the model intercomparison exercise. Such an intercomparison for the Eyjafjallajökull eruption, with approximately 20 models from Europe, USA and Canada participating in it, will be performed in the Joint Research Centre (JRC) in Ispra [12] at the end of 2010. The common source term will be used for all the models as well as the same grid system and content for the output files, but each model will use its own meteorological input. An interesting and major outcome of this intercomparison will be the ensembles, which will give a hint about uncertainty of the calculations.

The main goal of this report is a description of the volcano version of the SNAP model used as operational for the Eyjafjallajökull eruption and which will be operational at met.no for the potential future volcano eruptions. In the report, we also present and discuss the source term for the model run and compare it with the source terms used by other models. The SNAP results are shown for the first 10 days of the eruption, the period which includes the highest concentration of volcanic ash over Europe causing the interruption of air traffic in prevailing part of the European air space. The model results are only compared with the official VAAC forecasts showing similar shape of the ash cloud and some differences in the concentrations. A more thorough verification of the SNAP volcano version results is planned for the future (most likely end of 2010), when the measurements database for Eyjafjallajökull eruption will be established at JRC [12].

Since the development of SNAP volcano version was motivated and forced by the event of Eyjafjallajökull eruption, we begin this report with a summary of the main facts related to Eyjafjallajökull volcano and its eruption starting on 14 April 2010.

2 The Eyjafjallajökull Eruption in 2010

There are 30 volcanic systems on Iceland of which more than 200 eruption events identified in the historical time. Of these events, 124 were recorded as explosive, when more than 95% of the erupted magma is tephra [49]. The eruption which caused significant traffic problems in April and May 2010 was that of Eyjafjallajökull.

2.1 Eyjafjallajökull Volcano and its Location

The Eyjafjallajökull volcano, as seen from the air is shown in Fig. 2. The Eyjafjallajökull glacier (up to 200 m thick) covers the caldera of this volcano with a summit elevation of 1666 m. The mountain, a stratovolcano, stands 1651 m at it highest point, and has a crater 3-4 kilometres in diameter, open to the north. It is located in the south of Iceland (Fig. 2) with the co-ordinates: 63^o 38'N 19^o 36'W [53] .

Figure 2: The view of Eyjafjallajökull volcano from the air.

The Eyjafjallajökull volcano erupted in 1612 and again from 1821 to 1823 when it caused a glacial lake outburst flood. It has erupted twice in 2010 - on 20 March and in April/May. The March event forced a brief evacuation of around 500 local people, but the 14 April eruption was ten to twenty times more powerful and caused substantial disruption to air traffic across Europe. The first 2010 eruption is thought to have begun on 20 March 2010, about 8 kilometres east of the top crater of the volcano. This eruption, in the form of a fissure vent, did not occur under the glacier and was smaller in scale than had been expected by some geologists [53].

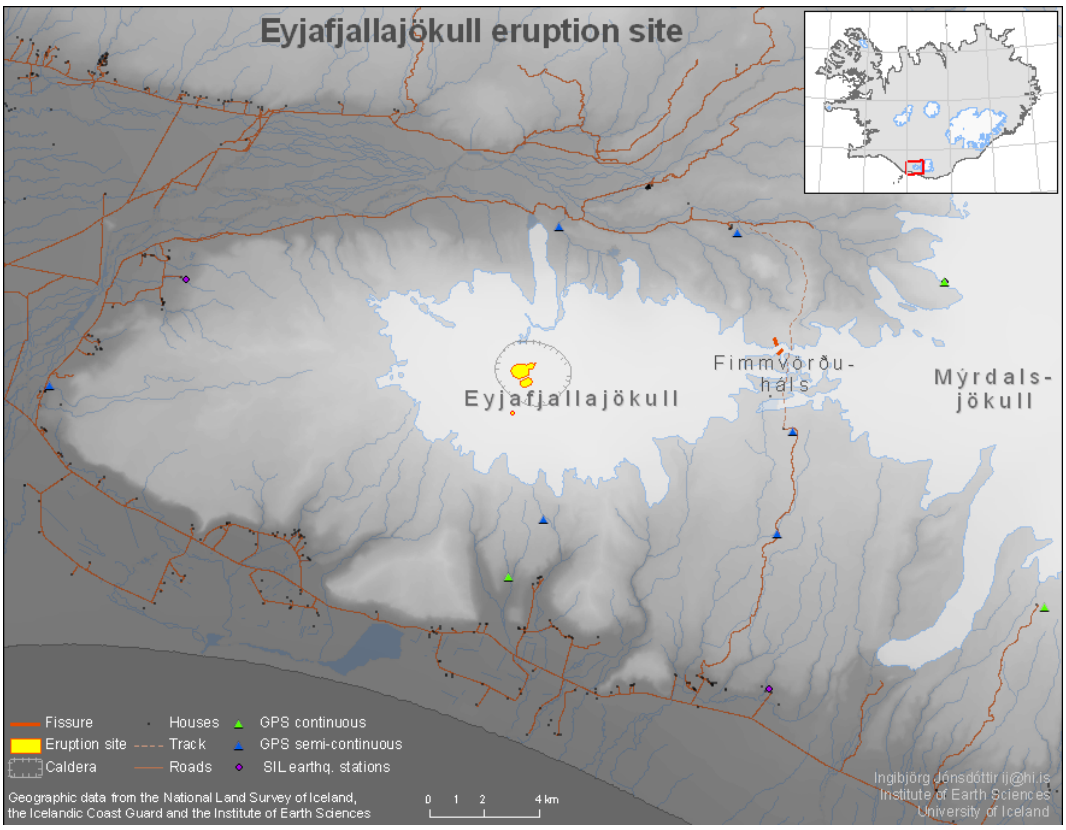

Figure 3: Geographical location of Eyjafjallajökull volcano on Iceland.

On 14 April 2010 Eyjafjallajökull resumed erupting after a brief pause, this time from the top crater in the centre of the glacier, causing melt water floods to rush down the nearby rivers, and requiring 800 people to be evacuated. This eruption was explosive in nature, due to melt water getting into the volcanic vent. It is estimated to be ten to twenty times larger than the previous one. This second eruption threw volcanic ash several kilometres up in the atmosphere which led to air travel disruption in northwest Europe in April and May 2010, including the closure of airspace over many parts of Europe. On 23rd May 2010, the London VAAC declared the eruption to have stopped, but continued to monitor the volcano [53].

Eyjafjallajökull lies 25 km west of another volcano, Katla, under the Mýrdalsjökull ice cap, which is much more active and known for its powerful sub glacial eruptions and its large magma chamber. Each of the eruptions of Eyjafjallajökull in 920, 1612, and 1821-1823 had preceded an eruption of Katla [48]. Katla has not displayed any unusual activity (such as expansion of the crust or seismic activity) during the 2010 eruptions of Eyjafjallajökull, though geologists have been concerned about the general instability of the larger volcano since 1999. Some geophysicists in Iceland believe that the Eyjafjallajökull eruption may trigger an eruption of Katla, which would cause major flooding due to melting of glacial ice and send up massive plumes of ash [53]. Therefore, it is very important to maintain the operational volcano modelling capacity for the coming months or perhaps years at met.no.

From the modelling perspective, information about the volcano source term and meteorological conditions is the most important for a proper description of volcanic ash dispersion in the air. Meteorological input data for the dispersion models are routinely available from the Numerical Weather Prediction (NWP) models at met.no, usually every 3-6 hours. There is a problem, however, with the source term data for the erupting volcano. There is a large uncertainty (one or two orders of magnitude) in the source strength, as well as in the released ash particle spectrum, especially in the initial phase of the eruption. The eruption height is usually better known than the mass eruption rate, assuming that the visibility around volcano is good enough. In any case, the information about the eruption height is easier available and more certain than the estimation of the source strength. Therefore, a common procedure in the VAAC centers, including London VAAC, is the estimation of the source strength from the eruption height. The same approach is used in the operational volcano version of SNAP.

2.2 Plume Height and Eruption rate

For the operational SNAP runs in the period of Eyjafjallajökull eruption, the information about the observed daily plume top was obtained directly from the Icelandic Meteorological Office (IMO) together with some comments. There was also some information provided by IMO to met.no about the range of eruption rate.

2.2.1 Plume Height

The information about the observed daily plume tops is summarized in Table 1, for each day of the period 14.04.2010 - 21.05.2010. The maximum height of eruption can be noticed for the first five days of the eruption and then in May 13-17.

Based on the information from Table 1, the value of daily plume top was estimated for each day of the operational SNAP run in the Eyjafjallajökull eruption period: 14.04.2010 - 21.05.2010. The daily heights of the plume top used in the operational SNAP run were calculated as an average of daily minimum and maximum in Table 1 and are shown in Fig. 4.

The maximum (8500 m) of the plume height in the SNAP runs is in the first, second and fourth day in the eruption period. The next local maximum (7250 m) is seen on 6 May and finally there are two local maxima (8000 m) closer to the end of eruption, on 14 and 16 May. The minimum (2500 m) of the plume height occurs in the 12th day of the eruption on 25 April.

There are some differences in the daily plume heights used by different models. Estimation of the daily tops of plume heights in the EMEP model was based on the VAAC London reports [52], whereas in case of SILAM model it was based on optical futures of the plume [44]. To illustrate these differences we compare the daily plume heights used by SNAP with those used by EMEP model [45] and SILAM model [44]. Comparison of daily top plume heights used by these three models is shown in Fig 5.

Compared to SNAP, the daily tops of plume height used by EMEP and SILAM are more smooth. The maximum difference between the heights used by the three models is approximately 3 km on 16 May. The comparison shown in Fig 5 indicates some uncertainties associated with the estimation of the top of plume height in case of volcano eruption. There are also some uncertainties related to estimation of the bottom of the plume. In SNAP model we use

Table 1: Volcanic Ash Clouds - Observed daily plume tops throughout the eruption. VOLCANO: EYJAFJALLAJOKULL 1702-02, PSN: N6338 W01937, AREA: ICELAND, SUMMIT ELEV: 1666M Heights indicated refer to MSL as reference surface. Source: The Icelandic Meteorological Office.

Date	Height (km)	Remarks
20100414	6 - 11	first plumes at 6km, later on up to 11km
20100415	6 - 11	significant eruption continuing
20100416	5.5 - 7	significant eruption continuing
20100417	8 - 9	significant eruption continuing
20100418	4.5 - 8	significant eruption continuing
20100419	2.5 - 5	eruption virtually ceased a few hours around 1200Z
20100420	3.5 - 5.5	eruption continuing
20100421	3.5 - 5	eruption continuing
20100422	3 - 5	eruption continuing
20100423	3 - 5	eruption continuing
20100424	2.5 - 4	magma flow as recently, plume acty. is slowly declining
20100425	2 - 3	magma flow as recently, plume acty. is slowly declining
20100426	2 - 4	plume+magma dischrg levels similar to preceding 3 days
20100427	3 - 5	plume+magma dischrg levels similar to preceding 4 days
20100428	3 - 4.5	plume+magma dischrg levels similar to preceding 5 days
20100429	3 - 4	plume+magma dischrg levels similar to preceding 6 days
20100430	3.5 - 4.5	plume+magma dischrg levels similar to preceding 7 days
20100501	3.5 - 4.5	plume+magma dischrg levels similar to preceding 8 days
20100502	3.5 - 4.5	ash darker and more dense than on recent days
20100503	4.5 - 5.5	overall activity has not changed much since yesterday
20100504	5 - 6	explosive acty. + ash product. increased since yesterday
20100505	5 - 7.5	incr. seismicity, new material intruding from deep below
20100506	5.5 - 9	higher eruption column, increased tephra fallout
20100507	5 - 8	explosive acty. decreased, ash plume lower / brighter
20100508	4.5 - 6.5	less explosive than on 6th, weak earthquakes only
20100509	4 - 6	acty. pulsating, further changes in acty. can be expected
20100510	4 - 6	incr. nbr of quakes M1-2, magma inflow fm mantle
20100511	4.5 - 6	16 earthquakes below M2, dark grey plume
20100512	4 - 6	few quakes only, marginally decreasing plume
20100513	6 - 9	the ash plume has increased since yesterday
20100514	7 - 9	above 50 lightn/last 24h, few quakes
20100515	6 - 8	ca. 30 lightn/last24h, increased nbr of quakes
20100516	7 - 9	above 150 lightn/last 24, few quakes
20100517	6 - 8	up to 10 ltn/h, explosivity slightly lower than on 13th
20100518	5 - 6.5	up to 6 ltn/h, explosivity slightly lower than yesterday
20100519	5 - 6	decreased nbr of lightnings, otherwise no major changes
20100520	4.5 - 5.5	activity lower than during last weekend
20100521	3 - 4	eruption declined, low magma flow, no lava out

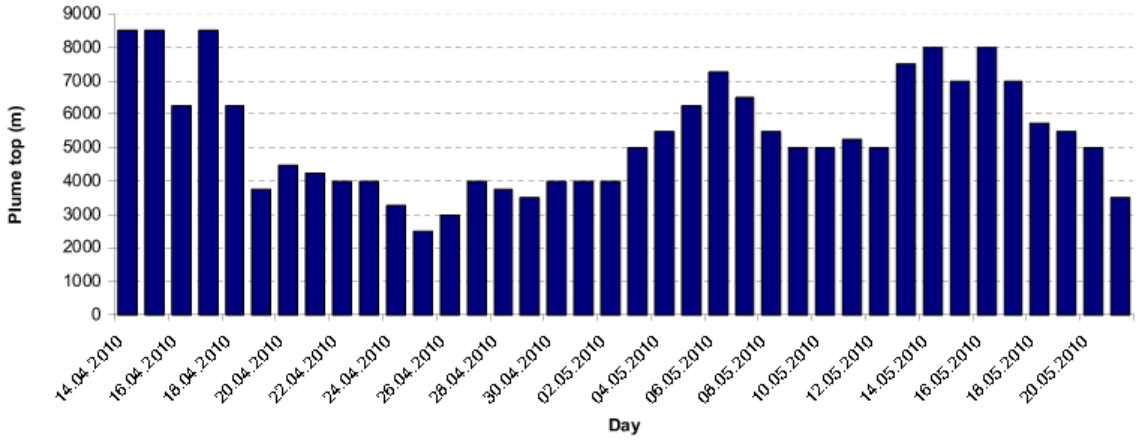

Figure 4: Daily plume top for each day of Eyjafjallajökull eruption period 14.04.2010 - 21.05.2010, as used in the operational SNAP runs.

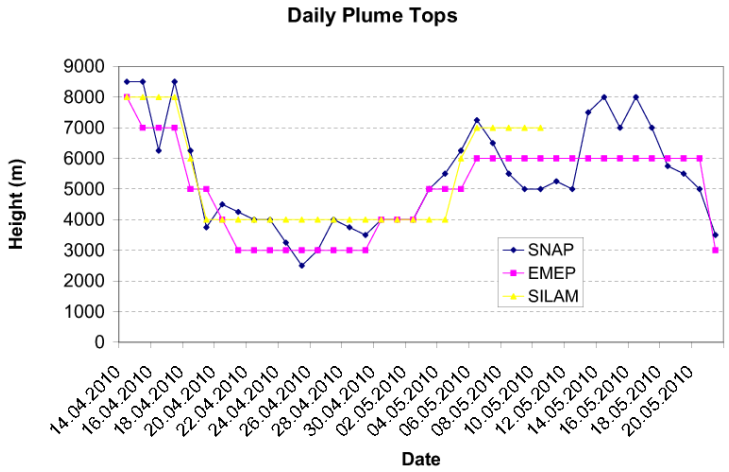

Figure 5: Daily plume tops used by three different dispersion models: SNAP, EMEP and SILAM, for each day of Eyjafjallajökull eruption period.

the volcano elevation summit (1666 m) as a base of the plume height. In EMEP model, the the lower model level corresponding to the ground level is taken as the base of the plume height. Finally, an elevation of 500 m above volcano top is assumed to be the plume base in SILAM model. These differences have also an important effect on the estimation of the eruption rate discussed in the next Section.

2.2.2 Eruption Rate

It is difficult to estimate the eruption rate from the direct measurements, because usually they do not exist. Other options are satellite images, if available, or indirect estimation of the eruption rate from the plume height.

An effort to estimatie the eruption rate based on the plume height can be found in [20]. In this effort, a list of eruptions for which the source parameters were well constrained was compiled first. Than the list was reviewed and updated. Finally, 35 different eruptions were chosen to estimate the relationship between the mass eruption rate and the plume height which is shown in Fig. 6.

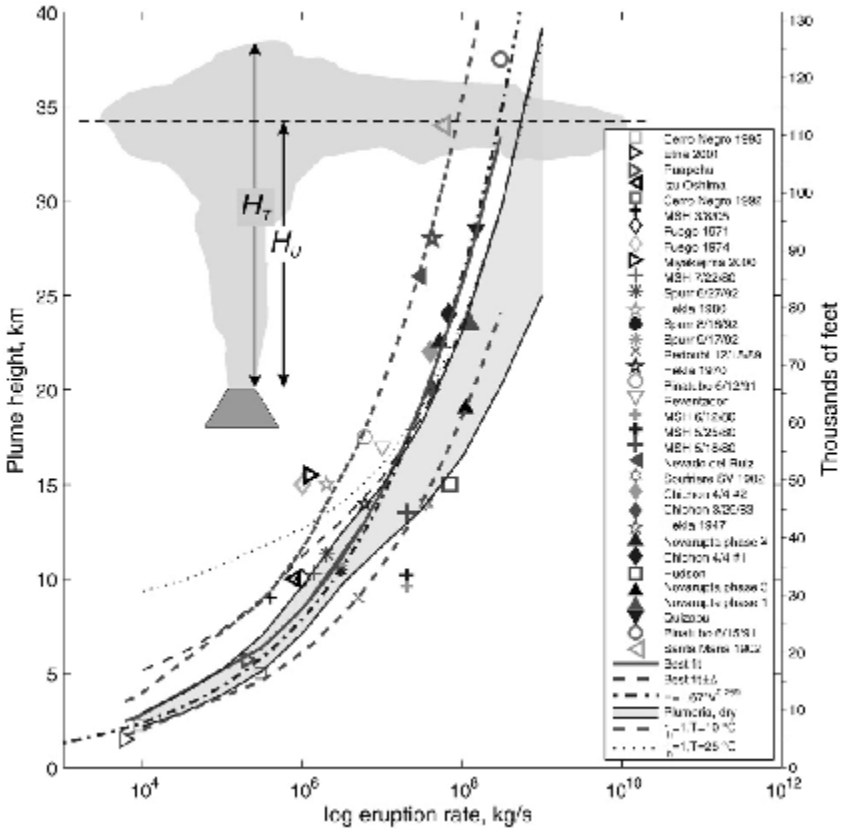

Figure 6: Plume height above the vent versus mass eruption rate as estimated in [20]. Symbols for each eruption are given in the legend. The bold solid line gives the best fit to the data.

In Fig. 6, plume height H is the elevation at which most of the ash spreads laterally from the plume into the ash cloud. It is expected to be equal to the height H_u at the center of the umbrella cloud. The upper light solid line is a theoretical curve of H_T calculated using the 1-D steady-state model Plumeria [19] using a magma temperature of 900^{o}C and a Standard dry atmosphere. The lower light solid curve is the elevation of neutral buoyancy, assumed to approximate H_u, calculated from the same model runs. The region between these two curves

is shaded. The dashed light curve represents predictions of H_T by Plumeria using properties of a Standard Atmosphere, but with 100% relative humidity and a temperature at ground level of 10^oC. The light dotted curve is a similar prediction using a relative humidity of 100% and a temperature at ground level of 25^oC. The bold solid line gives the best fit to the data which is represented by the following equation:

$$H = 2000(\dot{M}/\rho)^{0.241} \quad (1)$$

where H is in m, ρ is the density in kg m^{-3} and $\dot{M}$ is the eruption rate in kg s^{-1}.

In the operational SNAP runs, the information about the daily observed plume top is used, both for estimation of the source geometry and for estimation of the source strength. Following [20], it is assumed in the SNAP model that the erupted ash particles are uniformly distributed in the cylinder, with the base located at volcano summit elevation (1666 m) and top at the observed plume top.

Because of large uncertainty associated with the estimation of the eruption mass rate as a function of the plume height, we have used only six classes of the source strength. These six classes, based on Mastin's article [20] are used in the SNAP runs and are shown in Table 2.

Table 2: The source strength classes for Eyjafjallajökull eruption used in the SNAP simulations. H_T is the daily observed plume top.

Class	Observed Plume Top (m)	Eruption Rate (kg s^{-1})
1	$8850 \leq H_T$	10^6
2	$5800 \leq H_T < 8850$	10^5
3	$4050 \leq H_T < 5800$	10^4
4	$3000 \leq H_T < 4050$	10^3
5	$2500 \leq H_T < 3000$	10^2
6	$H_T < 2500$	0

The daily eruption rates from Eyjafjallajökull for the SNAP model simulations have been developed based on the information about the daily plume top (Fig. 4) and definitions of source strength classes included in Table 2. The total daily eruption rates for the SNAP simulation are shown in Fig. 7. For comparison, the daily eruption rates as used in the EMEP and SILAM models are also shown in Fig. 7. The SNAP rates are much higher (one-two orders of magnitude) than EMEP and SILAM rates, but SNAP particles classes, described in the next Section, have much broader spectrum (0.3-30 μm) than EMEP (2.5-10.0 μm) and SILAM (only 3.0 μm). Therefore, the SNAP daily rates in individual classes corresponding to EMEP and SILAM are much lower.

2.3 Ash Particle Size Distribution

During the Eyjafjallajökull eruption, the ash particles were not measured in the air, but in the deposits located 20-60 km away from the volcano. Therefore, there is also a large un-

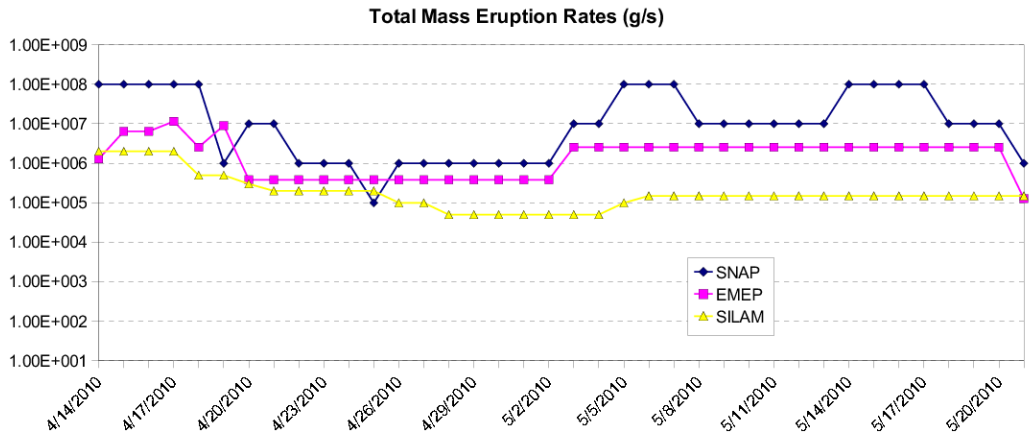

Figure 7: Comparison of the daily eruption rates for total mass used by three dispersion models: SNAP, EMEP and SILAM.

certainty in the estimation of ash particle size transported in the atmosphere. The samples of deposited ash from Eyjafjallajökull eruption were collected on 15 April 2010 by Sigurdur Reynir Gislason and Helgi Arnar Alfredsson from the Institute of Earth Sciences, University of Iceland. Samples were measured at Innovation Center Iceland at the request of The Environment Agency of Iceland and then analyzed and made public on the web by Thröstur Thorsteinsson [16]. After making some assumptions, such as same spherical shape and density for all particle sizes (1 to 300 μm), he calculated the number of particles of a given size range from the data about mass fraction below a certain grain size. The results are presented in Fig. 8. In this particle size spectrum, approximately 25% is the fraction of particles with diameter smaller than 10 μm.

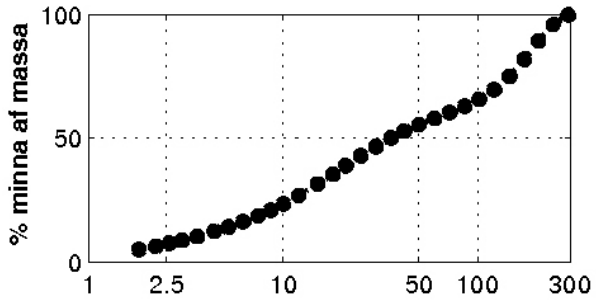

Figure 8: Particle size distribution in the ash from Eyjafjallajökull eruption. Sample from 15 April 2010 [16].

Following application of the NAME model [54] for London VAAC forecasts, we have chosen similar size-classes to parameterize the ash-particle size distribution in the SNAP model.

We assumed that 50% of the total eruption rate is assigned to the selected particle classes with a maximum characteristic diameter equal to 30 μm. The remaining mass belongs to ash particle with diameter larger than 30 μm. Characteristic diameter for each class, as well as the percent of the mass released in each class are shown in Table 3.

Table 3: Particle size-classes used in the SNAP model.

Class	1	2	3	4	5
Diameter (μm)	0.3	1.0	3.0	10.0	30.0
% of mass	0.1	0.6	6.0	26.0	67.3

The amount of erupted ash carried by small particles is much lower than ash mass carried by larger particles. The particle density is the same for each class 2.3 g cm^{-3}. Based on the information about the daily total rate included in Fig. 7 and particle sized distribution in Table 3, the daily emission rates were calculated for each of the particle class in the SNAP model. The results are shown in Fig. 9.

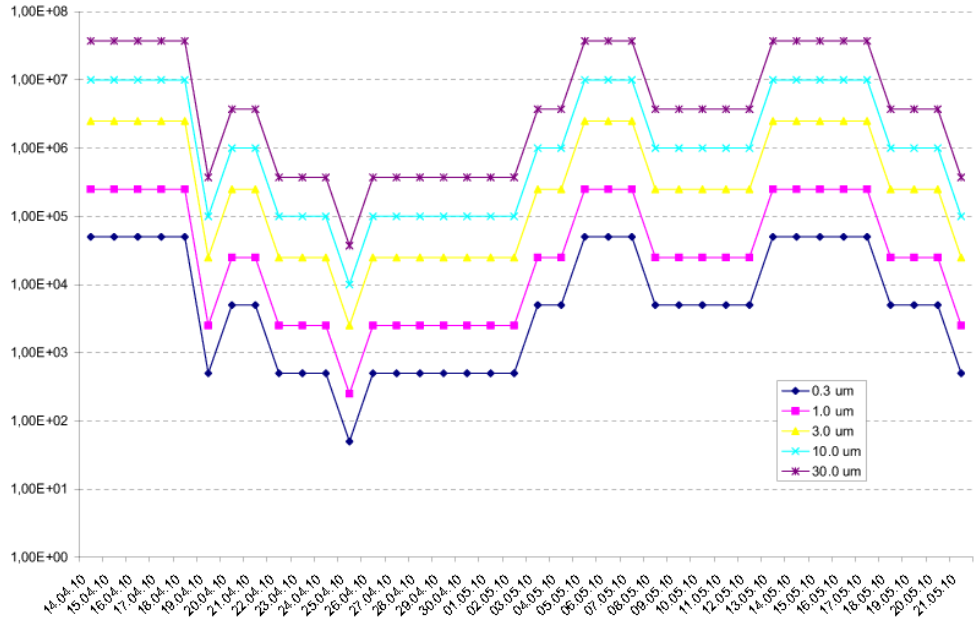

Figure 9: Daily eruption rates for five size-classes of the ash particles in SNAP.

3 Volcano Version of SNAP

The Severe Nuclear Accident Program (SNAP) model is a Lagrangian particle model, which has been developed at met.no (former DNMI) for simulating atmospheric dispersion of radioactive debris, first from nuclear accidents and then from nuclear explosions.

The basic concept of a Lagrangian particle model is rather simple in principle. The emitted mass of radioactive debris or volcanic ash, as in this model version, is distributed among a large number of model particles. After the release, each model particle carries a given mass of selected pollutant which can be in the form of gas, aerosol or particulate matter. A model particle in this approach is given an abstract mathematical definition, rather than a physical air parcel containing a given pollutant. It is used in SNAP as a vehicle to carry the information about the pollutant emitted from the source. The model particle is not given a definite size and can be not subdivided or split into parts. On the other hand, the mass carried by the particle can be subdivided and partly removed during the transport.

As in case of many other models, the development of SNAP started after the Chernobyl accident which occurred in April 1986. The first, preliminary version of SNAP [29] was based on the early version of the NAME model [17]. This SNAP version became fully operational at DMNI in December 1995 [30], [28], [31] as a part of the major Management Project (MEMbrain), in the framework of EUREKA (EU-904) activity. This operational version of SNAP was tested against tracer measurements in the European Tracer Experiment (ETEX) [32], [33] and then improved [2]. In 1996, SNAP was compared with two other models, one of Lagrangian type (NAME model from UK meteorological Office) and one Eulerian (EMEP model modified for radioactive pollution from the Norwegian Meteorological Institute) [18]. These three models produced similar results concerning the location of radioactive cloud, but the differences in concentrations were larger. The SNAP model was compared with many other models and tested on measurements available from the tracer releases in the frame of ETEX experiments and ATMES experiment [35].

Within the joint project between met.no and NRPA, SNAP was used for analysis of potential threat from hypothetical accident in Kola nuclear power plant [3], [34], [36]. The results of SNAP calculations indicated that, in case of accident the radioactive cloud can reach Northern Norway already after six hours and Oslo after two days from the accident start.

In the early versions of the SNAP models only small (diameter below 1 μm) particles were taken into account in the model equations. Some measurements, performed by University of Life Sciences after Chernobyl accident, showed that in certain cases also much larger (of the order of 20 μm) particles, so called hot particles were transported for long distances reaching Norway. Therefore, parameterization of particles with arbitrary diameter and density was introduced into the SNAP model and this model version was applied to simulate the Chernobyl accident again [4], [5]. This version was also applied for simulating the potential release from Kola once again, this time focusing on radioactive particle of different size and density [7].

SNAP has been an active member of the ENSEMBLE group [12] and project for the last 10 years. There are at least three important advantages of this on-going project: 1) possibility of comparing SNAP results with more than 20 other models in the same grid system, 2) possibility for the backup in case of problems with SNAP, and 3) possibility of creating the ensemble forecast giving a hint on uncertainty of the results, very important for the decision

makers [13], [14].

Introduction of arbitrary particles into the SNAP equations made it possible to create a SNAP version for nuclear explosion [38], [5]. This model version was a basis for implementing the parameterization related to volcano eruption into SNAP, described in this report.

3.1 Meteorological Input and Model Domain

The SNAP model is flexible concerning, both model domain and meteorological data. The spatial and vertical structure of the SNAP model domain is in fact defined by the meteorological input. In case of Ejafjallajöokull eruption, the results of the HIRLAM Numerical Weather Prediction model version 7.1.3 [50] were used as the meteorological input for SNAP. This model is currently operational at met.no and it is being run in different resolutions. Original forecasts for SNAP applications of Ejafjallajöokull eruption came from HIRLAM-12 version with approximately 12 km spatial resolution and 66 hrs time horizon for the forecast. The HIRLAM-12 is run 4 times a day, to produce 66 hour forecasts starting at 00, 06, 12 and 18 UTC. In addition, short 9 hour re-runs from the latest ECMWF analysis are done prior to each 6-hour interval. The main features of the HIRLAM-12 NWP model are summarized in Table 4 and the HIRLAM-12 model domain is shown in Fig. 10.

Table 4: Main features of the HIRLAM-12 NWP model.

Horizontal grid points (lon $\times$ lat)	864×698
Vertical levels	60
Mesh size (deg)	0.108×0.108
Analysis	3D-Var
Initialization	IDFI
Host model	ECMWF, IFS Cycle 36r, Richardson [23]
Boundary age	6
Boundary interval (h)	3
Forecast length (h)	66
Time step (min)	5
Condensation scheme	ISBA
Surface scheme	STRACO
Turbulence scheme	TKE-l
Radiation scheme	Savijärvi [40]

For historical reasons the FORTRAN code of SNAP has been developed for a single processor computer and was implemented on several platforms at met.no with the possibility of external use of the model by the Norwegian Radiation Authority (NRPA). This solution created some backup and security for operational applications in nuclear emergency, but at the same time it created some limits for the model use in case of volcano eruption with much longer emission period. The main limits were: the available memory and the time of the computations. The consequences of these limits for the volcano application lead to reduced

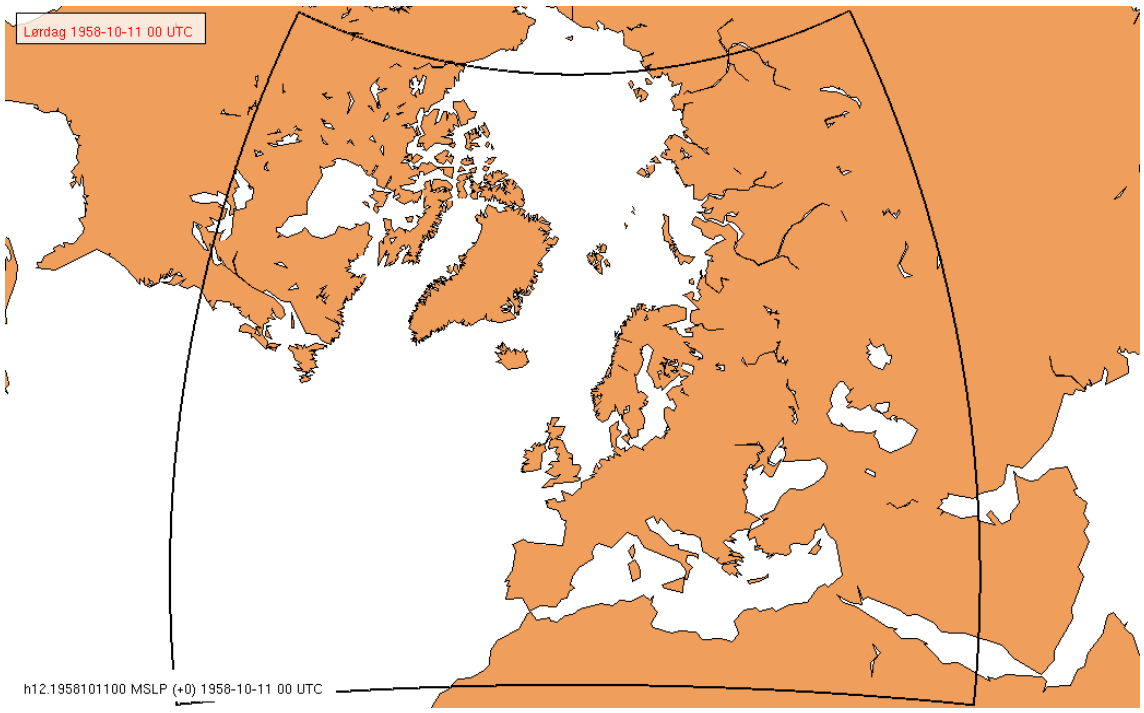

Figure 10: Computational domain of the operational HIRLAM-12 NWP model, used as meteorological input provider for SNAP.

resolution of the meteorological input data. For volcano applications, the results of HIRLAM-12 were interpolated into the new grid system with approximately 22 km horizontal resolution and 40 layers in vertical. Taking into account large uncertainties in the volcano source term this solution did not affected much the quality of the SNAP results. The model domain used for SNAP simulations of Ejafjallajöokull eruption is the same as the domain of HIRLAM-12 shown in Fig. 10.

3.2 Source Definition

The source geometry is time dependent in the SNAP model and can be specified differently for each time segment of the eruption. However, the number of model particles released at each model time step is the same for the entire period of eruption. The source term can be specified separately for each substance which is released into the atmosphere. Gases, aerosols and large particles can be included for dispersion simulation in SNAP. In case of volcano eruption, the ash is represented in the model by particle classes with different size and density. It is also possible to simulate SO_2 and SO_4 atmospheric transport from the volcanic eruption in the SNAP model, but in a very simplified form compared to Eulerian models with a sophisticated chemistry, e.g. EMEP model [45]. Therefore, the volcano version of SNAP is mostly focused on the transport of ash particles of different size. The release rate is separate for each particle class and can vary in time.

3.2.1 Source Geometry

Following the bomb version of SNAP [38], [5], there are two options for parameterizing geometry of the source for volcano eruption: cylinder or two cylinders one above another (mushroom shape in the bomb version). Only the cylinder version has been used for volcano applications. This version assumes that all model particles are uniformly mixed and distributed in the cylinder volume immediately after eruption. Different model particles are used for each substance - pollutant and therefore the trajectories of these model particles can also differ. The radius of the cylinder, as well as the bottom and top of the cylinder are specified in the input file for the model run. All parameters necessary for SNAP run specification are included in the file "snap.input". The definitions of the cylinder parameters in the snap.input file are the following:

```
RELEASE.RADIUS.M= 1250
RELEASE.LOWER.M=  2000
RELEASE.UPPER.M=  8500
```

According to the definition above, all model particles are uniformly distributed in the cylinder with the radius 1250m, with the cylinder base at 2000 m above the ground and the cylinder top at 8500 m above the ground.

3.2.2 Particle Classes

The volcanic ash particles can be represented by the particle classes in the model simulations. Each particle class is given a unique name and parameters: particle size and particle density. For each class there are three options for calculating gravitational settling: 1) gravitational settling neglected, 2) constant value of gravitational settling velocity for each class and 3) gravitational settling velocity calculated for each class at each model time step depending on temperature and pressure. The last option was used and five particle classes defined in the simulations of Ejafjallajökull eruption. The particle classes were different in size, but had the same density - 2.3 g cm^{-3}. The following diameters (in μm) were assigned to each particle class: 0.3, 1.0, 3.0, 10.0, 30,0. The definitions of model particle classes (components) in the snap.input file are given below:

```
COMPONENT= Aerosol.0.3
DRY.DEP.ON
WET.DEP.ON
RADIUS.MICROMETER= 0.15
DENSITY.G/CM3= 2.3
FIELD.IDENTIFICATION=01
*
COMPONENT= Aerosol.1.0
DRY.DEP.ON
WET.DEP.ON
RADIUS.MICROMETER= 0.5
DENSITY.G/CM3= 2.3
FIELD.IDENTIFICATION=02
*
COMPONENT= Aerosol.3.0
DRY.DEP.ON
WET.DEP.ON
RADIUS.MICROMETER= 1.50
DENSITY.G/CM3= 2.3
FIELD.IDENTIFICATION=03
*
COMPONENT= Aerosol.10.0
DRY.DEP.ON
WET.DEP.ON
RADIUS.MICROMETER= 5.0
DENSITY.G/CM3= 2.3
```

```
FIELD.IDENTIFICATION=04
*
COMPONENT= Aerosol.30.0
DRY.DEP.ON
WET.DEP.ON
RADIUS.MICROMETER= 15.0
DENSITY.G/CM3= 2.3
FIELD.IDENTIFICATION=05
```

The statements: DRY.DEP.ON and WEP.DEP.ON mean that each component is a subject of dry and wet deposition during the atmospheric transport.

3.2.3 Source Variability in Time

The source term in the SNAP model is time dependent and can be specified separately for each particle class. Three options - commands for this specification are used in the SNAP input file: ”BOMB”, ”STEPS” and ”LINEAR”. In the ”BOMB” option all model particles are injected into cylinder only at time zero of the simulation. In the ”STEPS” option emission rates are kept constant for each time sequence which is specified by the user. In the ”LINEAR” option, there is a linear interpolation of the emission rates between each time step, which is specified by the user. The ”STEPS” option has been used for the volcano version, however the ”LINEAR” option can be useful as well.

3.2.4 An Example of Source Specification

An example of source term specification in the input file for the SNAP run simulating the Eyjafjallajökull eruption is given below.

```
TIME.RELEASE.PROFILE.STEPS
RELEASE.HOUR=              0,     24,     48,     96,    120,    144,    168,    192,    216,    240
RELEASE.RADIUS.M=       1250,   1250,   1250,   1250,   1250,   1250,   1250,   1250,   1250,   1250
RELEASE.LOWER.M=           0,      0,      0,      0,      0,      0,      0,      0,      0,      0
RELEASE.UPPER.M=        8500,   8500,   6500,   5000,   3500,   4500,   4500,   4500,   4000,   3500
RELEASE.BQ/SEC.COMP=  5.0e+4, 5.0e+4, 5.0e+4, 5.0e+4, 5.0e+4, 5.0e+2, 5.0e+3, 5.0e+3, 5.0e+2, 5.0e+2 'Aerosol.0.3'
RELEASE.BQ/SEC.COMP=  2.5e+5, 2.5e+5, 2.5e+5, 2.5e+5, 2.5e+5, 2.5e+3, 2.5e+4, 2.5e+4, 2.5e+3, 2.5e+3 'Aerosol.1.0'
RELEASE.BQ/SEC.COMP=  2.5e+6, 2.5e+6, 2.5e+6, 2.5e+6, 2.5e+6, 2.5e+4, 2.5e+5, 2.5e+5, 2.5e+4, 2.5e+4 'Aerosol.3.0'
RELEASE.BQ/SEC.COMP=  1.0e+7, 1.0e+7, 1.0e+7, 1.0e+7, 1.0e+7, 1.0e+5, 1.0e+6, 1.0e+6, 1.0e+5, 1.0e+5 'Aerosol.10.0'
RELEASE.BQ/SEC.COMP= 37.2e+7,37.2e+7,37.2e+7,37.2e+7,37.2e+7,37.2e+5,37.2e+6,37.2e+6,37.2e+5,37.2e+5 'Aerosol.30.0'
```

This source term specification was used for the simulation of the first 10 days of Eyjafjallajökull eruption.

3.3 Mixing Height

As good as possible determination of the mixing height, which represents in the model the depth of atmospheric boundary layer (ABL), is very important for modelling atmospheric transport and deposition of air pollution. The turbulent diffusion is significantly more intensive in the ABL and only pollution in the boundary layer is a subject of dry deposition.

The procedure to identify and calculate the mixing height h is based on critical Richardson Number formulation R_{iC}. The gradient Richardson Number, R_i, is calculated for a given model layer from

$$R_i = \frac{g\Delta\theta_i/\Delta z}{\bar{T}(\Delta\mathbf{u}/\Delta z)^2} \tag{2}$$

where $\Delta\theta_i/\Delta z$ and $\Delta\mathbf{u}/\Delta z$ are the gradients of potential temperature and wind speed, g is the acceleration due to gravity and $\bar{T}$ is the mean temperature of the layer. It is assumed that the mixing height can be determined from the meteorological input data at which a small positive number of R_i is reached, below which turbulent motion tends to persists and above which it is suppressed. The critical value R_{iC} is used to identify the top of the ABL that is, the mixing height h. The model gradients of potential temperature and wind, $\Delta\theta/\Delta z$ and $\Delta\mathbf{u}/\Delta z$, are used to search for R_{iC} layer by layer, starting from the surface and stepping upward trough the model layers. The value $R_{iC} = 1.8$ is used for determining the mixing height in the SNAP model.

3.4 Advection and Diffusion

The advective displacement of each model particle is calculated at each model time step, Δt, which is equal to 5 minutes (300 s) in the present SNAP version. For this calculation, three-dimensional velocity is interpolated to particle position from the eight nearest nodes in the model grid. Bilinear interpolation in space is applied to horizontal components of the velocity field and linear interpolation for the vertical component. In addition, linear interpolation in time is applied between three-hourly meteorological input fields. The advective displacement of each particle in one model time step is calculated according to

$$\mathbf{x}'_{t+\Delta t} = \mathbf{x}_t + [\mathbf{u}(\mathbf{x}_t) + \mathbf{u}_g(\mathbf{x}_t)]\Delta t \tag{3}$$

where $\mathbf{x}_t = (x, y, \eta, t)$ is the position of particle, $\mathbf{u} = (x, y, \eta, t)$ is velocity from the numerical weather prediction model and $\mathbf{u}_g = \mathbf{u}_g(x, y, \eta, t)$ is the gravitational setting velocity for the given model particle, all at time t. The intermediate position of the particle after advection is denoted by the vector $\mathbf{x}'_{t+\Delta t}$.

The calculation of gravitational settling velocity included in Equation 3 is described in the next Section. A relatively simple iterative procedure developed by Petersen [21] is used for numerical solution of Equation 3. We have found two iterations in this procedure to be entirely sufficient for calculating the new position of the model particle.

3.4.1 Gravitational Settling Velocity

For conditions when the Stokes law is valid, gravitational settling velocity with spherical shape of particles is a function of particle size, particle density and air density [41]:

$$v_g = \frac{d_p^2 g(\rho_p - \rho_a)C(d_p)}{18\nu} \tag{4}$$

where:
d_p is the particle diameter,
g is the acceleration due to gravity,
ρ_p is the particle density,
$\rho_a = \rho_a(p, T)$ is the density of the air at particle location,
$C(d_p)$ is Cunningham correction factor,

$\nu = \nu(T)$ is the dynamic molecular viscosity of the air at particle location.

The density of the air is calculated from the equation of state

$$\rho_a = \frac{p}{RT} \tag{5}$$

where
p is the atmospheric pressure,
T is the absolute temperature,
$R = 287.04$ is the gas constant for dry air ($Jkg^{-1}K^{-1}$)

Viscosity of the air is a function of temperature [22]:

$$\nu = 1.72 \times 10^{-5} \frac{393}{T+120} (\frac{T}{273})^{\frac{3}{2}} \tag{6}$$

and Cunningham correction factor for small particles [41]) is calculated as:

$$C(d_p) = 1 + \frac{2\lambda}{d_p}(1.257 + 0.4e^{-0.55\frac{d_p}{2\lambda}}) \tag{7}$$

where $\lambda = 6.53 \times 10^{-8}$m is the mean free path of air molecules. Equation 4 is not valid for particles with the radius larger than 10-15 μm. In case of the larger particle classes, correction to account for high Reynolds numbers is necessary. Such a correction was introduced in the SNAP model (Bartnicki et al., 2003) leading to the following set of equations [41]:

$$\begin{array}{ll} v_g(1 + \frac{3}{16}Re + \frac{9}{160}Re^2 \ln 2Re) = \frac{d_p^2 g(\rho_p - \rho_a)C(d_p)}{18\nu} & 0.1 < Re \leq 2 \\ v_g(1 + 0.15Re^{0.578}) = \frac{d_p^2 g(\rho_p - \rho_a)C(d_p)}{18\nu} & 2 < Re \leq 500 \end{array} \tag{8}$$

where $Re = v_g d_p \rho_a / \nu$ is the Reynolds Number. Equation 8 is non-linear and requires a numerical solution, which may significantly slow down the model performance, if it is applied to each individual particle at each model time step. However, in the volcano version of SNAP, we have used the tabulated values of gravitational settling velocities for each of the selected particle class. This table is calculated only once at the beginning of each model run, so that application of these equations did not significantly reduced the model performance.

3.4.2 Random Walk Method

Random walk techniques giving effect to diffusion are described in detail in [26]. The Wiener-type of process used here is governed by a length scale, the sequence of steps following the description by Mayron [17]. A slightly different parameterization is used for particles located within boundary layer and for those above, but can be described by the same equations. The new particle position is calculated as:

$$\begin{array}{l} x'' = x' + r_x l \\ y'' = y' + r_y l \\ \eta'' = \eta' + r_\eta l_\eta \end{array} \tag{9}$$

where $\mathbf{x}''_{t+\Delta t} = (x'', y'', \eta'')$ is the particle position vector at time $t + \Delta t$ after application of the diffusion algorithm; r_x,r_y,r_η are randomly sampled numbers from the range (-0.5,+0.5), generated from uniform distribution; l and l_η are the length scales from the horizontal and vertical turbulent motion. Horizontal diffusion above the ABL in SNAP is parameterized in the same way as for the particles below, but the value of the coefficient of proportionality is different for two regions. We assume horizontal length-scale for the turbulent motion, defining horizontal diffusion:

$$l = ax^b \tag{10}$$

where $x = |\mathbf{u}|\Delta t$, $|\mathbf{u}| = \sqrt{u^2 + v^2}$ is the wind speed in m/s, $b = 0.875$, $a = 0.5$ in ABL and $a = 0.25$ above.

The scale of vertical diffusion is $l_\eta = 0.08$ within ABL and $l_\eta = 0.001$ above the boundary layer. Parameterization of vertical diffusion in the volcano version of SNAP is relatively simple, probably too simple especially in the ABL. However, as seen from the aviation perspective, the most important for the model results is the diffusion above ABL. In most of the dispersion models, vertical diffusion is very week and in some models it is even neglected [24]. The advantage of the simplification related to vertical diffusion parameterization is a better performance of the model in relation to computational time.

3.4.3 Boundary Conditions

When displaced, particles can reach the boundaries of the model domain. Since SNAP is a model of the Lagrangian type, formulation of boundary conditions is relatively simple.

For particles with larger diameter like 20 μm and above, the mechanism of gravitational settling can be effective in moving them quickly to the ground. If the position of model particle in the next time step is lower than the ground level $\eta > 1.0$, the entire particle is removed from the further computations and its entire mass is added to dry deposition matrix. In the random walk process, the model particles cannot penetrate the surface - the bottom boundary of the model domain. If the particle hits the ground in the random walk procedure, it is reflected back into the boundary layer.

A similar procedure is applied to the model particles reaching the upper boundary of the model domain. At the top of the model domain, there is no exchange of particles. This assumption implies the closed upper boundary conditions.

Particles can flow out of the lateral boundaries of the model domain, but none can enter the model domain from the outside. This implies open lateral boundary conditions.

3.5 Dry Deposition

Many particles of different size are released into the atmosphere in the volcano eruption. For the relatively large particles, the dry deposition process is dominated by the gravitational settling. However, for the relatively small particles with the diameter below 3 μm, other processes are dominating the removal of particles from the air. Therefore, not only gravitational settling, but also other surface related processes are included in the parameterization of dry deposition.

A key parameter in the dry deposition process is the dry deposition velocity v_d, which can be calculated based on the resistance analogy [41]. For particles of arbitrary size:

$$v_d = \frac{1}{r_a + r_s + r_a r_s v_g} + v_g \tag{11}$$

In Equation 11, the aerodynamic resistance r_a accounts for turbulent diffusion from the free atmosphere to surface laminar sub-layer and it is a function of meteorological parameters such as wind speed, atmospheric stability and surface roughness. The surface layer resistance r_s is related to diffusion trough a laminar sub-layer and is more dependent on molecular than turbulent properties. For the volcano version of SNAP, we have assumed the total resistance in Equation 11 to be 200 s m^{-1}. The gravitational settling velocity is dominating dry deposition process for large particles. For very large particles emitted into the atmosphere during the volcano eruption, this leads to the simplification $v_d \approx v_g$.

In the volcano version of SNAP we have assumed that the model particles located above the mixing height h are not affected by the dry deposition process. Reduction of the particle mass, m, due to dry deposition in one time step Δt, for each model particle located within the mixing layer can be calculated as:

$$m(t+\Delta t) = m(t) exp(-\frac{v_d}{h}\Delta t) \tag{12}$$

The above parameterization of dry deposition is relatively simple, except gravitational settling velocity calculations. This simple approach can affect the deposition field and concentrations in the ABL. However, for volcano applications, concentrations at the higher levels are the most important and those are not affected by the simplifications in dry deposition parameterization.

3.6 Wet Deposition

Wet deposition is the most effective process in removing particles of different size from the atmosphere. This process includes absorption of particles into the droplets in the clouds and then droplet removal by precipitation. Wet deposition process depends on many complicated factors, which are difficult to take into account, like for example occult deposition related to fog, scavenging by snow, effect of convective precipitation and orographic effects.

In the volcano version of the model, we have assumed that the mass of particle, m affected by precipitation is reduced during one model time step Δt in the following way:

$$m(t+\Delta t) = m(t) e^{-k_w \Delta t} \tag{13}$$

Following Baklanov and Sørensen [1], the coefficient of wet deposition k_w is a function of the particle radius r (in μm) and the precipitation intensity q (in mm per hour):

$$k_w = \begin{cases} a_0 q^{0.79} & r \leq 1.4 \\ (b_0 + b_1 r + b_2 r^2 + b_3 r^3) f(q) & 1.4 < r \leq 10.0 \\ f(q) & 10.0 < r \end{cases} \tag{14}$$

where

$f(q) = a_1 q + a_2 q^2$,
$a_0 = 8.4 \times 10^{-5}$, $a_1 = 2.7 \times 10^{-4}$, $a_2 = -3.618 \times 10^{-6}$,
$b_0 = -0.1483$, $b_1 = 0.3220133$, $b_2 = -3.0062 \times 10^{-2}$, $b_3 = 9.34458 \times 10^{-4}$.

In Equation 14, the wet deposition coefficient for small particles ($r \leq 1.4$) and for large particles ($10.0 < r$) does not depend on the particle size, but on precipitation intensity. Only for particles in the range ($1.4 < r \leq 10.0$), the wet deposition coefficient is a function of both particle size and precipitation intensity.

In many cases and in convective situation especially, precipitation does not occur in the entire model grid square. The area of the model grid square covered by precipitation as a function of precipitation intensity was originally estimated in [15]. In the SNAP model we use a probability curve Fig.11 based on this estimation. From the probability curve we can find the probability of the model particle to be affected by precipitation in a given model grid as a function of precipitation intensity. If the probability ϕ of precipitation for a given location of the model particle is above zero, we replace the precipitation intensity q in Equation 14 by the effective precipitation intensity $q_{eff} = q/\phi$.

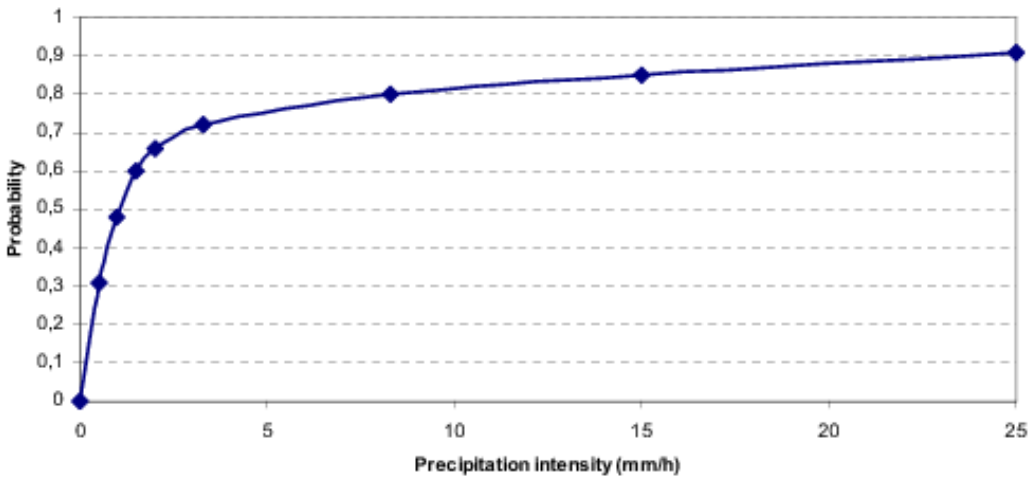

Figure 11: The probability curve for precipitation used in the SNAP, model and taken from [15].

In addition, there is an elevation limit for model particles to be a subject of wet deposition. In the volcano version of SNAP, we have assumed that only those particles located below the model level $\eta = 0.67$ are loosing mass due to wet deposition. This η level corresponds roughly to 3000 m.

4 SNAP Simulations of Eyjafjallajökull Eruption

The SNAP model can be run in two modes. In the graphical mode, the selected SNAP results are shown on the screen during the model run. These results include the locations of model particles on the map within the model domain, which are continuously updated. In the batch mode, no graphics is shown on the screen, but the model execution is much faster. An example of screen display during the SNAP run for radioactive pollutants is shown in Fig. 12. In the operational SNAP version for radioactive debris, the isolines of pressure and precipitation are shown together with the model particles. Different colors are used for marking the model particles. Those affected by precipitation are red and those in dry environment are black. A ”gold” color is used to show the contaminated part of the model domain where the radioactive debris is deposited in dry or wet process. An example of on-line screen display during the SNAP run for radioactive pollutants is shown in Fig. 12.

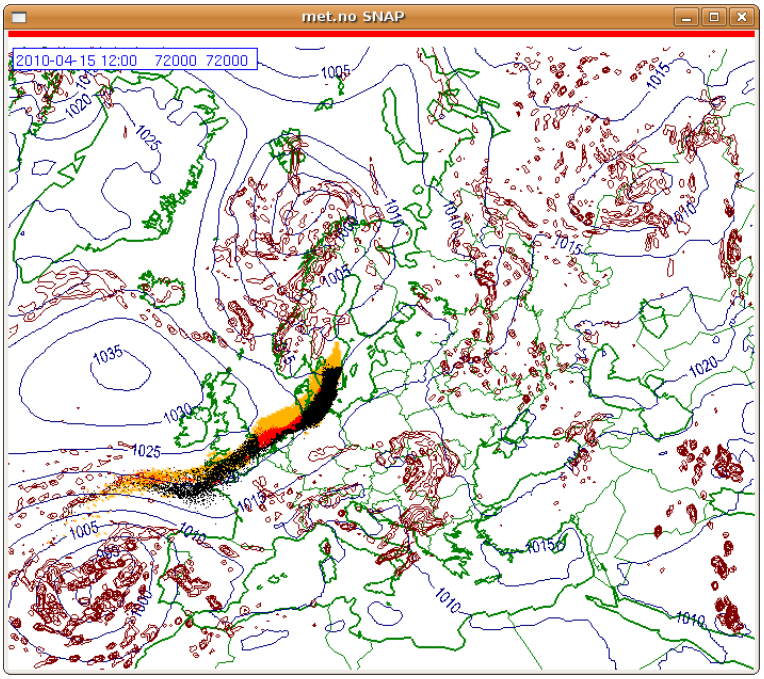

Figure 12: An example of on-line screen view during the SNAP run for radioactive pollution.

4.1 Results of Preliminary Run

The operational volcano version of SNAP did not exist in time of Eyjafjallajökull eruption on 14 April 2010. Therefore the standard ”radioactive” version of SNAP had to be used with some crude modifications in the early phase of the eruption. In the first, preliminary model runs the volcanic ash was represented by two classes of particles: ”small” with the radius 1.0 μm and ”large” with the radius 2.2 μm. The density of particles was the same for both classes and equal to 3 g cm^{-3}. The eruption rates for these particles were of the same order as typical

radioactivity releases in case of nuclear accident and did not reflect the reality. However, the model particles were very useful to illustrate the location of the ash cloud from Eyjafjallajökull eruption. Daily eruption rates applied in the preliminary SNAP runs were the same for both classes and are shown in Fig. 13.

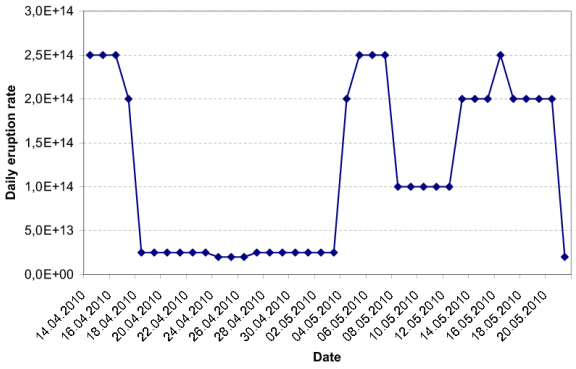

Figure 13: Daily eruption rates for two classes of particles used in the preliminary SNAP runs. Units: g hr^{-1}.

Compared to radioactive pollutants, the on-line screen display was different for operational SNAP runs simulating the volcano eruption in the later phase. All model particles were shown in black color and deposition was not shown at all. An example of the map with model particles for volcano eruption is shown in Fig. 14. The results of preliminary model runs, with the daily eruption rate as specified in Fig. 13, are shown in Appendix **??**. These results are presented as maps with the model particles for each day of the period 14.04.2010 - 21.05.2010.

4.2 Results of the Operational Model Version

The present (October 2010) operational volcano version of the SNAP model, as described in Chapter 3 has been also used to simulate the dispersion of volcanic ash from Eyjafjallajökull eruption. The results of the model run in operational applications include different kinds of maps such as: maps with model particles, maps with the average air concentrations in three layers and maps with atmospheric column of ash. After the model run it is also possible to use the met.no's DIANA software for displaying instantaneous ash concentration, as well as dry, wet and total depositions.

The maps showing the locations of model particles in .png format are produced automatically during the operational run of SNAP. The updated, during the model run, maps can be seen on-line on the screen by the meteorologists on duty operating the model. In addition those maps are stored for a later display on the met.no's web, as well as for creation of the animations, which are also posted on the met.no's web. The complete set of maps with model particles created by the present volcano version of SNAP is given in Appendix **??**. These maps differ, sometimes significantly, from the maps created in preliminary SNAP runs, with the source term specified in Fig. 13. As an example, we show a comparison of maps with

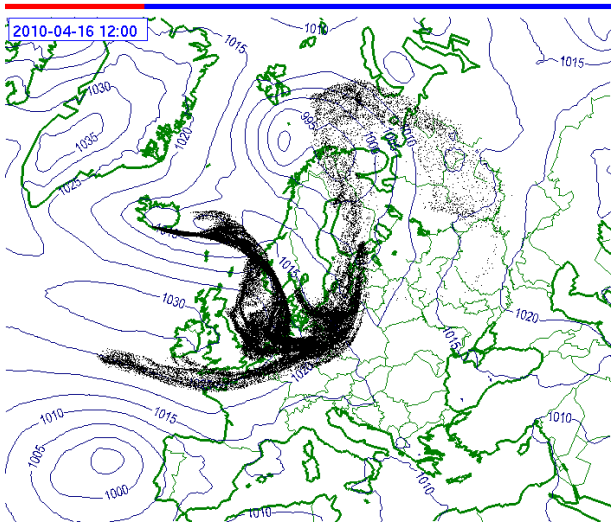

Figure 14: An example of on-line screen view during the SNAP run for volcano eruption. Simulation of Eyjafjallajökull eruption for 12:00 UTC 16.04.2010 with the source term defined in Fig. 13.

model particles from preliminary and present operational SNAP runs in Fig. 15. On 21 April at 12:00 UTC the density of the model particles on the map from operational run is much higher than on the map from preliminary SNAP run, especially over Norway.

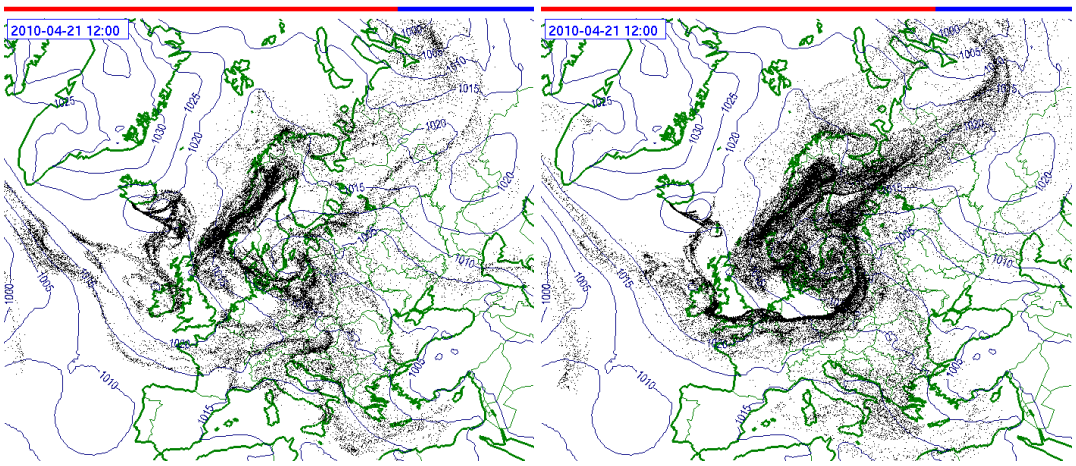

Figure 15: Comparison of the maps with model particles from preliminary run (left) and from operational run (right). Situation from 21 April 12:00 UTC.

4.2.1 Model Output Compatible With VAAC

The model output compatible with VAAC consists of three maps with ash concentrations averaged over the last six hours and over the entire layer between the selected flight levels. The first - bottom layer SFC/FL200 extends between the surface and 20000 ft, the second - middle layer FL200/FL350 is located above 20000 ft and below 35000 ft and the third one - the top layer FL350/FL550 extends from 35000 ft to 55000 ft. The official VAAC maps are coming from the results of the NAME model [27] run at the UK Meteorological Office. They include only isolines of the threshold concentrations at these three selected layers. As a support to the official VAAC forecasts, the results of the NAME model are also presented on the web [51] as different zones on the maps. In April 2010, in the first week of the Eyjafjallajökull eruption only two zones were in use - red and black. Later on a new gray zone was introduced and the zones currently in use by the UK Meteorological Office are the following:

- **Red zone.** The outer range of this zone represents the area with exceedance of standard threshold of ash concentrations (200 μg of ash per m^3) as used in the official VAAC products.
- **Gray zone.** The gray areas represent the ash concentrations that are 10 to 20 times higher than the standard (red) threshold, with the ash concentrations in the range 2000 - 4000 μg m^{-3}. To operate in this new zone airlines need to present the CAA with a safety case that includes agreement of their aircraft and engine manufacturers.
- **Black zone.** The black areas represent ash concentrations that are 20 times the standard (red) threshold and twice the gray threshold with concentrations higher than 4000 μg m^{-3}. These are areas within which engine manufacturers tolerances are exceeded.

In the SNAP output, we follow the initial definitions of the zones, which are valid in Norway at present (October 2010). This means no gray zone and a lower level (2000 μg m^{-3}) for the black zone. Three zones in the SNAP model are defined as follows:

- **Yellow zone.** Represents areas with non-zero ash concentrations calculated by the SNAP model. Since the average values are shown here, the actual ash concentrations in this area can be higher.
- **Red zone.** Is the same as defined by UK Meteorological Office, with ash concentration limits between 0.2 mg m^{-3} and 2.0 mg m^{-3}.
- **Black zone.** It is the same as in SNAP as the initial black zone defined by the UK Meteorological Office with a lower limit of the ash concentrations - 2 mg m^{-3}.

The future definitions of the zones in the SNAP output will depend on the requirements of the Norwegian Aviation Authority and will be changed according to their needs.

Some examples of the simulated ash concentrations, in three selected layers, on 21 April 06:00 UTC are shown in Fig. 16. The top map shows the concentrations in the top layer FL350/FL550 one week ofter the eruption start and this is the first time when the ash entered

this layer. For the first week of the simulation the top layer was free of ash. The concentrations are higher in the bottom layer than in the middle layer, because of the assumptions in the source term parameterization, with most of the release in the bottom layer.

The complete set of maps with the concentrations in three selected layers, for the entire period of the simulation and with 6-hour resolution is given in Appendix C. It should be noticed that already after 12 hours from the eruption start the volcanic ash in the middle layer is approaching the coast of Northern Norway. On 16 April 12:00 UTC, 54 hours after the eruption start, the ash is present over the whole Norway, both in the bottom layer and in the middle layer.

4.2.2 Maps of Atmospheric Column

The maps of atmospheric column of ash show the horizontal distribution of ash mass which is present in the air. The range of atmospheric column is consistent with the horizontal envelope over ash concentrations in three selected layers shown in the previous Section. The examples of simulated atmospheric column are shown in Fig. 17. The first map of ash column comes from an early phase of the eruption on 14 April 18:00 UTC, when the volcanic ash arrives to the coast of Northern Norway. The map in the middle of Fig. 17 shows the situation 30 hours after eruption start when volcanic ash is present in the air over the entire Norwegian territory. The bottom map represents the situation at the end of the simulation on 24 April 12:00 UTC when the ash column covers most of the model domain. The complete set of maps with atmospheric column, for the entire period of the simulation and with 6-hour resolution is given in Appendix C.

4.2.3 Deposition Maps

In some cases, the volcanic ash can include certain substances, which are not especially dangerous for people, but can cause animal diseases. Such cases are of interest for Veterinary Authorities and require information about the distribution of ash deposition. Therefore, the maps with ash deposition should be also considered as a part of an operational output. Maps of ash deposition from individual size classes on 24 April at 06:00 UTC, 10 days after the eruption start are shown in Fig. 18. The total ash deposition from all classes is also shown for comparison. An interesting feature in Fig. 18 is a relatively large contribution from class 5 (particle diameter 30 μm) to total deposition. On one hand this is not surprising, taking into account a relatively high emissions in this class (75%) of total emissions. On the other hand, the range of the transport of these large particles is very long, perhaps longer than expected. Those results confirm that atmospheric transport of large ash particles can not be neglected in modelling volcano eruptions.

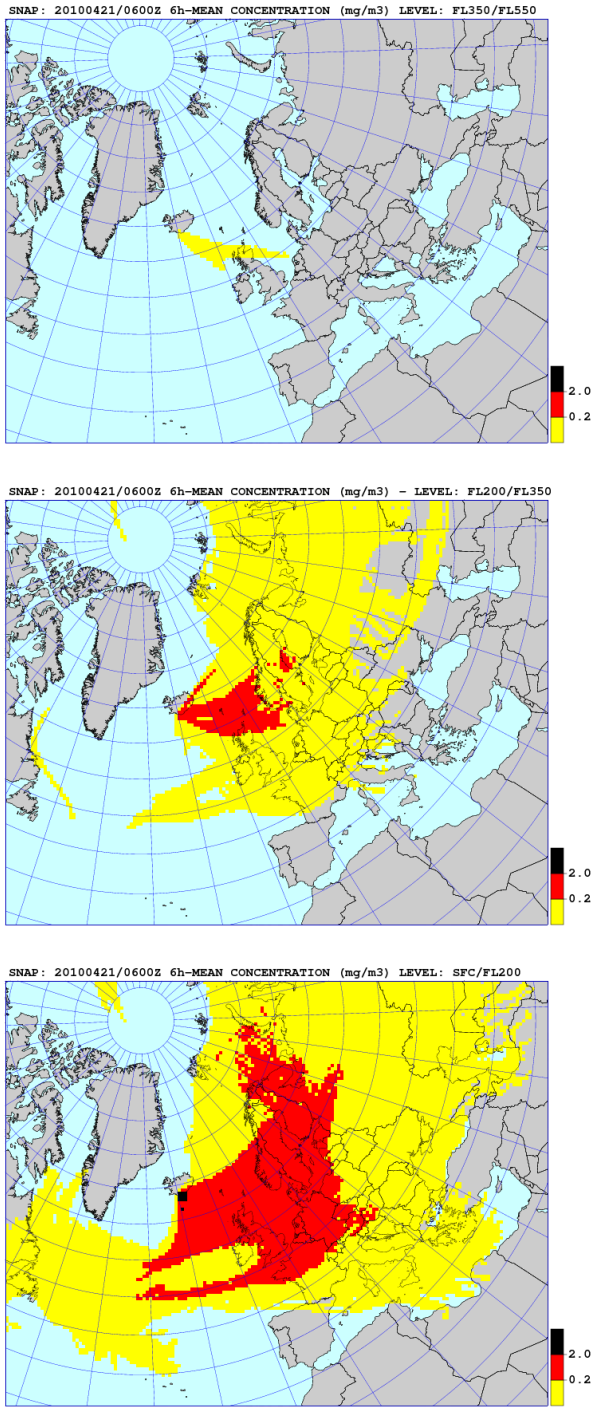

Figure 16: An example of simulated ash concentrations in three VAAC compatible layers on 21 April 2010 at 06:00 UTC.

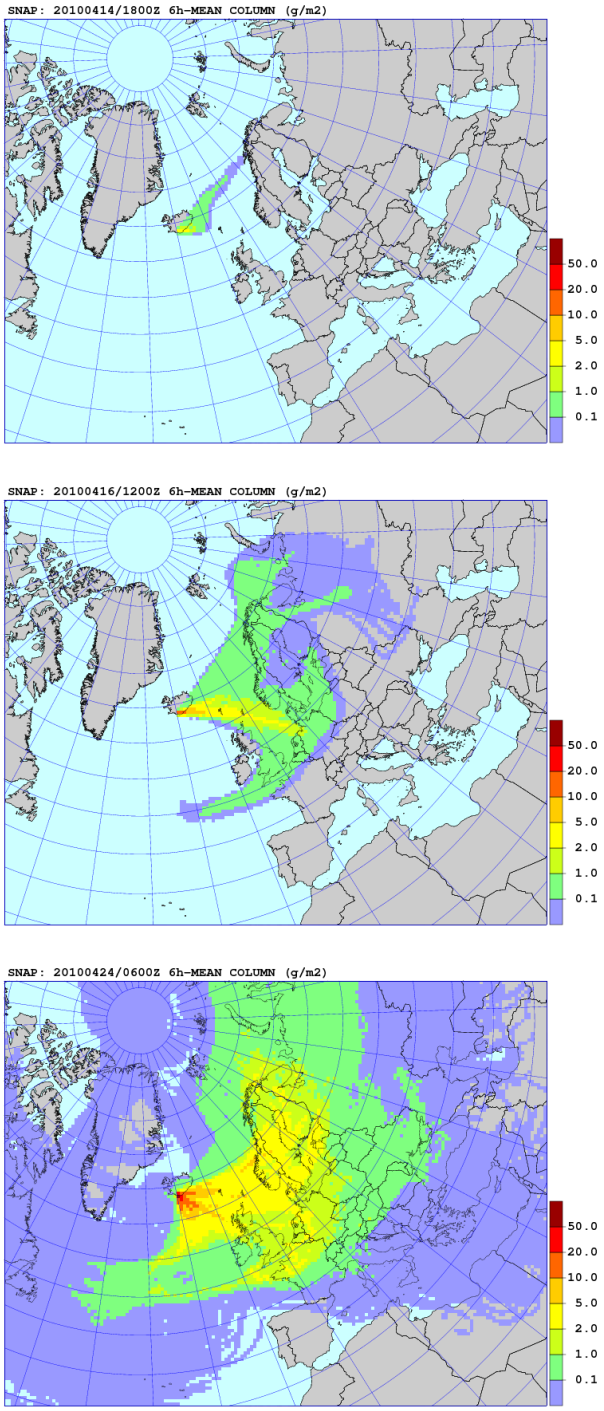

Figure 17: Examples of simulated atmospheric column of ash in early phase of eruption (14 April 12:00 UTC), when the cloud covers the whole Norwegian territory and at the end of the simulation (24 April 06:00 UTC).

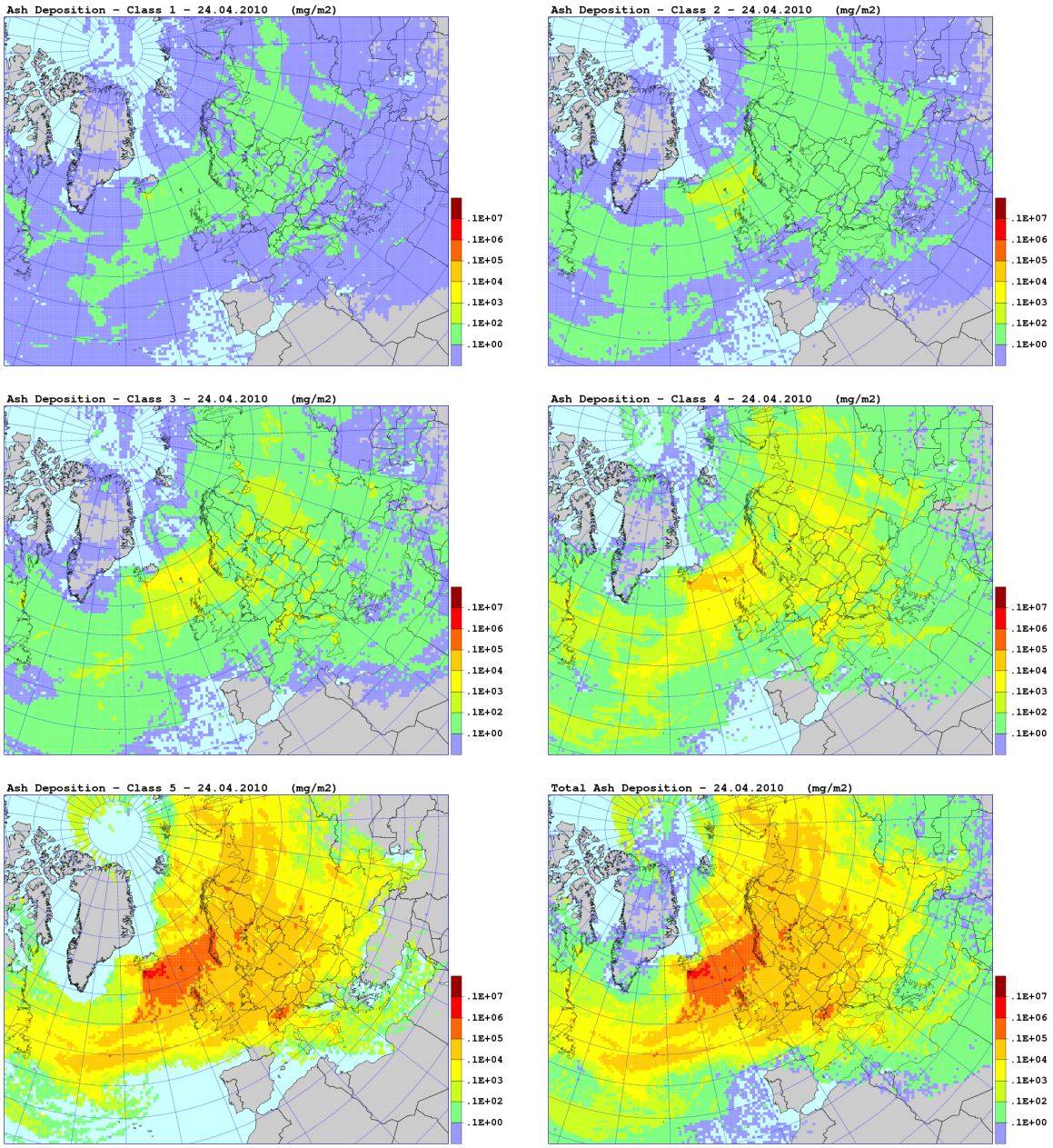

Figure 18: Maps of ash deposition in individual size classes on 24 April at 06:00 UTC, 10 days after the eruption start. Total ash deposition as a sum of depositions from all classes is also included.

5 Comparison of SNAP Results With VAAC Forecasts

A systematic comparison of the SNAP volcano version results with available measurements has not been performed yet. A large part of this very important task will be done in the frame of the ENSEMBLE project [12] organized by JRC in Ispra, at the end of 2010. A dedicated measurements database for Eyjafjallajökull eruption will be established at JRC for this project, in which more than 20 dispersion models from all over the world will take part. Here, we only present a comparison of the SNAP results with the official VAAC forecasts during the Eyjafjallajökull eruption. The VAAC forecasts are available in the form of maps with three isolines representing the threshold level for ash concentration (200 μg m^{-3}) in three layers. The red isoline in VAAC maps represents the threshold in the bottom SFC/FL200 layer, green in the middle FL200/FL3500 layer and dark blue in the top FL350/FL500 layer. The present comparison of SNAP results with VAAC forecasts should be seen as a first step towards extended model verification which will take place at the end of 2010 and in 2011.

5.1 First 24 Hours After Eruption Start

Comparison of the SNAP results with the VAAC maps for the first 24 hours after the eruption start is presented in Fig. 19 - for the bottom layer and in Fig. 20 - for the middle layer. SNAP results have not shown any ash concentration in the top layer in the first 24 hours of the simulation and therefore we do not show the empty SNAP maps for this layer. Because of different projections on the VAAC maps (Geographic) and on the SNAP maps (Polar Stereographic), comparison is a bit more difficult than with the same projections, but still possible.

The shapes of the ash clouds in the VAAC forecasts and in the SNAP maps are quite similar in the bottom layer (Fig. 19). However, the size of the SNAP cloud defined by the red color is much smaller than the size of the VAAC cloud limited by the corresponding red isoline with the same concentration threshold in Fig. 1. The VAAC cloud is more similar to SNAP yellow cloud with smaller concentrations bellow the threshold level. These differences in the concentration levels in SNAP and VAAC results occur because of the differences in the source term used by VAAC and SNAP. Namely, the VAAC eruption rate was at least one order of magnitude higher than the the SNAP eruption rate especially in the beginning of the eruption period. In addition, the plume top used in VAAC simulations was approximately 3 km higher than the plume top used by SNAP, also mostly in the beginning of the eruption period. In fact, in the first SNAP simulations (April, 2010), we used similar source term as VAAC with the VAAC and SNAP results being then more similar than now, but later on the SNAP source term was modified with the eruption rate and plume height reduced as suggested by satellite measurements and observations as used in EMEP [11] and SILAM [44] models.

The same remarks, as for the bottom layer, also apply for the middle layer which is marked by a green isoline on the VAAC maps(Fig. 20). Again, the shapes of the VAAC and SNAP ash clouds are quite similar, but the concentrations are lower on the SNAP maps. The area limited by the threshold isoline is larger in the middle layer than in the bottom layer in the VAAC maps. The situation is opposite in SNAP results where the ash concentrations and cloud range are slightly larger in the bottom than in the middle layer. These differences were caused again by the differences in the source terms used by VAAC and SNAP. Only relatively small part

of the erupted volcanic ash is reaching the middle layer in the SNAP parameterization of the source term, whereas it is quite significant in the NAME source used for the official VAAC forecasts.

Some indications concerning the dynamics of the ash cloud are also visible in Fig. 19 and 20. According to both, SNAP and VAAC results, the ash cloud in the bottom layer is arriving to Northern Norway after 18 hours from the eruption start. However, concentrations predicted by SNAP are below the threshold level, whereas the VAAC concentrations are above the threshold level. The winds are stronger in the middle layer and this is the reason for the faster transport of the ash cloud in this layer. According to SNAP results, ash cloud in the middle layer is reaching North Norway already 12 hours after the eruption start, but with very low concentrations. The transport in the middle layer is also faster according to VAAC results, but the the ash cloud as defined by the threshold layer does not reach Norway before 18 hours from the eruption start. The VAAC maps show that after 18 hours from the eruption start, the ash cloud with concentrations above the threshold level is present over North Norway in all three layers.

5.2 Two Days After Eruption Start

Figures 19 and 20 show the situation up to 24 hours from the eruption start. In addition, comparison of the SNAP results with the VAAC maps on 21 April 12:00 UTC, 54 hours after the eruption start is presented in Fig. 21. In general there is a good agreement between the SNAP and VAAC forecast in the bottom layer also for the concentrations above the threshold level with the exception of the Eastern part of the VAAC cloud which is not present on the SNAP map. On the other hand, there is a yellow SNAP zone present in the Eastern part of the VAAC cloud location with the concentration below the threshold level. The location of the North Eastern part of the VAAC cloud extending to Novaya Zemlya and further is confirmed by several single red grids in the SNAP prediction. The South East part of the VAAC cloud is also reasonably well reproduced on the SNAP maps, but in same areas and with concentrations below the threshold level.

In the middle layer, the location of the ash cloud predicted by SNAP is similar to VAAC forecasts, but the concentrations in SNAP are significantly lower due to differences in the source terms.

5.3 General Agreement

In general, there is a satisfied agreement between SNAP and VAAC results despite the differences in the concentration levels caused by the different source term applied. The agreement is better in the middle than in the bottom layer. The problem remains in the top layer, where SNAP does not predict ash presence for most of the simulation. On the meteorological side, the agreement between VAAC and SNAP is good in terms of the direction and the range of volcanic ash transport in the air.

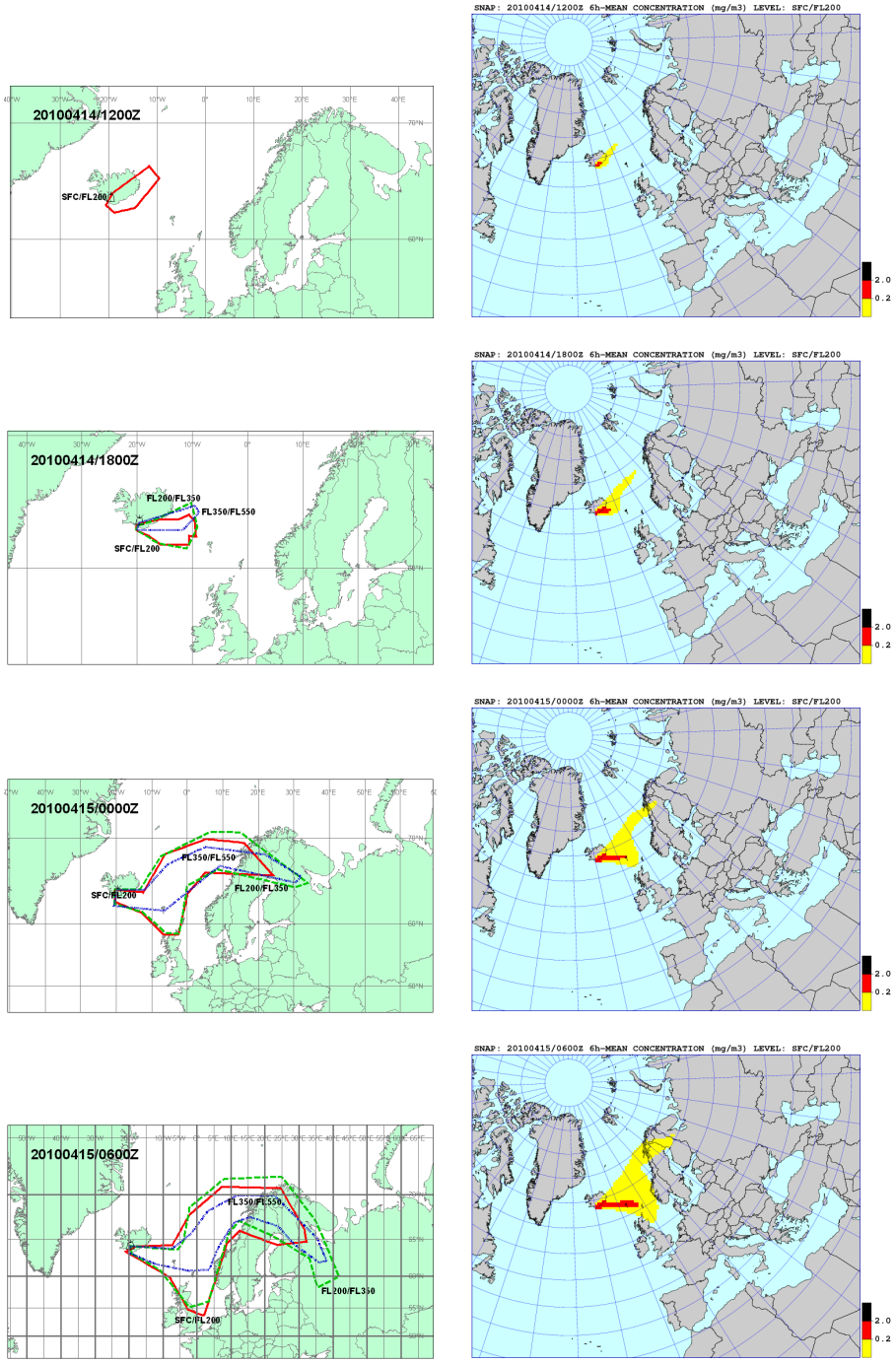

Figure 19: Comparison of VAAC forecasts (left column) with SNAP concentrations in the bottom layer SFC/FL200 (right column) for the first 24 hours after the eruption start. The red line in the left column should be compared with the border of red area in the right column.

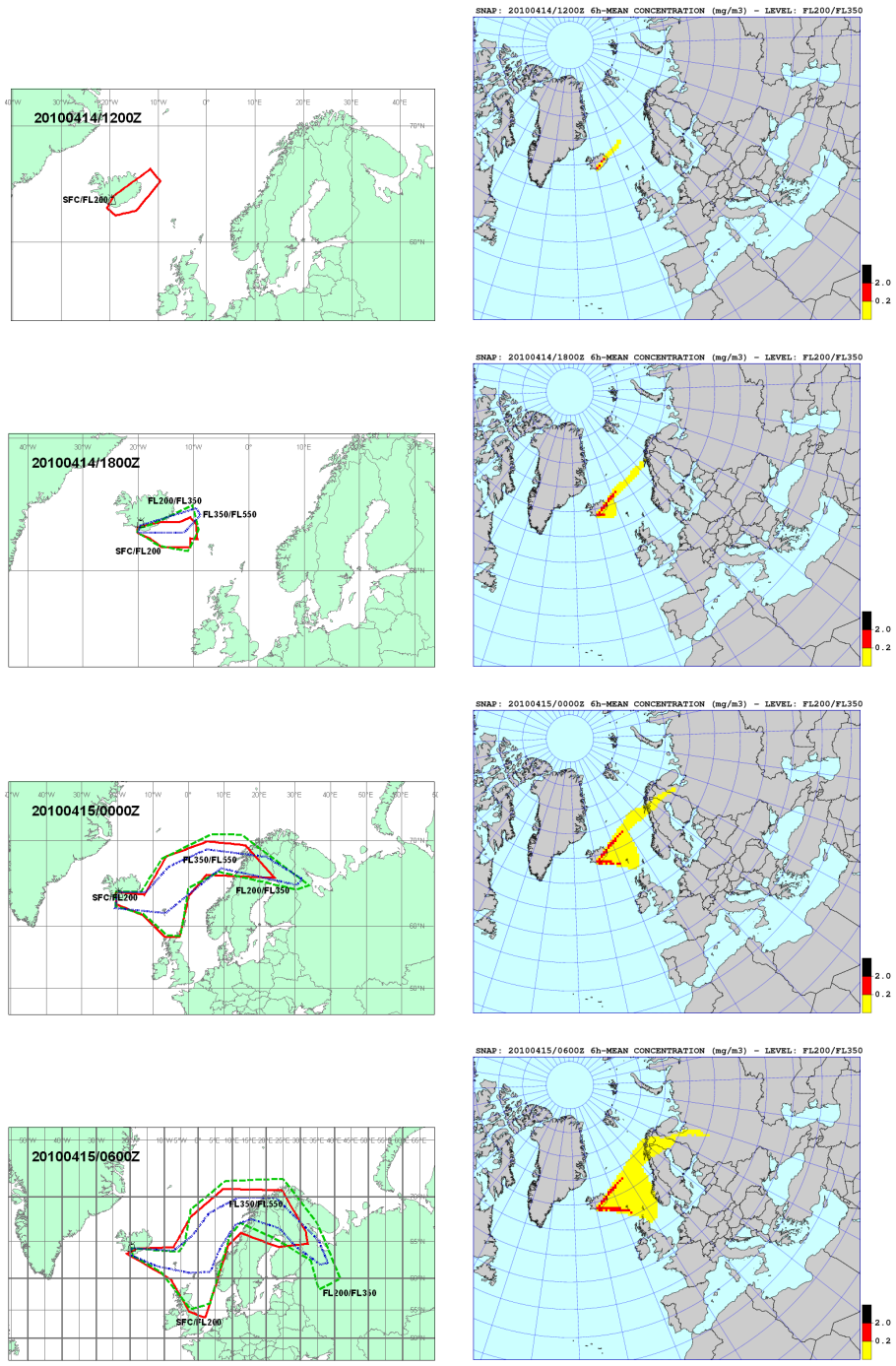

Figure 20: Comparison of VAAC forecasts (left column) with SNAP concentrations in the middle layer FL200/FL350 (right column) for the first 24 hours after the eruption start. The green line in the left column should be compared with the border of red area in the right column.

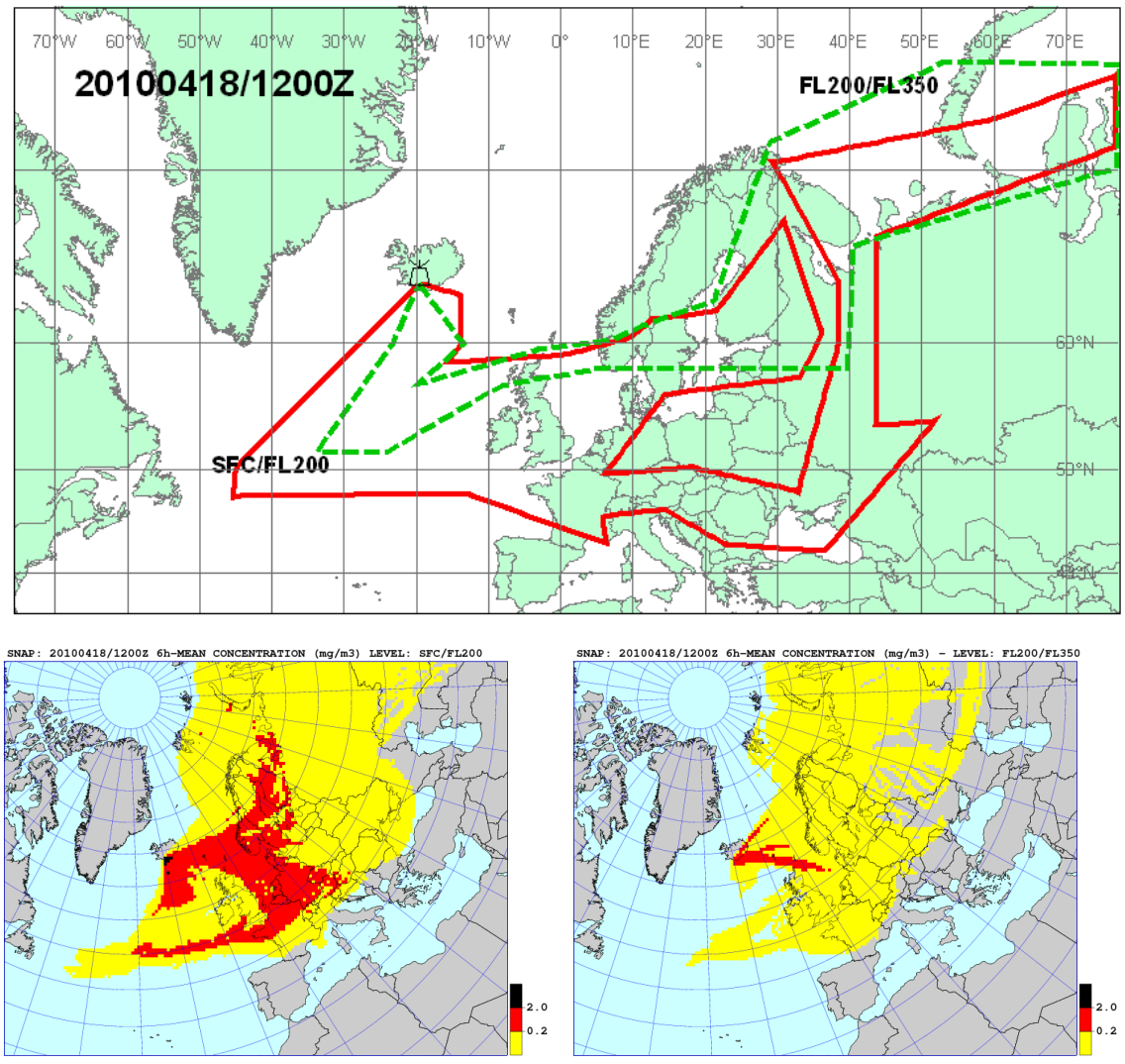

Figure 21: Comparison of VAAC forecasts (top) with SNAP concentrations in the bottom layer SFC/FL200 (bottom left) and in the middle layer (bottom right) on 21 April 12:00 UTC, 54 hours after the eruption start. The red and green lines on the VAAC map should be compared with the border of red area on the SNAP maps.

6 Conclusions

A new version of the SNAP model has been developed for simulating atmospheric transport of ash particles from the volcano eruption. This model version has been used for the event of Ejafjallajökull eruption in April 2010 for calculating ash concentrations and deposition over Europe. At the beginning of eruption, the volcano version of SNAP did not exist and a bomb version of SNAP had to be quickly modified and used. The model modifications and development were also continued after the emergency period resulting in a new version of SNAP, which can be called a volcano version and which has been described in this report. The main conclusions from operational model runs in the emergency period as well as model development and testing after the emergency period are presented below.

- The maps with model particles, as well as animations based on these maps were made public from the beginning of the emergency period. They were updated every day in the emergency period on the met.no and yr.no web sites. They were received with a great interest both, from the general public and decision makers and should continue to be a part of the standard output from the operational model at present and in the future.

- Application of SNAP in the emergency period in April and further tests showed that uncertainties in the source term have a major influence on the uncertainty of the model results, mainly on the range of the cloud with volcanic ash. The uncertain range, in turn, can be extremely costly for the aviation business and, what is even more important, create very dangerous situation in the flights. Therefore, the improvement of the source term parameterization, mainly the release height and release rate estimation, is of the first priority for the future research.

- In the present source term parameterization in SNAP, the erupted volcanic ash is represented by five particle classes with different size, in the range 0.3 μm - 30.0 μm. Model results indicated that all five classes of particles and especially class 5, are important for simulating atmospheric dispersion for volcano eruption.

- Parameterization of the vertical diffusion above the mixing layer is very simple, too simple in SNAP, but also in most of the volcano models. The coefficient of vertical diffusion is constant and does not take into account the current meteorological situation at the place where the ash cloud is located. A better parameterization of vertical diffusion above the mixing layer has a high priority in the future model development.

- Also a parameterization of wet deposition in SNAP is relatively simple and has to be improved in the future. This parameterization is important because wet deposition is a main and most efficient mechanism removing ash particles from the air.

- At present, there is no convection and deep convection parameterization in the SNAP model. The convection and especially deep convection process can very quickly change the vertical locations of ash particles making the advection and diffusion processes much more intense than in usual conditions. The convection can also enhance the wet deposition of ash. Both diffusion and wet deposition are closely related to convection and all of them will be important topics in the future studies.

- Systematic sensitivity tests have not been performed with the present version of the model. They are important and will be performed with the next model version, in which improvement of physical processes mentioned above will be taken into account.

- The verification of the present SNAP volcano version has been very limited and only comparison of the model results with the VAAC maps is shown in the report. The SNAP results were also compared with some results of the EMEP and FLEXPART models showing good consistency, but these comparisons were not discussed in the report. A major SNAP verification based on the comparison with available measurements and the results of other 20 models is planned within the ENSEMBLE project organized by the Joint Research Centre in Ispra at the and of 2010.

- The transport of volcanic ash from Iceland to Norway can be very fast. The experience with the Ejafjallajökull eruption shows that already after 12 hours from the eruption start the volcanic ash can reach the territory of Norway. Therefore, the response triggering the emergency modeling system needs to come about at a very short notice. The operational SNAP execution time, including preliminary source term specifications, is approximately 30 minutes, which is short enough.

- The event of Ejafjallajökull eruption in April 2010 confirms that, in emergency situation, met.no is ready and prepared for modeling atmospheric dispersion of not only radioactive debris, but volcanic ash as well. The volcano version of SNAP is fully operational at present (October, 2010) at met.no. Meteorologist on duty can run the model at any time - 24 hours a day. However, some work is necessary for improving the operational application. From the model user side, we are working at present on the efficient Graphic User Interface, which will speed up the preparation of the model run and will limit a possibility for errors in the preparation phase. The future work on the SNAP-VOLCANO model will be focused on improving parameterization of crucial physical processes related to volcano eruption and on improvement of the operational model applications.

References

[1] Baklanov A. and J. H. Sørensen (2001) Parameterization of radionuclide deposition in atmospheric long-range transport modeling. Physics of the Chemistry of the Earth (B) 26(10), 787-799.

[2] Bartnicki, J. and J. Saltbones (1996) Severe Nuclear Accident Program (SNAP) - A real time dispersion model. In: Development and Application of Computer Techniques to Environmental Studies VI. (P. Zannetti and C.A. Brebbia, eds.), pp. 17-26. Computational Mechanics Publications, Southampton, Boston.

[3] Bartnicki, J. and J. Saltbones (1997) Analysis of Atmospheric Transport and Deposition of Radioactive Material Released During a Potential Accident at Kola Nuclear Power Plant. Research Report No. 43, ISSN 0332-9879. Norwegian Meteorological Institute, Oslo, Norway.

[4] Bartnicki J., Salbu B., Saltbones J., Foss A. and O. Ch. Lind (2001) Gravitational settling of particles in dispersion model simulations using the Chernobyl Accident as a test case. DNMI Research Report No. 131. Norwegian Meteorological Institute, Oslo, Norway.

[5] Bartnicki J., B. Salbu, J. Saltbones, A. Foss and O. Ch. Lind (2003) Long-range transport of large particles in case of nuclear accident or explosion. Preprints of 26th NATO/CCMS International Technical Meeting on Air Pollution Modelling and its Application, 26-30 May 2003. Istanbul Technical University, Istanbul, Turkey, pp. 53-60.

[6] Bartnicki, J., Salbu B., Saltbones J. and A. Foss (2005) Analysis of Atmospheric Transport and Deposition of Radioactive Material Released During a Potential Accident at Kola Nuclear Power Plant. Research Report No. 10, ISSN 1503-8025. Norwegian Meteorological Institute, Oslo, Norway.

[7] Bartnicki J., B. Salbu, J. Saltbones, A. Foss and O. C. Lind (2006) Long-range transport and deposition of radioactive particles from potential accidents at Kola Nuclear Power Plant. Proceedings of 1st Joint Emergency Preparedness and Response/Robotic and Remote Systems Topical Meeting. February 11-16, 2006 Salt Lake City, Utah, USA

[8] Bartnicki J. and J. Saltbones (2008) Atmospheric dispersion of radioactive debris released in case of nuclear explosions using the Norwegiain SNAP model. Proceedings of The 12th International Conference on Harmonization within Atmospheric Dispersion Modelling for Regulatory Purposes HARMO12. 6-10 October 2008 - Cavtat, Croatia. pp. 111-115.

[9] D'Amours R. (1998) Modeling the ETEX plume dispersion with the Canadian emergency response model. Atmospheric Environment 32(24): 4335-4341.

[10] Draxler R.R., and G.D. Hess (1998) An overview of the HYSPLIT-4 modelling system for trajectories, dispersion and deposition. Australian Meteorological Magazine 47: 295-308.

[11] EMEP web-site (2010) http://www.emep.int/

[12] ENSEMBLE web-site (2010) http://ensemble.jrc.ec.europa.eu/

[13] Galmarini, S., Bianconi, R., Klug, W., Mikkelsen, T., Addis, R., Andronopoulos, S., Astrup, P., Baklanov, A., Bartnicki, J., Bartzis, J.C., Bellasio, R., Bompay, F., Buckley, R., Bouzom, M., Champion, H., D'Amours, R., Davakis, E., Eleveld, H., Geertsema, G.T., Glaab, H., Kollax, M., Ilvonen, M., Manning, A., Pechinger, U., Persson, C., Polreich, E., Potemski, S., Prodanova, M., Saltbones, J., Slaper, H., Sofiev, M.A., Syrakov, D., SÃ¸rensen, J.H., Van der Auwera, L., Valkama, I., Zelazny, R., 2004a. Ensemble dispersion forecasting, part 1: concept, approach and indicators. Atmos. Environ. 38 (28): 4607-4617.

[14] Galmarini S., Bianconi R., Klug W., Mikkelsen T., Addis R., Andronopoulos S., Astrup P., Baklanov A., Bartnicki J., Bartzis J. C., Bellasio S., Bompay F., Buckley R., Bouzom M., Champion H., D'amours R., Davakis E., Eleveld H., Geertsema G. T., Glaab H., Kollax M., Ilvonen M., Manning A., Pechinger U., Persson C., Polreich E., Potempski S., Prodanova M., Saltbones J., Slaper H., Sofiev M. A., Syrakov D., SÃ¸rensen J. H., Van der Auvera L., Vaikama I. and R. Zelazny (2004) Can the confidence in long range atmospheric transport models be increased? The Pan-European experience on ENSEMBLE. Radiation Protection Dosimetry, 109 (1-2), pp. 19-24.

[15] Haga P.E. (1991) Hvordan influerer nedbørprocesser tids- og romskala pålangtransport av svoveldioksyd og partiklataert sulfat? (in Norwegian). Thesis, Oslo University.

[16] Institute of Earth Sciences. University of Iceland (2010) http://www2.norvol.hi.is/page/ies_EYJO2010_Grain/

[17] Maryon R.H., Smith J.B., Convay B.J., and D.M Godard (1991) The United Kingdom Nuclear Accident Model. Prog. Nucl. Energy, 26:85-104.

[18] Maryon R.H., J. Saltbones, D.B. Ryall, J. Bartnicki, H.A. Jakobsen and E. Berge (1996) An intercomparison of three long range dispersion models developed for the UK Meteorological Office, DNMI and EMEP. UK Met Office Turbulence and Diffusion Note 234. UK Meteorological Office, Bracknell, United Kingdom.

[19] Mastin, L.G. (2007) A user-friendly one-dimensional model for wet volcanic plumes. Geochemistry, Geophysics, Geosystems 8 (Q03014). doi:10.1029/2006GC001455.

[20] Mastin L.G., M. Guffanti, R. Servranckx, P. Webley, S. Barsotti, K. Dean, A. Durant, J.W. Ewert, A. Neri, W.I. Rose, D. Schneider, L. Siebert, B. Stunder, G. Swanson, A. Tupper, A. Volentik, C.F. Waythomas (2009) A multidisciplinary effort to assign realistic source parameters to models of volcanic ash-cloud transport and dispersion during eruptions. J. Volcanol. Geotherm. Res. 188(2009)1-21. doi:10.1016/j.jvolgeores.2009.01.008

[21] Pettersen S. (1956) Weather Analysis and Forecasting. McGraw-Hill, New York.

[22] RAFF (1999) Properties of nuclear fule particles and release of radionuclides from carier matrix. RAFF final report. A research programme carried out with the financial support from the Commision of EC - DG XII. Contract No. FICCT960007.

[23] Richardson D. (2010) Changes to the operational forecasting system. ECMWF Newsletter No.122, Winter 2009/2010.

[24] Robertson L. and J. Langner (1998) An Eulerian Limited-Area atmospheric transport model. Journal of Applied Meteorology, 38: 190-210.

[25] Rose W.I, Y. Gu1, I. M. Watson, T. Yu1, G. J. S. Bluth, A. J. Prata, A. J. Krueger, N. Krotkov, S. Carn, M. D. Fromm, D. E. Hunton, G. G. J. Ernst, A. A. Viggiano, T. M. Miller, J. O. Ballenthin, J. M. Reeves, J. C. Wilson, B. E. Anderson, D. E. Flittner (2000) The February-March 2000 Eruption of Hekla, Iceland from a Satellite Perspective. In: Volcanism and the Earth's Atmosphere, Robock A, Oppenheimer C. (eds). AGU Geophysical Monograph 139: Washington DC; 107-132.

[26] Ryall D.B. and Maryon R.H. (1996) The NAME2 dispersion model: a scientific overview. UK Meteorological Office. MetO(Apr) Turbulence and Diffusion note 217b.

[27] Ryall D.B. and Maryon R.H. (1998) Validation of thr UK Mte. Office's NAME model against the ETEX dataset. Atmospheric Environment 32(24): 4265-4276.

[28] Saltbones J.(1995) Real-time dispersion model calculations as part of NORMEM-WP19. Safety Science 20, 51-59.

[29] Saltbones J. and A. Foss (1994) Real-time dispersion model calculations of radioactive pollutants at DNMI. Part of Norwegian preparedness against nuclear accidents. Preprints of the XIX Nordic Meteorologists Meeting, June 1994, Kristiansand, Norway.

[30] Saltbones J., Foss A. and J. Bartnicki (1995) Severe Nuclear Accident Program. Technical Description. Research Report No. 15. Norwegian Meteorological Institute. Oslo, Norway.

[31] Saltbones J., Foss A. and J. Bartnicki (1995) Severe Nuclear Accident Program (SNAP) - A real time dispersion model. In: Proceedings of Oslo Conference on International Aspects of Emergency management and Environmental Technology. (K.H. Drager ed.), pp. 177-184.

[32] Saltbones J., Foss A. and J. Bartnicki (1995) ETEX - the European Tracer Experiment - DNMI's participation in an international program for evaluation of real time dispersion models. In: Proceedings of Oslo Conference on International Aspects of Emergency management and Environmental Technology. (k:H: drager ed.), pp. 129-138.

[33] Saltbones J., Foss A. and J. Bartnicki (1996) A real time dispersion model for severe nuclear accidents tested in the European Tracer Experiment. Systems Analysis Modelling Simulation 25, 263-279.

[34] Saltbones J. and J. Bartnicki (1997) Atmospheric transport of radioactive material from potential accident in Kola nuclear power plant (in Norwegian). Naturen 4, 178-188.

[35] Saltbones J., Foss A. and J. Bartnicki (1998) Norwegian Meteorological Institute's Real-Time Dispersion Model SNAP (Severe Nuclear Accident Program). Runs for ETEX and ATMES II Experiments with Different Meteorological Input. Atmospheric Environment 32(24), 4277-4283.

[36] Saltbones J., Foss A. and J. Bartnicki (2000) Threat to Norway from potential accidents at the Kola nuclear power plant. Climatological trajectory analysis and episode studies. Atmospheric Environment 34, 407-418.

[37] Saltbones J., Foss A. and J. Bartnicki (2002) Intercomparison of real time dispersion model results, supporting decision making in case of nuclear accident and focusing on quantification of uncertainty. In; Eighth International Conference on Harmonisation Within Atmospheric Dispersion Modelling for Regulatory Purpose. Sofia, Bulgaria, 14-17 October 2002. E. Batcharova and D. Syrakow (Eds.), pp.92-96.

[38] Saltbones J., Bartnicki J. and A. Foss (2003) Handling of Fallout Processes from Nuclear Explosions in Severe Nuclear Accident Program - SNAP. Research Report No. 157. Norwegian Meteorological Institute. Oslo, Norway.

[39] Sandu I, F. Bompay and S. Stefan S. (2003) Validation of atmospheric dispersion models using ETEX data. International Journal of Environment and Pollution 19(4): 367-389.

[40] Savijärvi H.(1990) Fast radiation parameterization schemes for mesoscale and short-range forecast models. J. Appl. Meteor., 29, 437-447.

[41] Seinfeld J.H. (1986) Atmospheric Chemistry and Physics of Air Pollution. John Wile & Sons. New York. 738 pp.

[42] Sigmundsson F, Einarsson P, Gudmundsson MT, Hognadottir T, Mortensen AK, Jakobsdottir S, Roberts M, Vogfjord K, Stefansson R. (2004) Eruption of the Grimsvotn volcano, Iceland: Summary of activity November 1-4 , 2004 (http://www.norvol.hi.is/html/grimsvotn2004/situationreport/nov5.html).

[43] SILAM model web site (2010) http://silam.fmi.fi/

[44] SILAM model web site (2010) http://silam.fmi.fi/AQ_forecasts/v4/forecasts_2010/index.html/

[45] Simpson D., Fagerli H., Jonson J. E:, Tsyro S., Wind P. and J.-P. Tuovinen. (2003) The EMEP Unified Eulerian Model. Model Description, EMEP MSC-W report 1/2003. The norwegian meteorological Institute, Oslo, norway.

[46] Sørensen, J. H. (1998) Sensitivity of the DERMA Long-Range Dispersion Model to Meteorological Input and Diffusion Parameters. Atmos. Environ. 32: 4195-4206.

[47] Stohl, A., Forster, C., Frank, A., Seibert, P., Wotawa, G. (2005) Technical note: The Lagrangian particle dispersion model FLEXPART version 6.2., Atmos. Chem. Phys., 5, 2461-2474.

[48] Sturkell E., Einarsson P,Sigmundsson F, Hooper H., Benedikt Ófeigsson B.G., Geirsson H and H. Ólafsson (2010) Katla and Eyjafjallajokull Volcanoes. Developments in Quaternary Sciences 13, 5-21.

[49] Thordarson T and G. Larsen (2010) Volcanism in Iceland in historical time: Volcano types, eruption styles and eruptive history. Journal of Geodynamics 43 (2007) 118-152.

[50] Undén, P., Rontu, L., Järvinen, H., Lynch, P., Calvo, J., Cats, G., Cuaxart, J., Eerola, K., Fortelius, C., Garcia-Moya, J.A., Jones, C., Lenderlink, G., McDonald, A., McGrath, R., Navascues, B., Nielsen, N.W., Ødegaard, V., Rodriguez,E., Rummukainen, M., Rööm, R., Sattler, K., Sass, B.H., Savijärvi, H., Schreur, B.W., Sigg, R., The, H. and Tijm,A. (2002) HIRLAM-5 Scientific Documentation, HIRLAM-5 Project. Available from SMHI, S-601767 Norrköping, Sweden.

[51] United Kingdom Meteorological Office - Volcano Hazard web-site (2010) http://http://www.metoffice.gov.uk/corporate/pressoffice/2010/volcano.html

[52] VAAC London web-site (2010) http://www.metoffice.gov.uk/aviation/vaac/vaacuk_vag.html

[53] Wikipedia web-site (2010) http://en.wikipedia.org/wiki/

[54] Witham C.S., M. C. Hort, R. Potts, R. Servranckx, P. Husson and F. Bonnardot (2007) Comparison of VAAC atmospheric dispersion models using the 1 November 2004 Grimsvötn eruption. Meteorol. Appl. 14: 27-38.

A Maps With Model Particles - Preliminary Run

In this Appendix, we present the results of the preliminary SNAP run as maps of the model particles for every day (at 12:00 UTC) of the entire period of the simulation: 14.05-2010 - 21.05.2010. The day and hour for which the map is valid is visible in the upper left corner of each Figure. The source term used for this run is specified in Fig. 13.

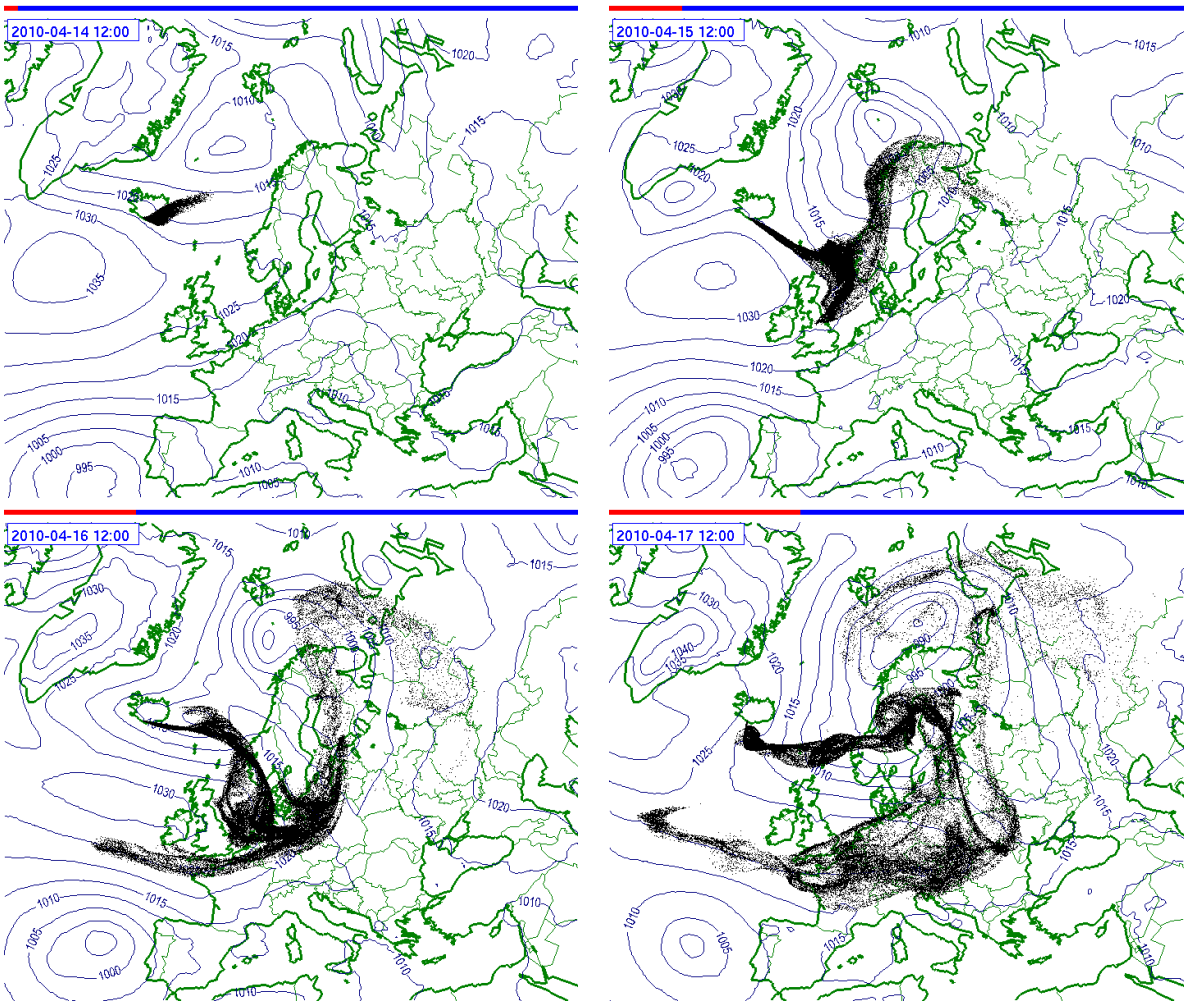

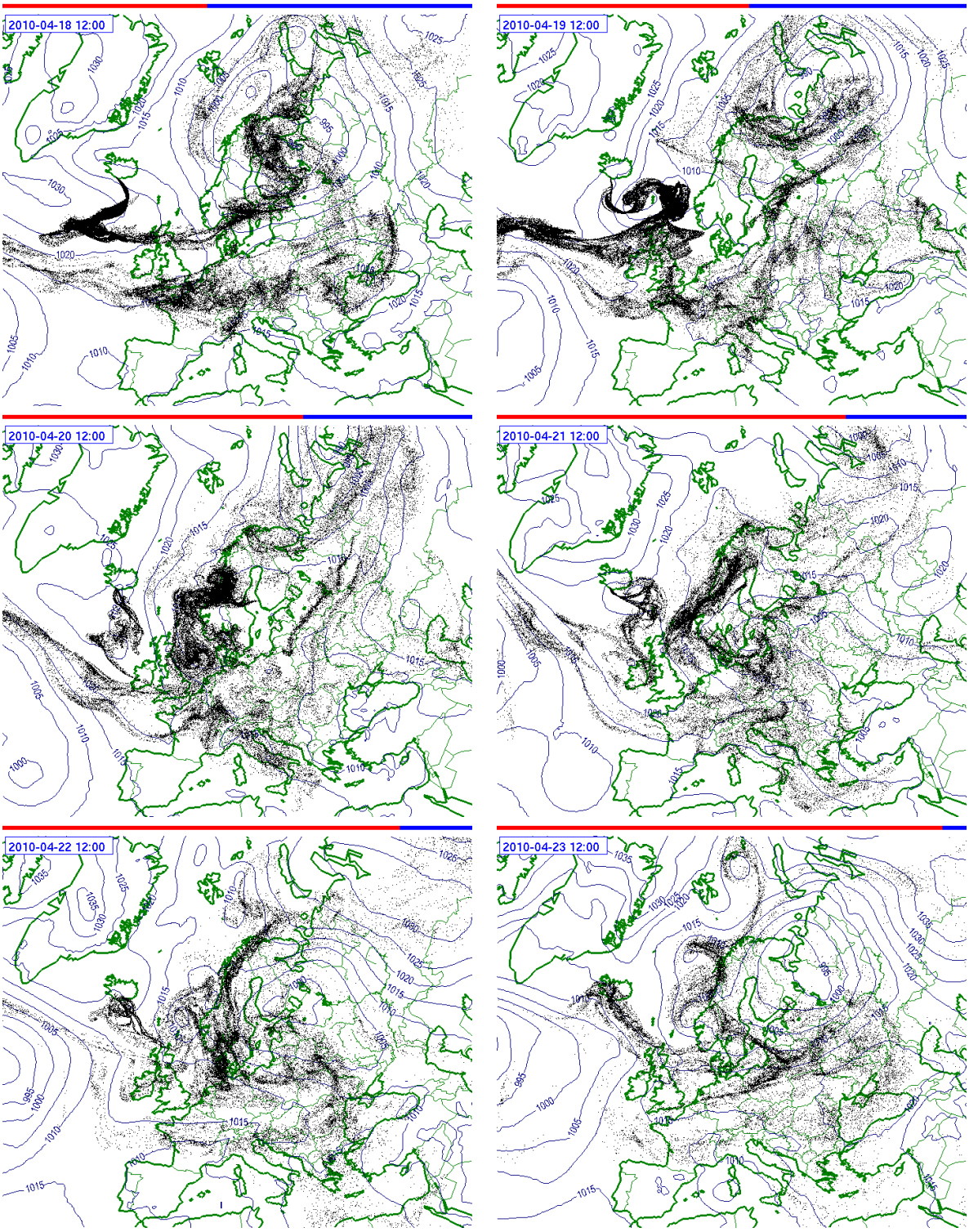
2010-04-18 12:00
2010-04-19 12:00
2010-04-20 12:00
2010-04-21 12:00
2010-04-22 12:00
2010-04-23 12:00

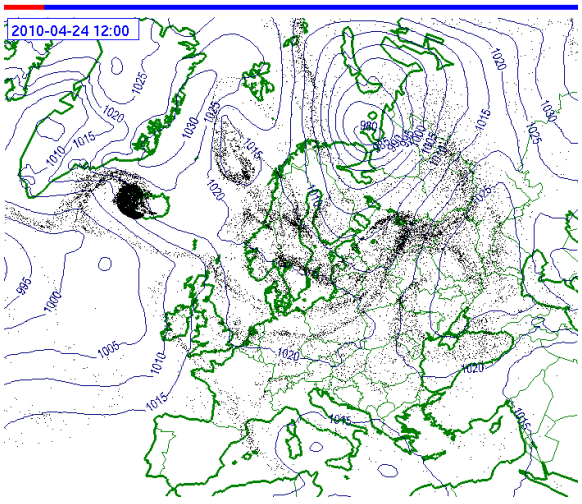
2010-04-24 12:00

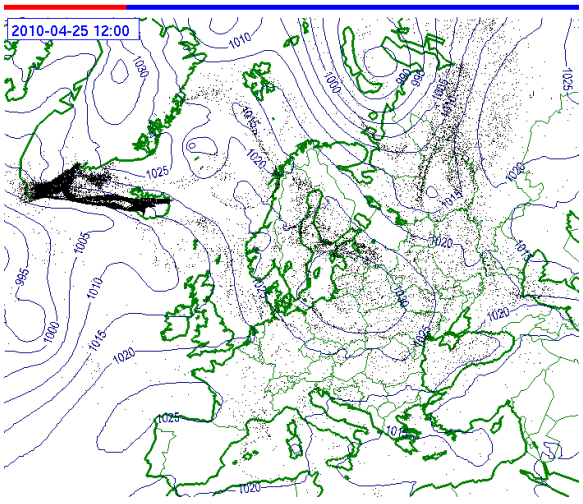
2010-04-25 12:00

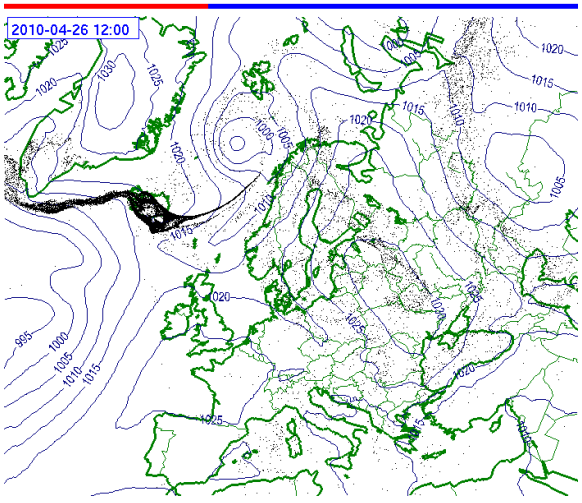
2010-04-26 12:00

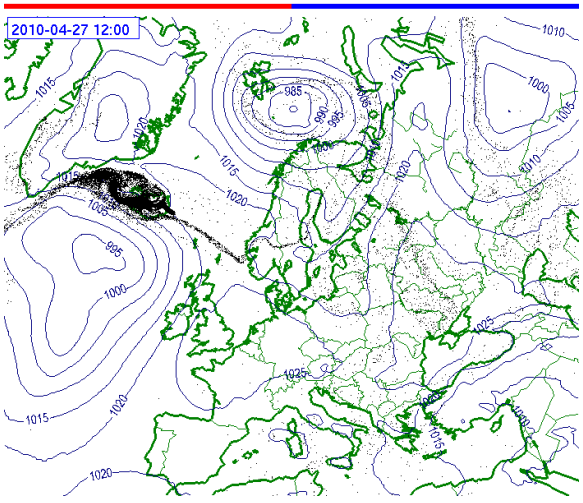
2010-04-27 12:00

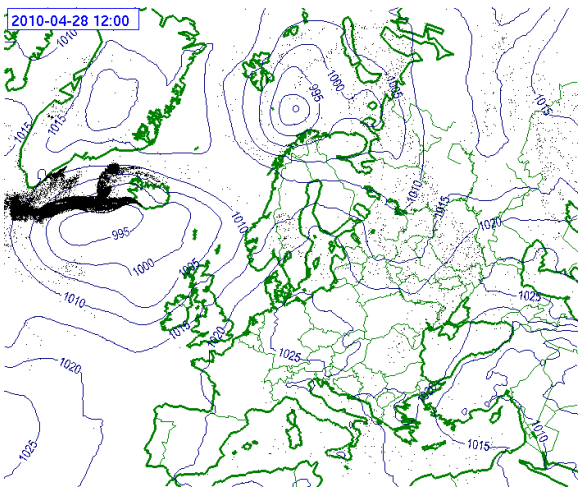
2010-04-28 12:00

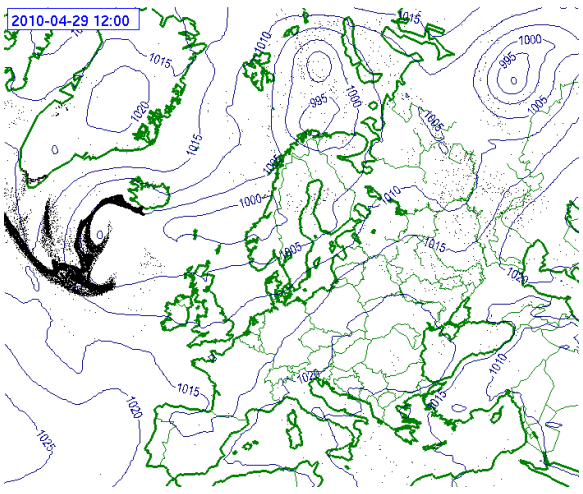
2010-04-29 12:00

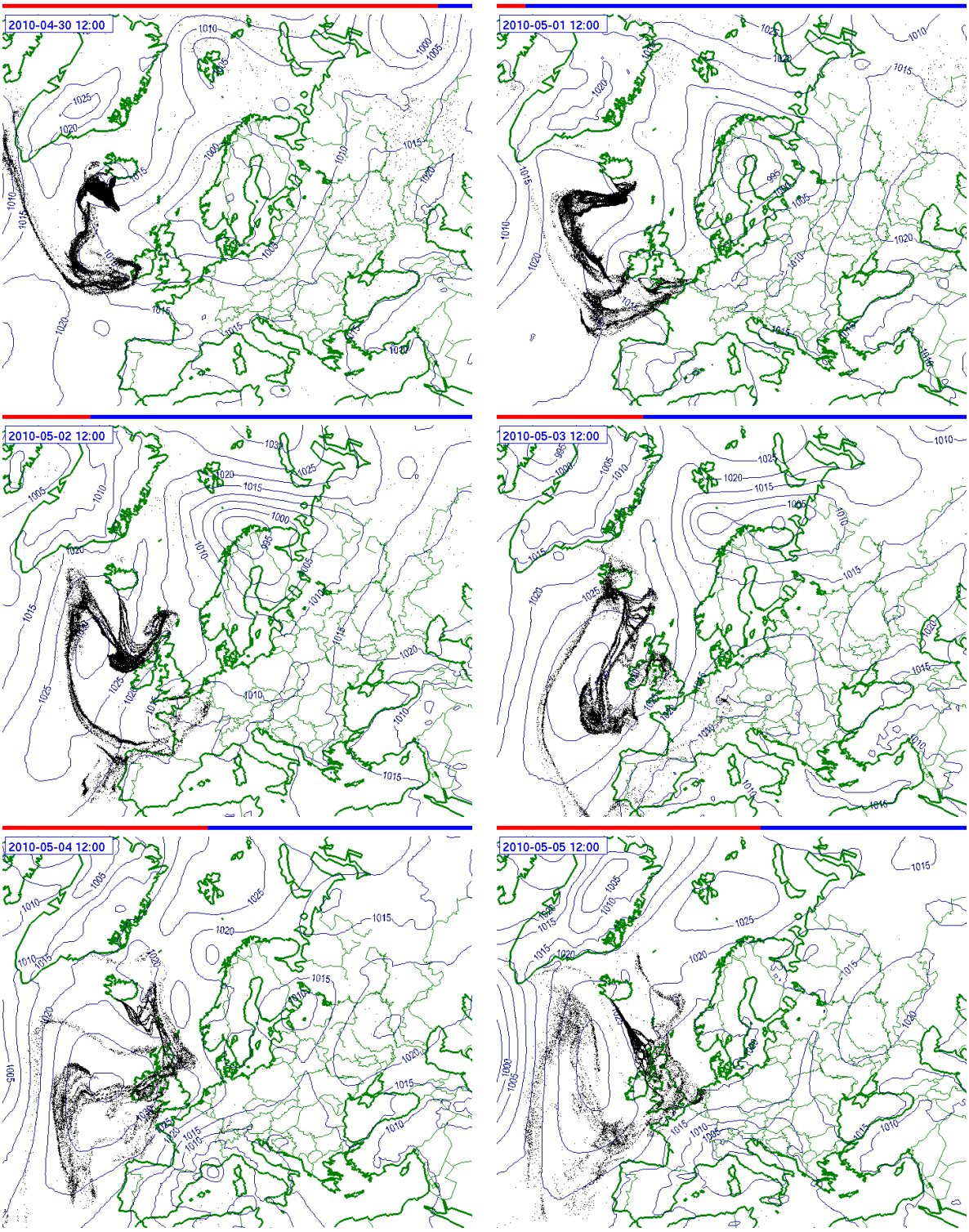
2010-04-30 12:00
2010-05-01 12:00
2010-05-02 12:00
2010-05-03 12:00
2010-05-04 12:00
2010-05-05 12:00

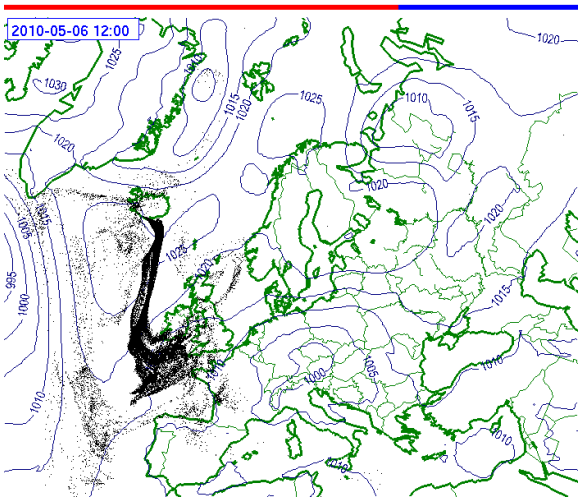
2010-05-06 12:00

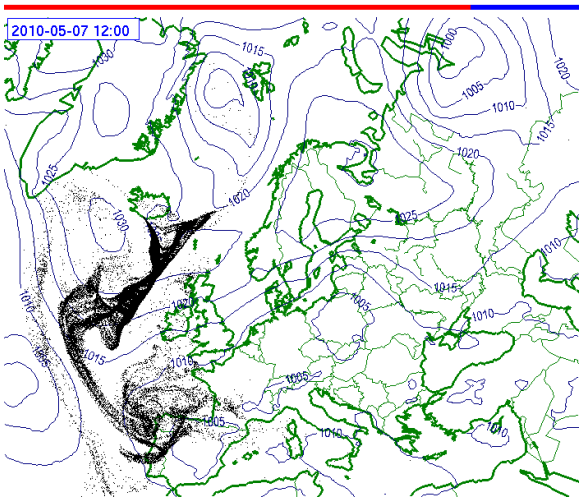
2010-05-07 12:00

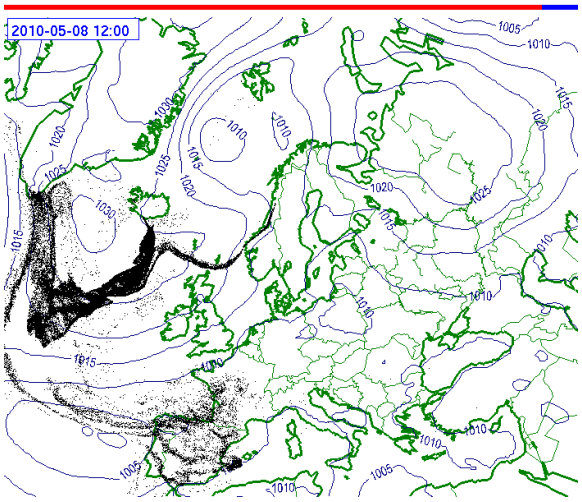
2010-05-08 12:00

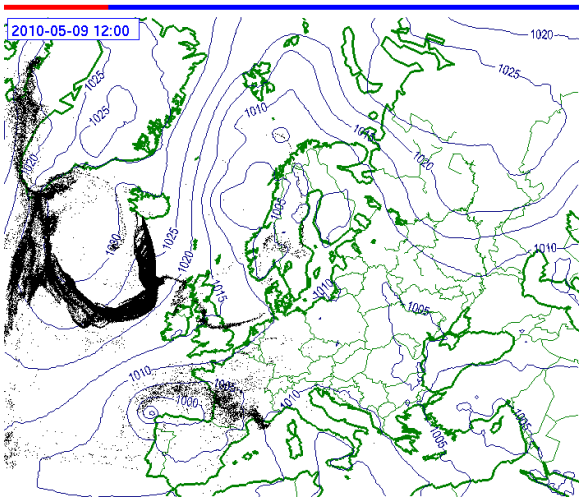
2010-05-09 12:00

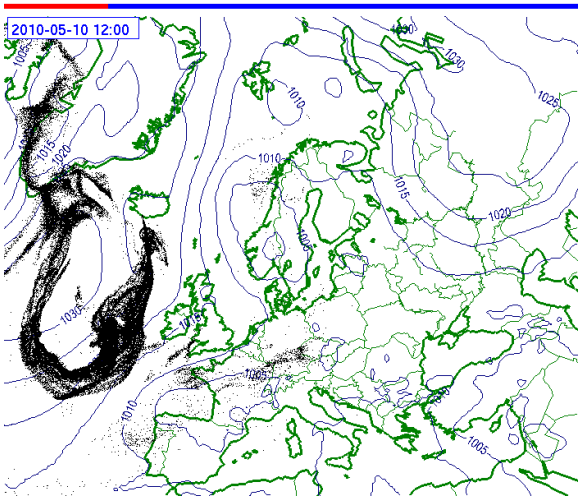
2010-05-10 12:00

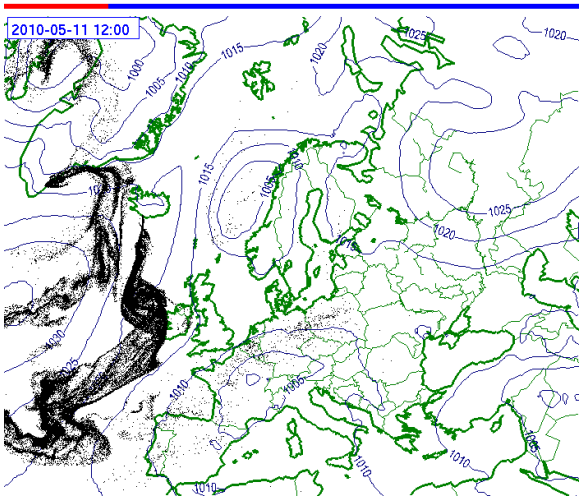
2010-05-11 12:00

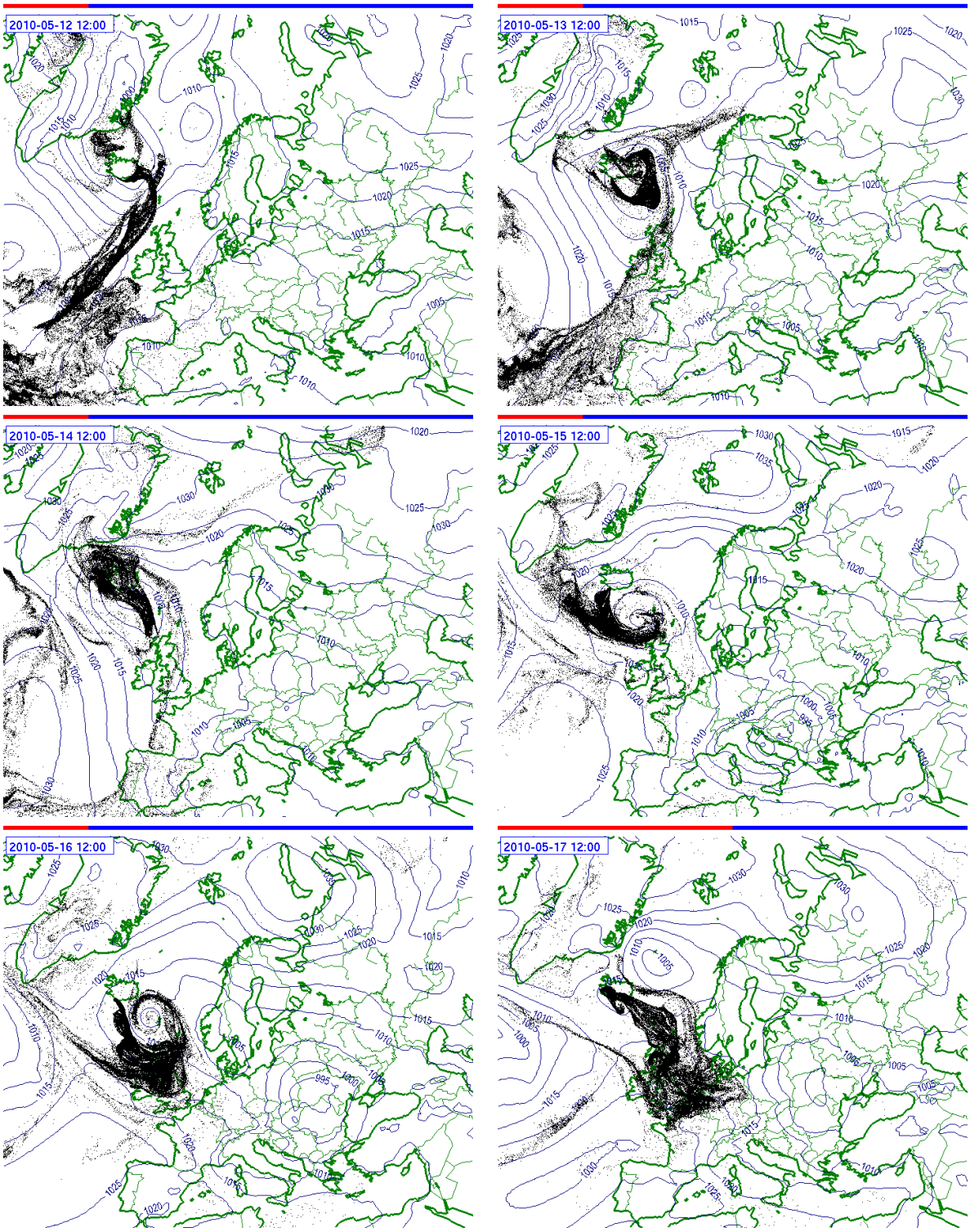
2010-05-12 12:00
2010-05-13 12:00
2010-05-14 12:00
2010-05-15 12:00
2010-05-16 12:00
2010-05-17 12:00

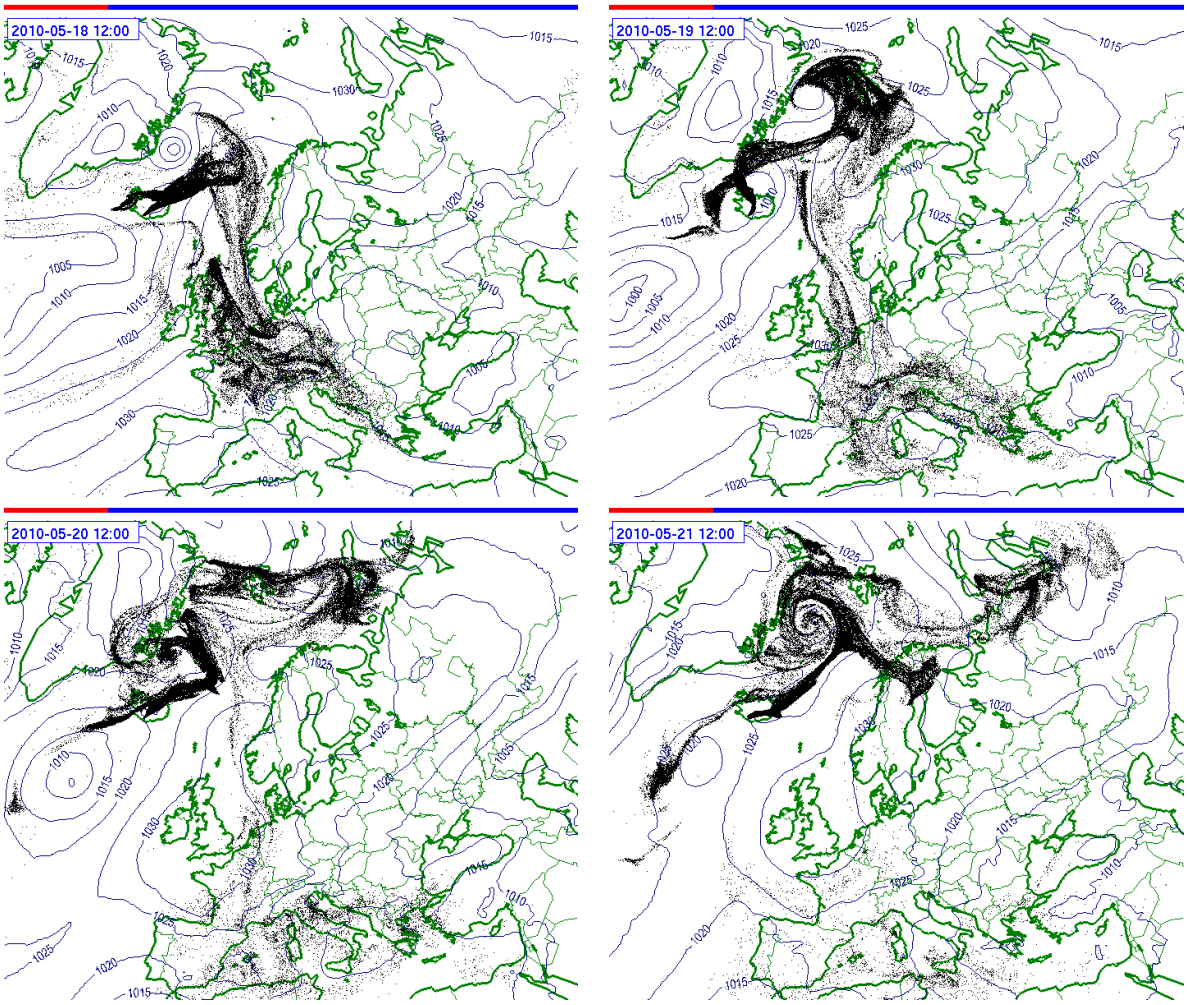
2010-05-18 12:00
2010-05-19 12:00
2010-05-20 12:00
2010-05-21 12:00

B Maps With Model Particles - Operational Run

In this Appendix, we present the results of the current (30 October 2010) operational SNAP calculations as maps of the model particles for every day (at 12:00 UTC) for the simulation period: 14.05-2010 - 21.05.2010. The day and hour for which the map is valid is visible in the upper left corner of each Figure.

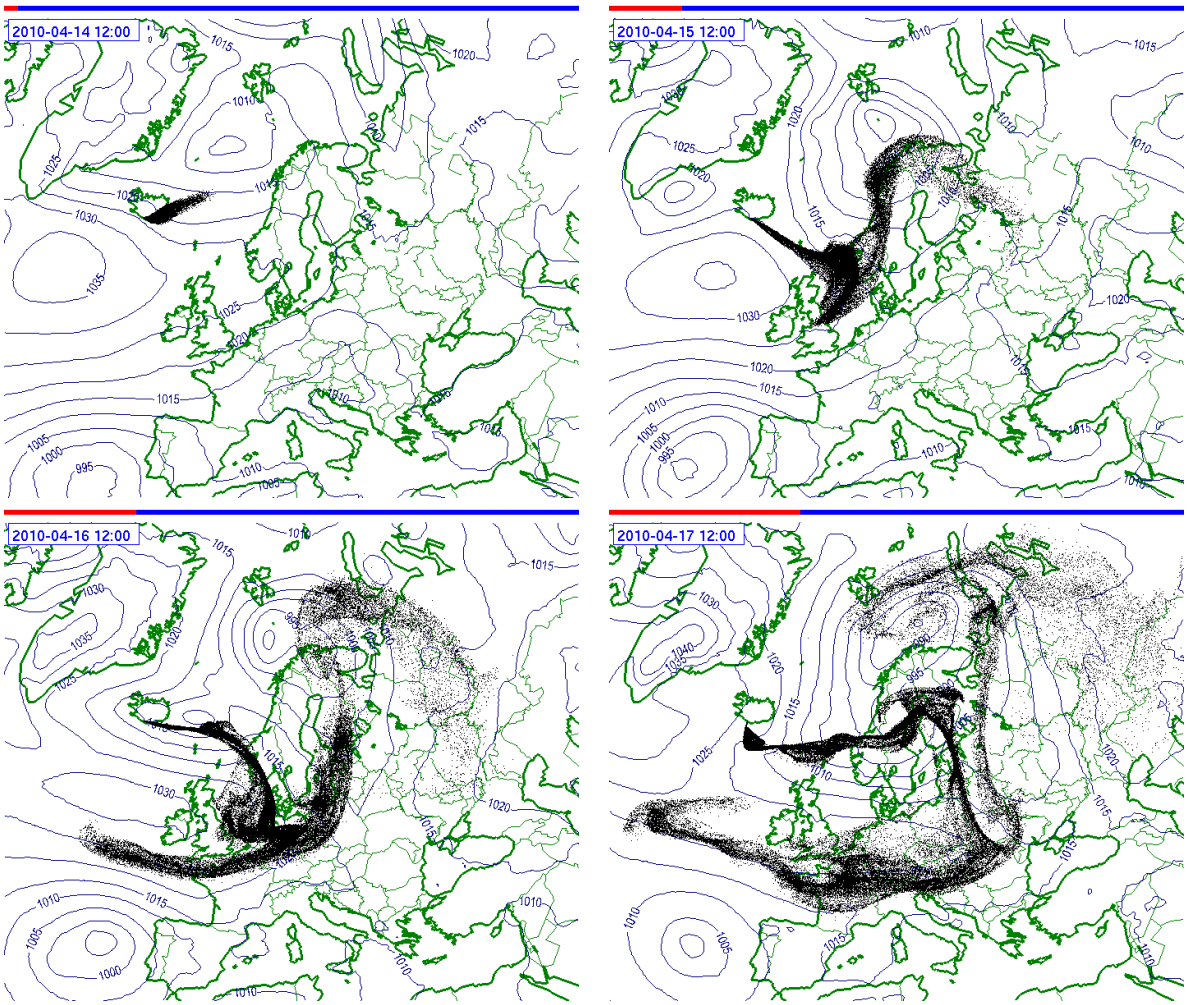

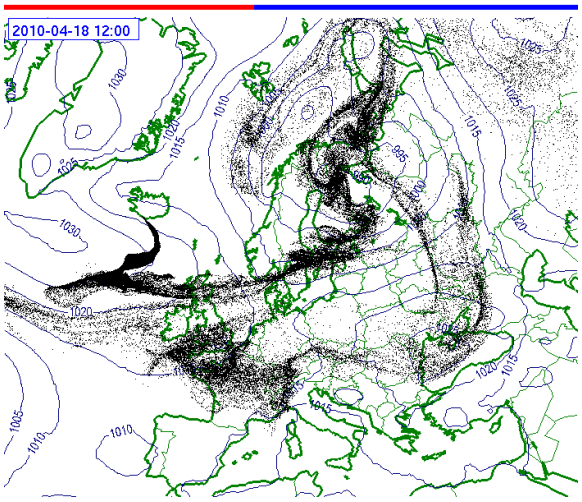
2010-04-18 12:00

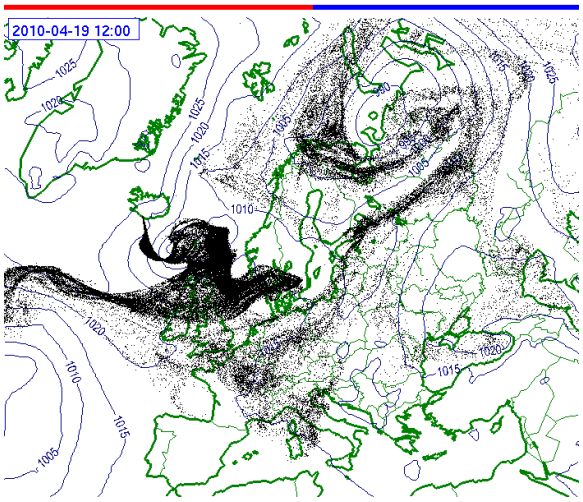
2010-04-19 12:00

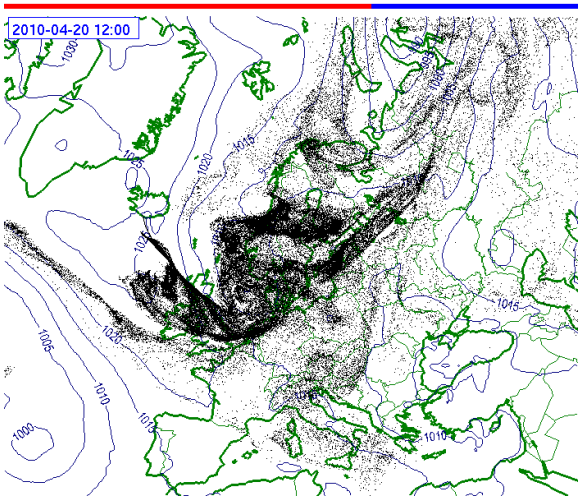
2010-04-20 12:00

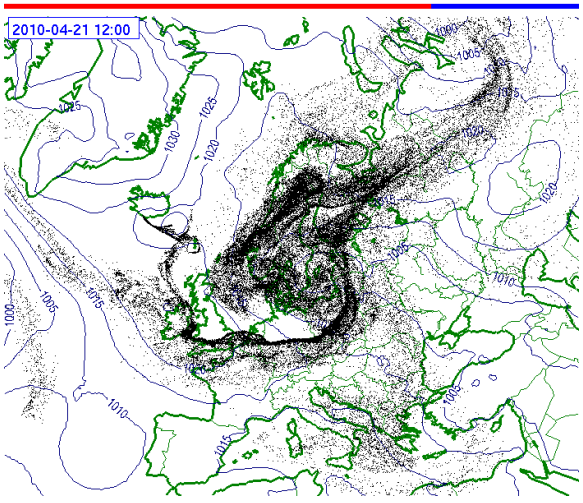
2010-04-21 12:00

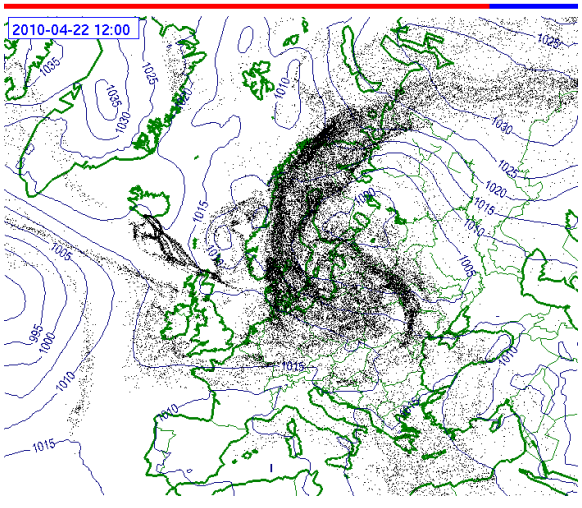
2010-04-22 12:00

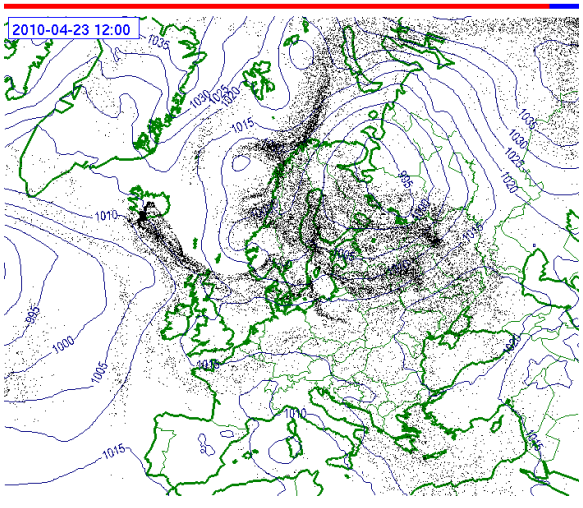
2010-04-23 12:00

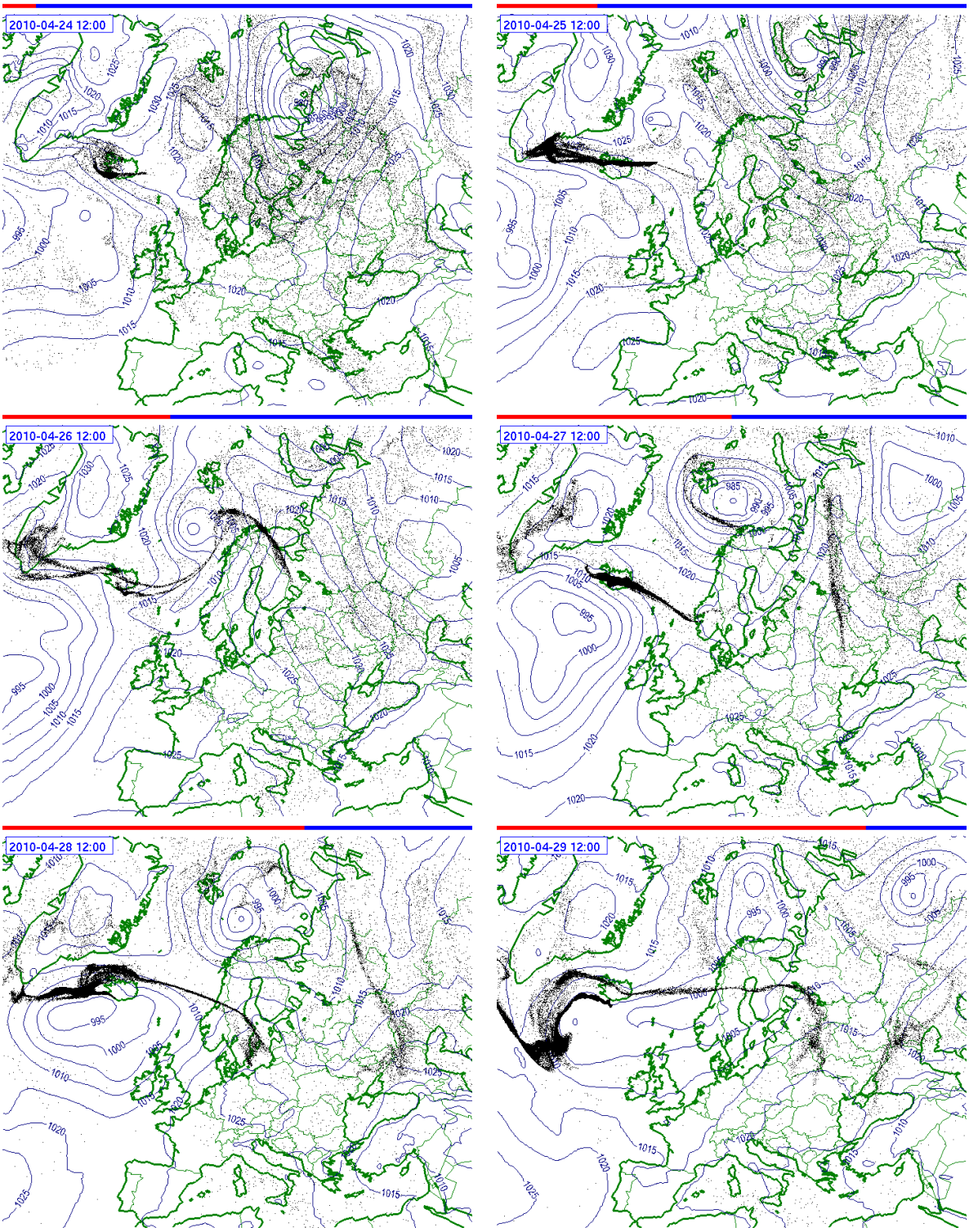
2010-04-24 12:00
2010-04-25 12:00
2010-04-26 12:00
2010-04-27 12:00
2010-04-28 12:00
2010-04-29 12:00

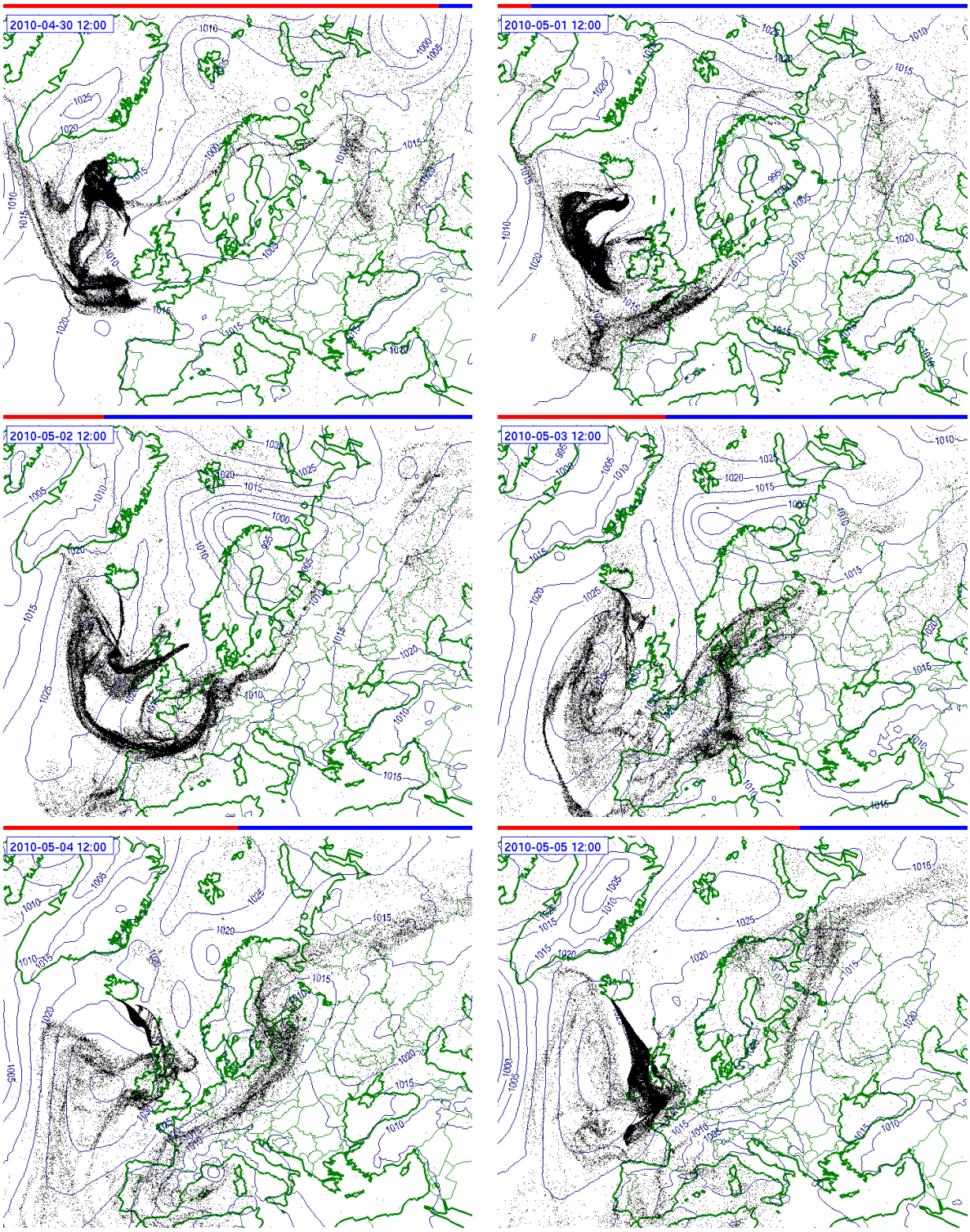
2010-04-30 12:00
2010-05-01 12:00
2010-05-02 12:00
2010-05-03 12:00
2010-05-04 12:00
2010-05-05 12:00

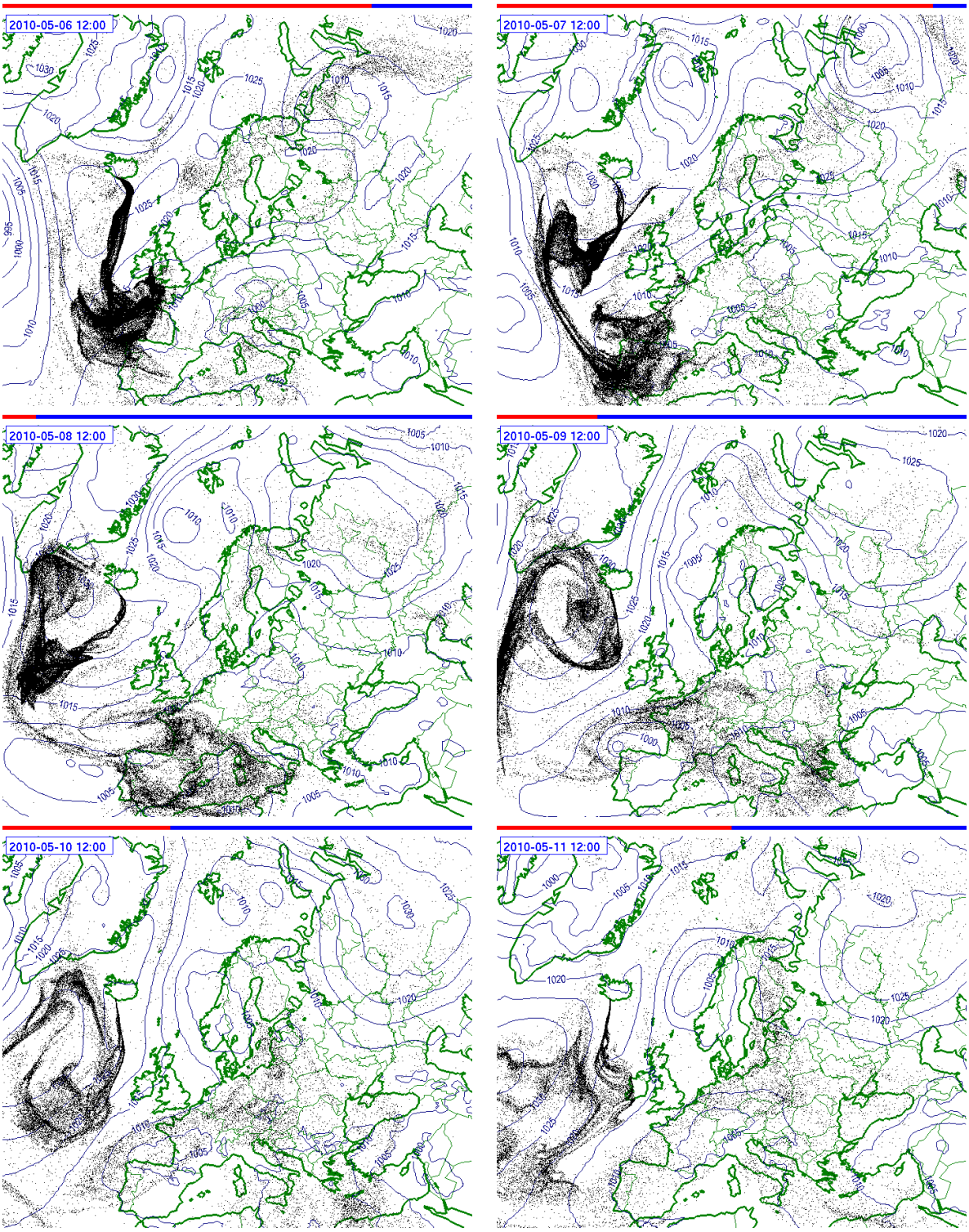
2010-05-06 12:00
2010-05-07 12:00
2010-05-08 12:00
2010-05-09 12:00
2010-05-10 12:00
2010-05-11 12:00

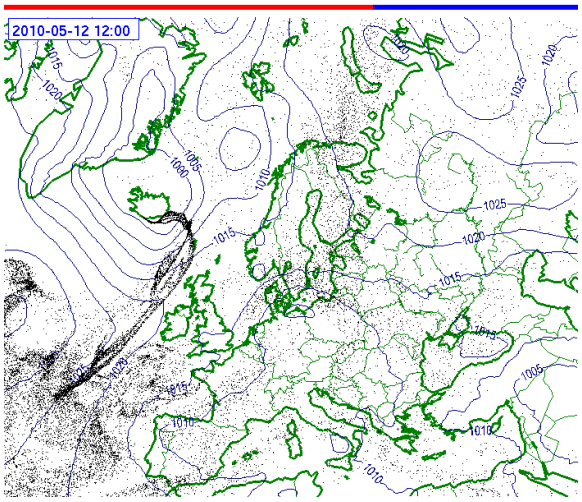
2010-05-12 12:00

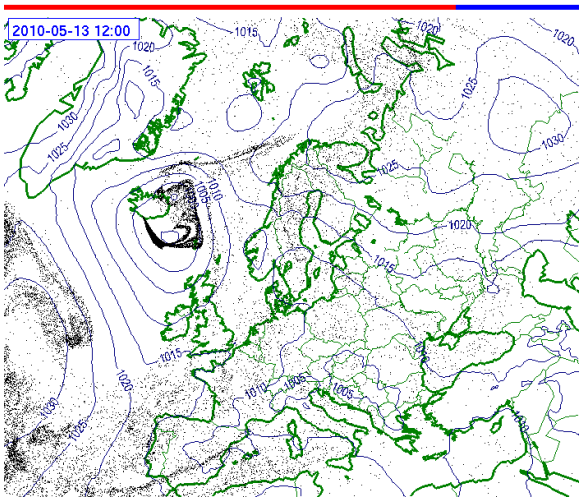
2010-05-13 12:00

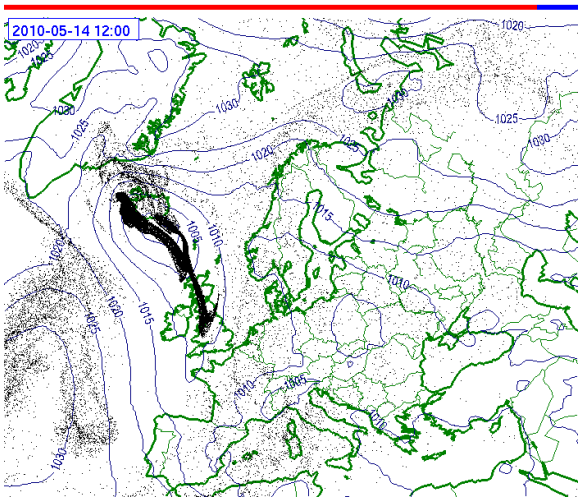
2010-05-14 12:00

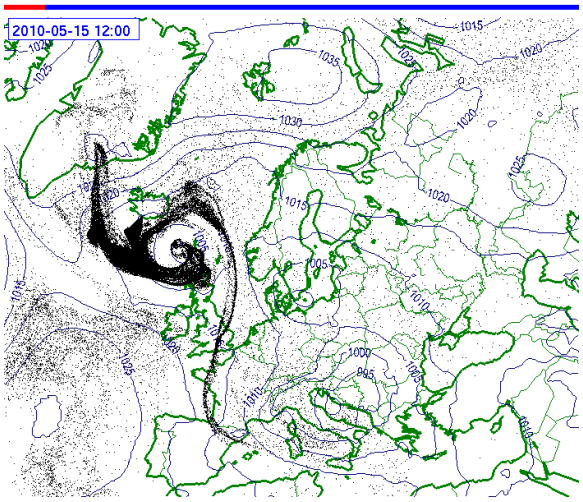
2010-05-15 12:00

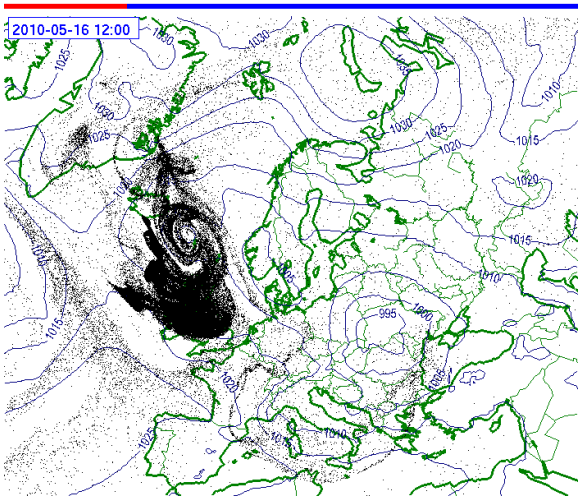
2010-05-16 12:00

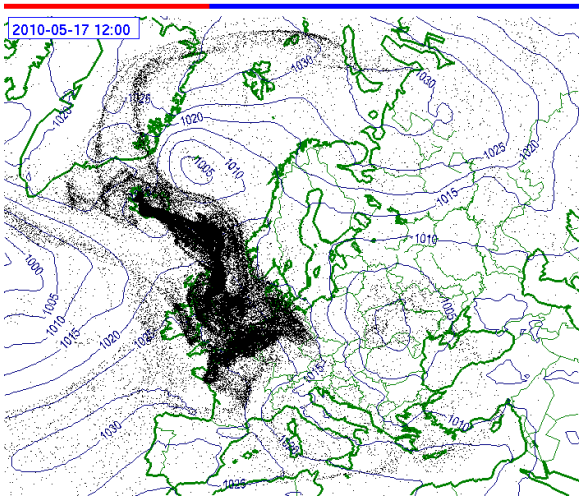
2010-05-17 12:00

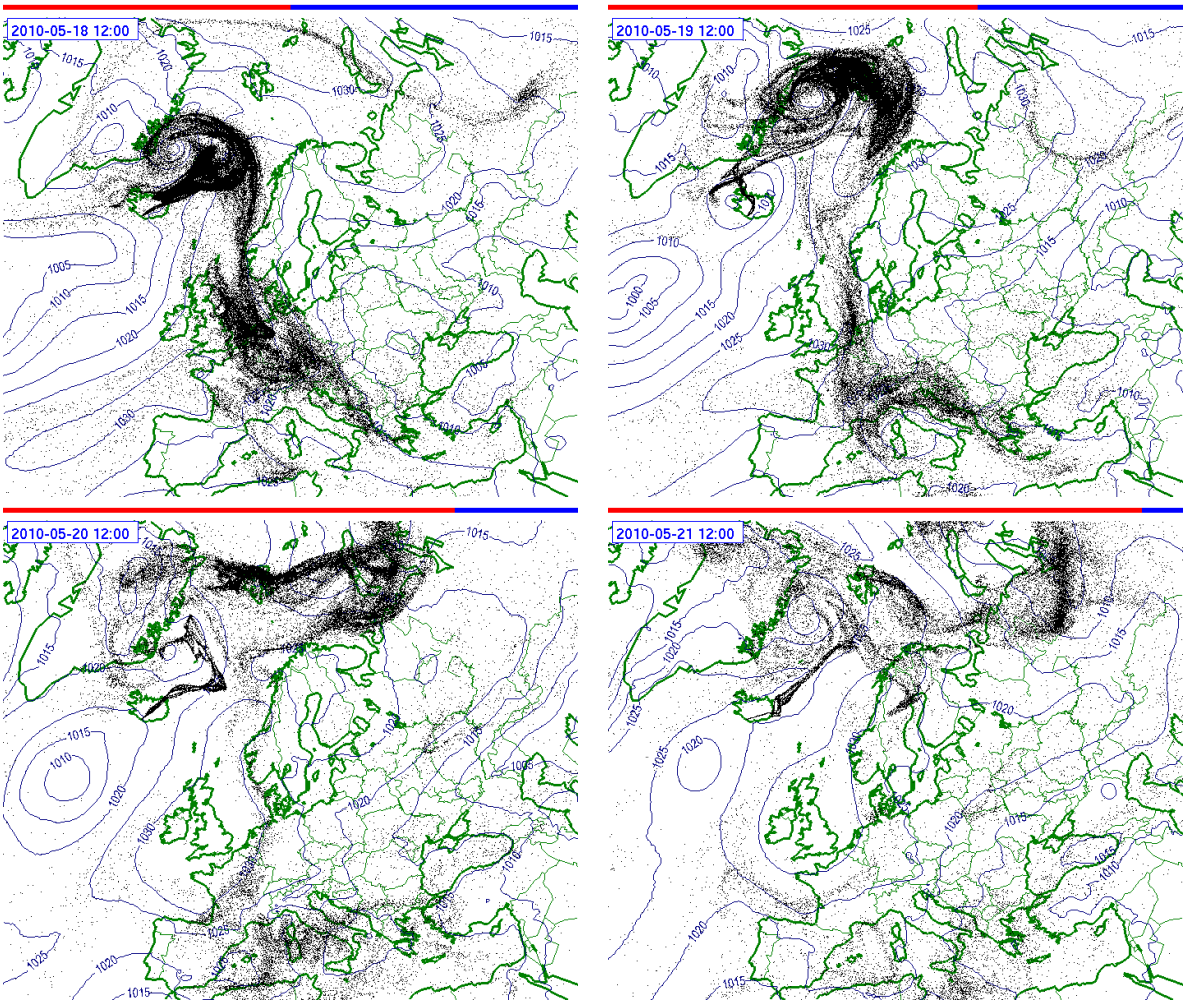
2010-05-18 12:00
2010-05-19 12:00
2010-05-20 12:00
2010-05-21 12:00

C SNAP Results: - Air Concentrations and Atmospheric Column

In this Appendix, we present the results of the operational SNAP version for every six hours, for the 10 days period of the simulation: 14.04-2010 - 24.05.2010. The results are shown as average concentration maps compatible with VAAC maps for the layers: SFC/FL200, FL200/FL350, FL350/FL550 (mg m^{-3}) and as maps of atmospheric column (g m^{-2}).

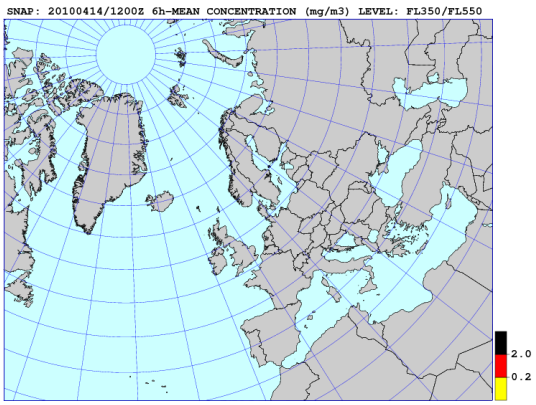
SNAP: 20100414/1200Z 6h-MEAN CONCENTRATION (mg/m3) LEVEL: FL350/FL550
2.0
0.2

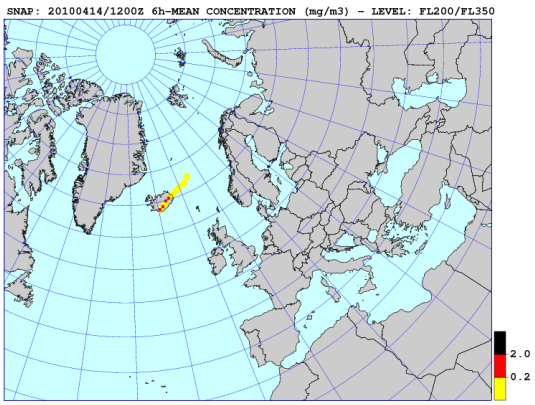
SNAP: 20100414/1200Z 6h-MEAN CONCENTRATION (mg/m3) - LEVEL: FL200/FL350
2.0
0.2

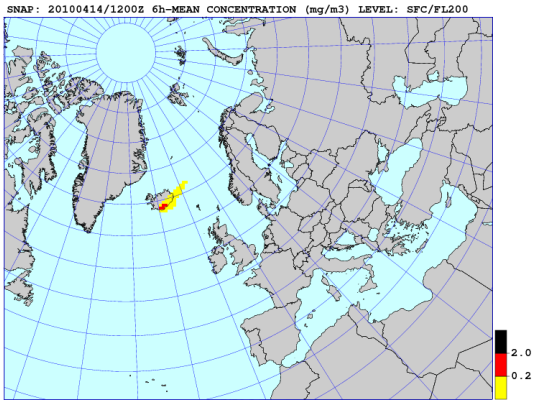
SNAP: 20100414/1200Z 6h-MEAN CONCENTRATION (mg/m3) LEVEL: SFC/FL200
2.0
0.2

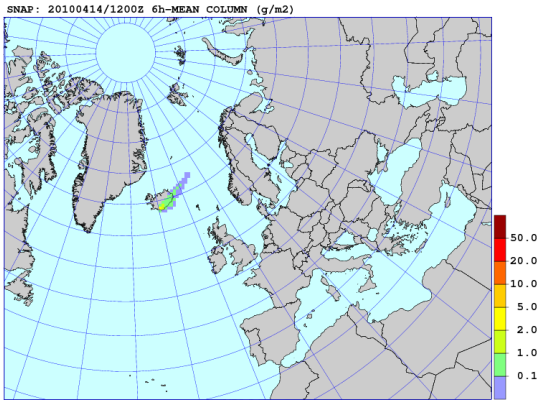
SNAP: 20100414/1200Z 6h-MEAN COLUMN (g/m2)
50.0
20.0
10.0
5.0
2.0
1.0
0.1

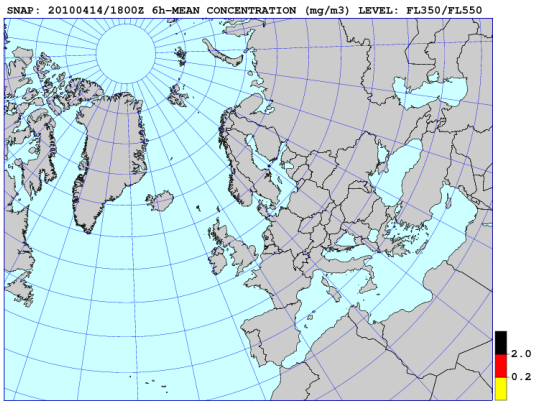
SNAP: 20100414/1800Z 6h-MEAN CONCENTRATION (mg/m3) LEVEL: FL350/FL550
2.0
0.2

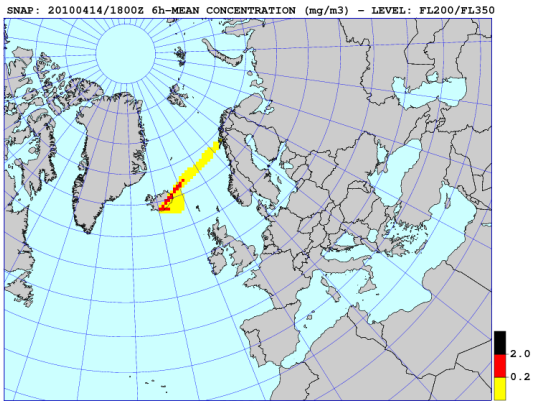
SNAP: 20100414/1800Z 6h-MEAN CONCENTRATION (mg/m3) - LEVEL: FL200/FL350
2.0
0.2

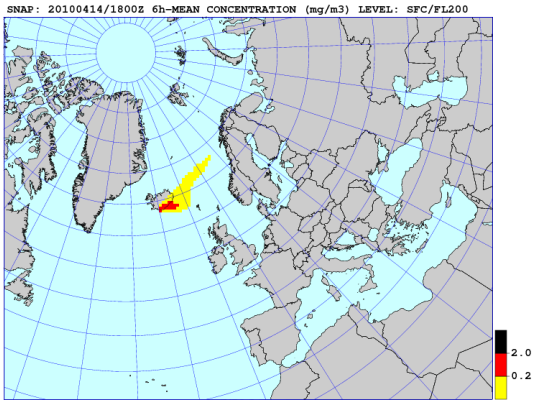
SNAP: 20100414/1800Z 6h-MEAN CONCENTRATION (mg/m3) LEVEL: SFC/FL200
2.0
0.2

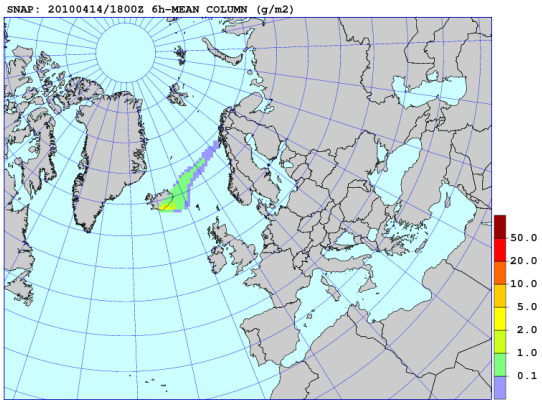
SNAP: 20100414/1800Z 6h-MEAN COLUMN (g/m2)
50.0
20.0
10.0
5.0
2.0
1.0
0.1

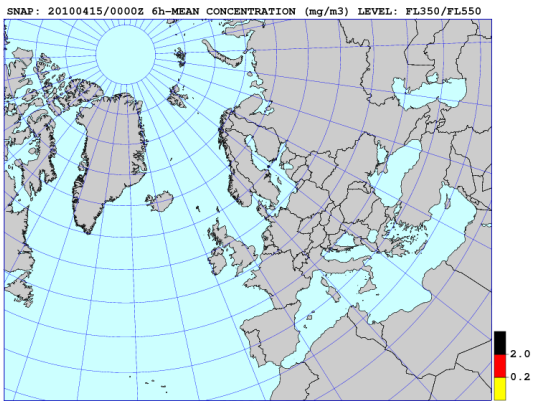
SNAP: 20100415/0000Z 6h-MEAN CONCENTRATION (mg/m3) LEVEL: FL350/FL550
2.0
0.2

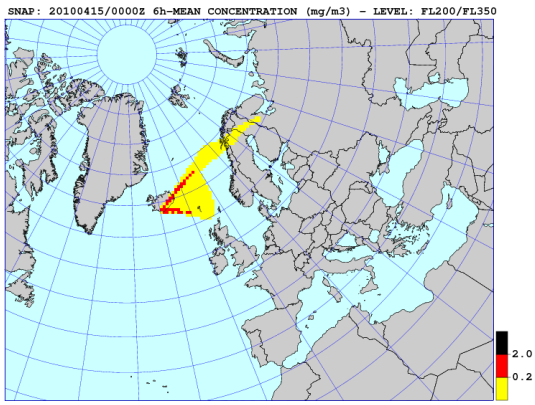
SNAP: 20100415/0000Z 6h-MEAN CONCENTRATION (mg/m3) - LEVEL: FL200/FL350
2.0
0.2

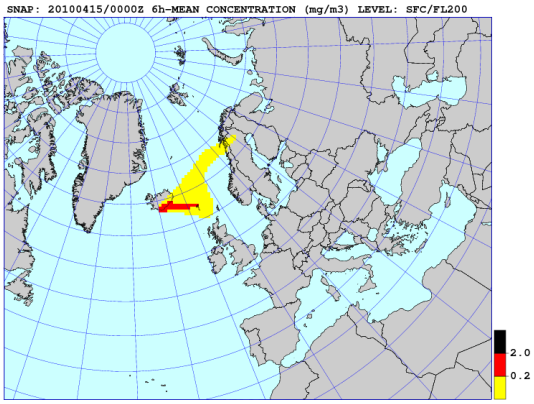
SNAP: 20100415/0000Z 6h-MEAN CONCENTRATION (mg/m3) LEVEL: SFC/FL200
2.0
0.2

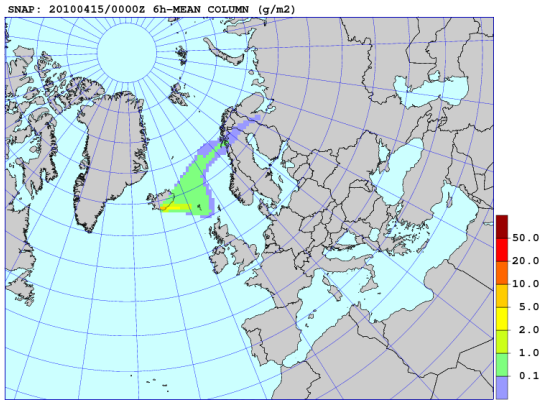
SNAP: 20100415/0000Z 6h-MEAN COLUMN (g/m2)
50.0
20.0
10.0
5.0
2.0
1.0
0.1

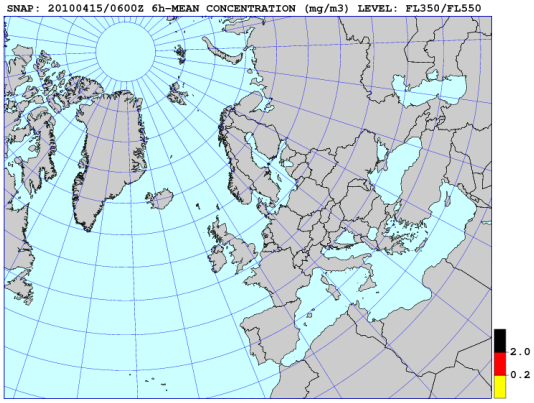
SNAP: 20100415/0600Z 6h-MEAN CONCENTRATION (mg/m3) LEVEL: FL350/FL550
2.0
0.2

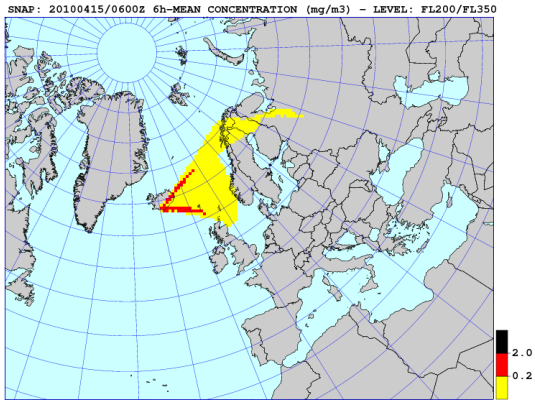
SNAP: 20100415/0600Z 6h-MEAN CONCENTRATION (mg/m3) - LEVEL: FL200/FL350
2.0
0.2

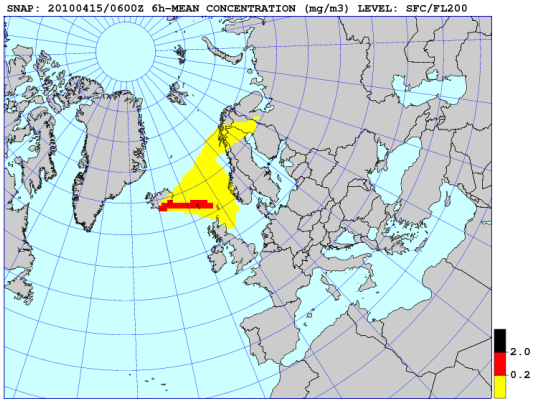
SNAP: 20100415/0600Z 6h-MEAN CONCENTRATION (mg/m3) LEVEL: SFC/FL200
2.0
0.2

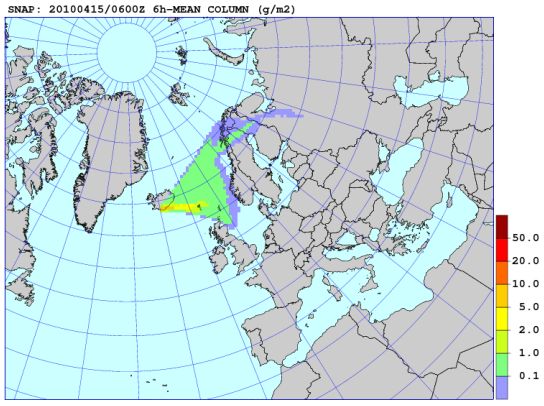
SNAP: 20100415/0600Z 6h-MEAN COLUMN (g/m2)
50.0
20.0
10.0
5.0
2.0
1.0
0.1

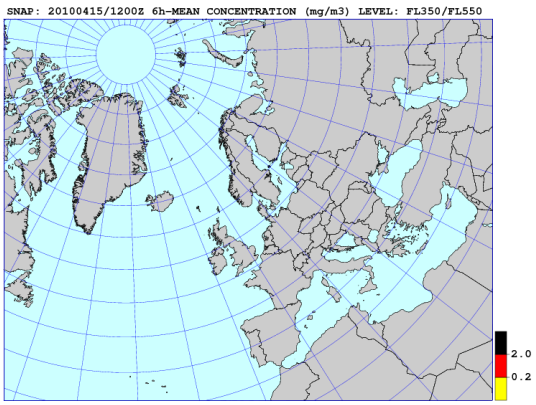
SNAP: 20100415/1200Z 6h-MEAN CONCENTRATION (mg/m3) LEVEL: FL350/FL550
2.0
0.2

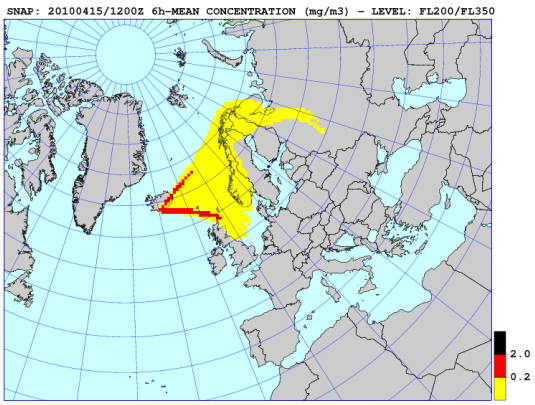
SNAP: 20100415/1200Z 6h-MEAN CONCENTRATION (mg/m3) - LEVEL: FL200/FL350
2.0
0.2

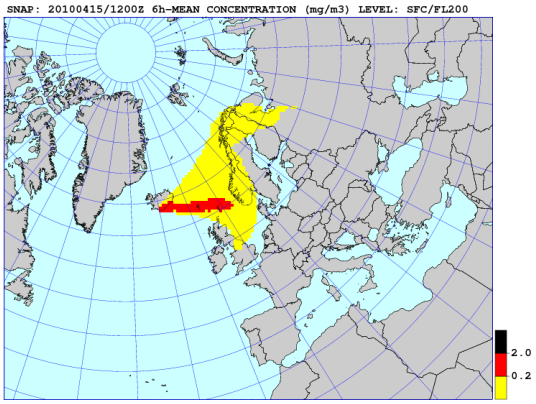
SNAP: 20100415/1200Z 6h-MEAN CONCENTRATION (mg/m3) LEVEL: SFC/FL200
2.0
0.2

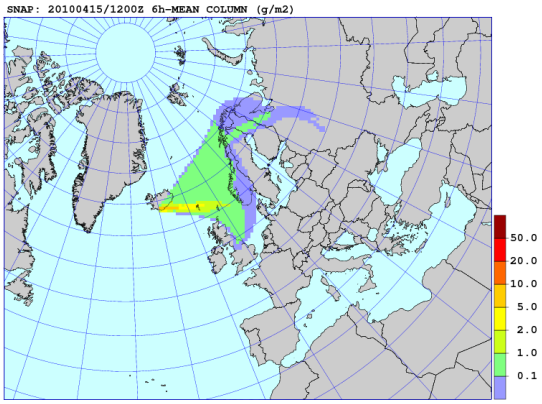
SNAP: 20100415/1200Z 6h-MEAN COLUMN (g/m2)
50.0
20.0
10.0
5.0
2.0
1.0
0.1

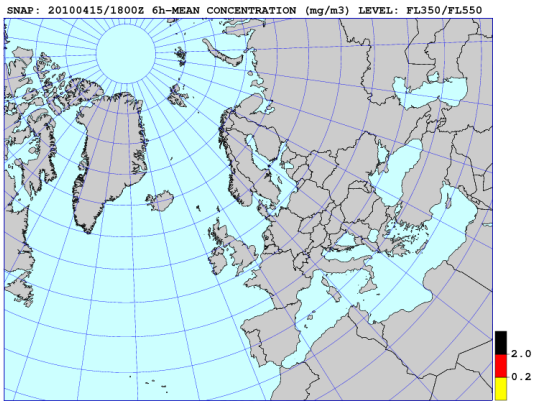
SNAP: 20100415/1800Z 6h-MEAN CONCENTRATION (mg/m3) LEVEL: FL350/FL550
2.0
0.2

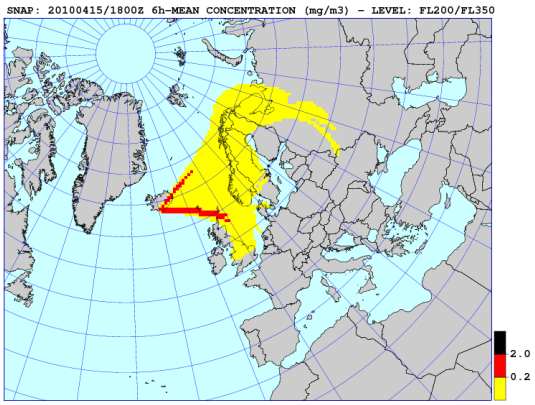
SNAP: 20100415/1800Z 6h-MEAN CONCENTRATION (mg/m3) - LEVEL: FL200/FL350
2.0
0.2

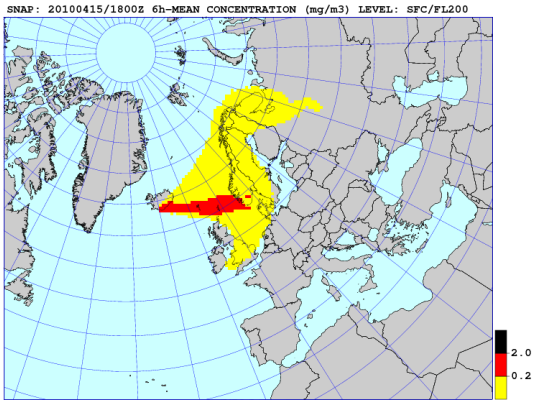
SNAP: 20100415/1800Z 6h-MEAN CONCENTRATION (mg/m3) LEVEL: SFC/FL200
2.0
0.2

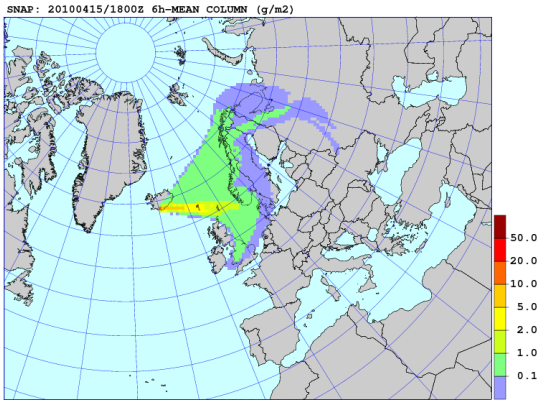
SNAP: 20100415/1800Z 6h-MEAN COLUMN (g/m2)
50.0
20.0
10.0
5.0
2.0
1.0
0.1

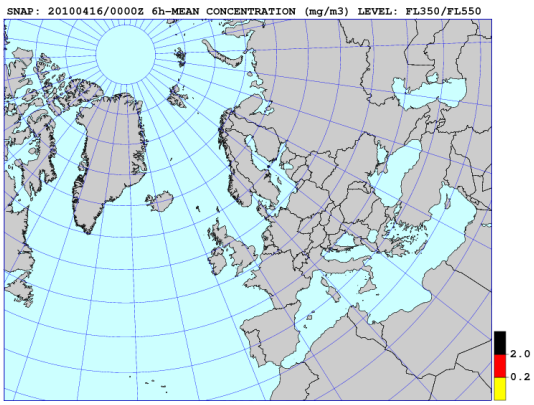
SNAP: 20100416/0000Z 6h-MEAN CONCENTRATION (mg/m3) LEVEL: FL350/FL550
2.0
0.2

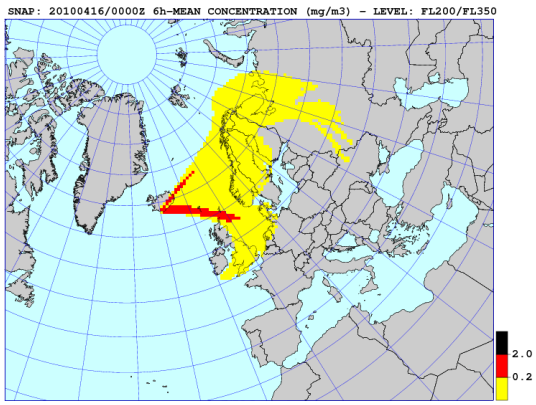
SNAP: 20100416/0000Z 6h-MEAN CONCENTRATION (mg/m3) - LEVEL: FL200/FL350
2.0
0.2

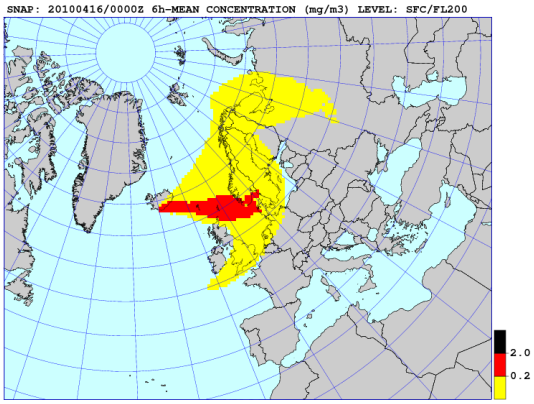
SNAP: 20100416/0000Z 6h-MEAN CONCENTRATION (mg/m3) LEVEL: SFC/FL200
2.0
0.2

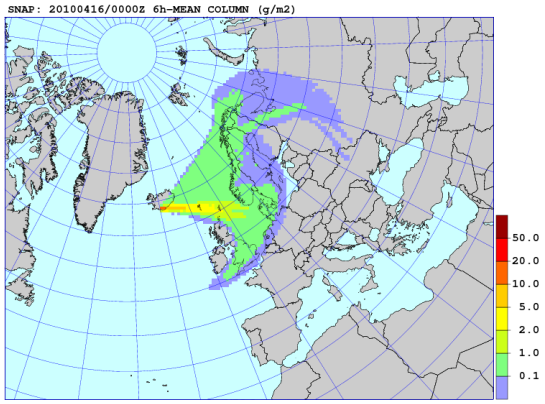
SNAP: 20100416/0000Z 6h-MEAN COLUMN (g/m2)
50.0
20.0
10.0
5.0
2.0
1.0
0.1

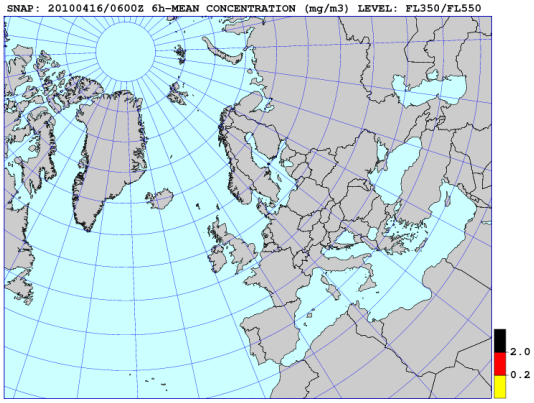
SNAP: 20100416/0600Z 6h-MEAN CONCENTRATION (mg/m3) LEVEL: FL350/FL550
2.0
0.2

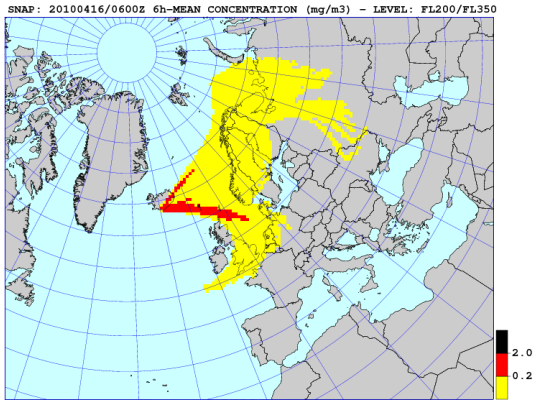
SNAP: 20100416/0600Z 6h-MEAN CONCENTRATION (mg/m3) - LEVEL: FL200/FL350
2.0
0.2

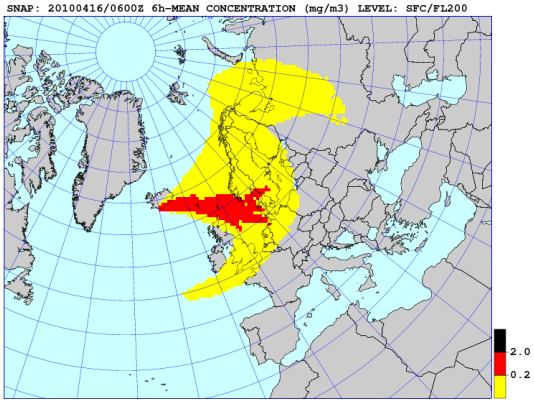
SNAP: 20100416/0600Z 6h-MEAN CONCENTRATION (mg/m3) LEVEL: SFC/FL200
2.0
0.2

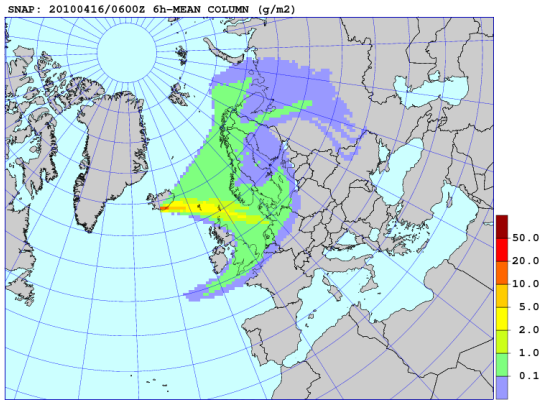
SNAP: 20100416/0600Z 6h-MEAN COLUMN (g/m2)
50.0
20.0
10.0
5.0
2.0
1.0
0.1

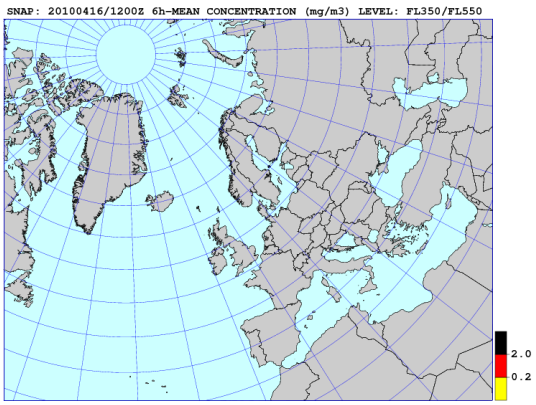
SNAP: 20100416/1200Z 6h-MEAN CONCENTRATION (mg/m3) LEVEL: FL350/FL550
2.0
0.2

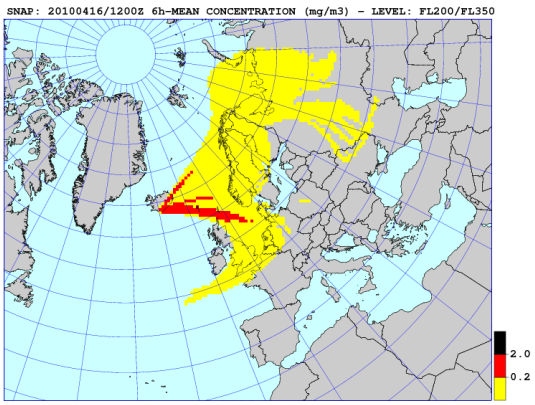
SNAP: 20100416/1200Z 6h-MEAN CONCENTRATION (mg/m3) - LEVEL: FL200/FL350
2.0
0.2

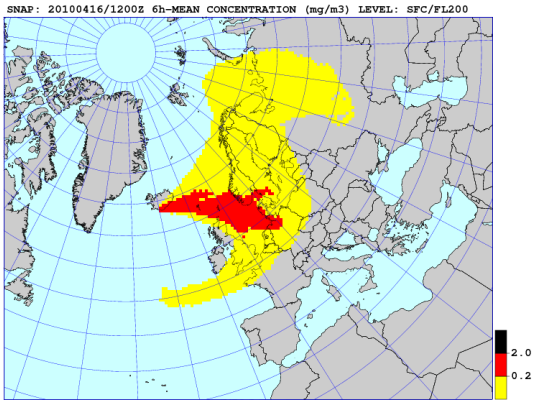
SNAP: 20100416/1200Z 6h-MEAN CONCENTRATION (mg/m3) LEVEL: SFC/FL200
2.0
0.2

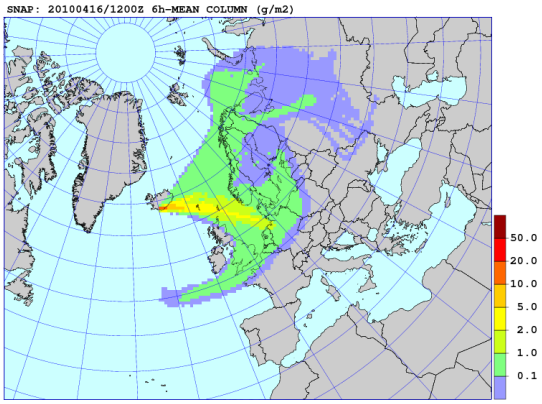
SNAP: 20100416/1200Z 6h-MEAN COLUMN (g/m2)
50.0
20.0
10.0
5.0
2.0
1.0
0.1

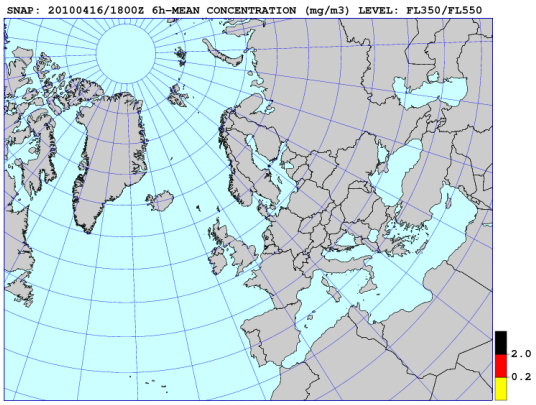
SNAP: 20100416/1800Z 6h-MEAN CONCENTRATION (mg/m3) LEVEL: FL350/FL550
2.0
0.2

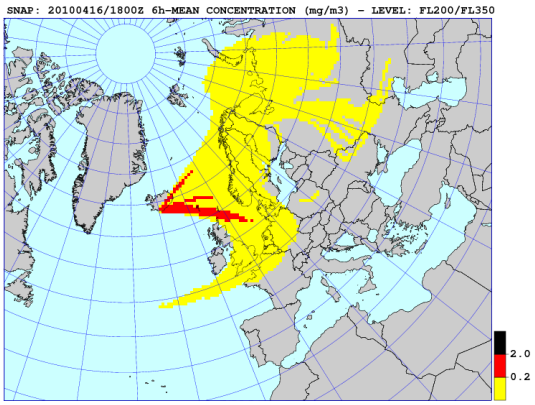
SNAP: 20100416/1800Z 6h-MEAN CONCENTRATION (mg/m3) - LEVEL: FL200/FL350
2.0
0.2

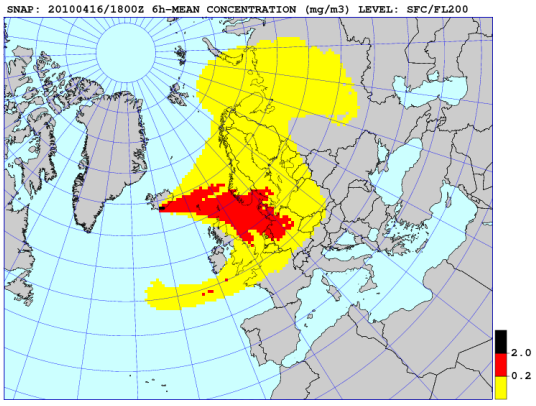
SNAP: 20100416/1800Z 6h-MEAN CONCENTRATION (mg/m3) LEVEL: SFC/FL200
2.0
0.2

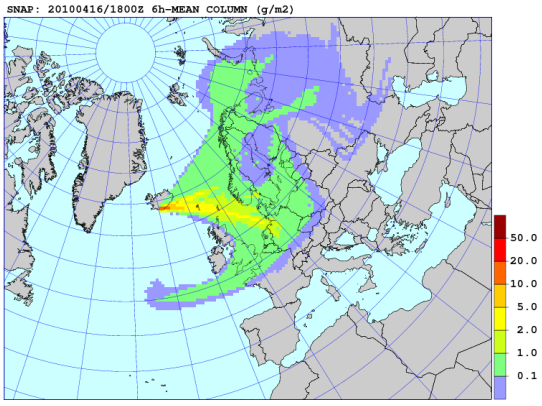
SNAP: 20100416/1800Z 6h-MEAN COLUMN (g/m2)
50.0
20.0
10.0
5.0
2.0
1.0
0.1

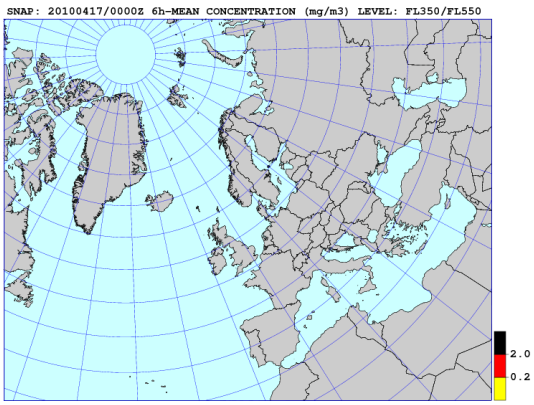
SNAP: 20100417/0000Z 6h-MEAN CONCENTRATION (mg/m3) LEVEL: FL350/FL550
2.0
0.2

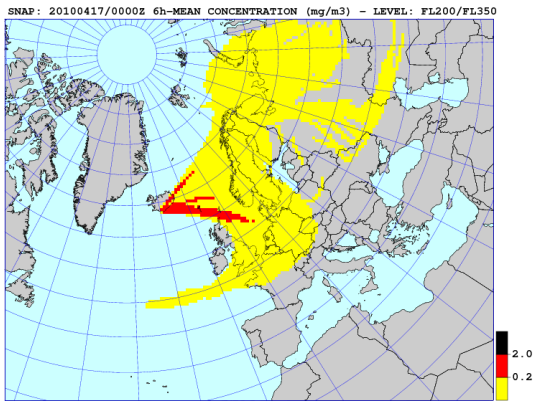
SNAP: 20100417/0000Z 6h-MEAN CONCENTRATION (mg/m3) - LEVEL: FL200/FL350
2.0
0.2

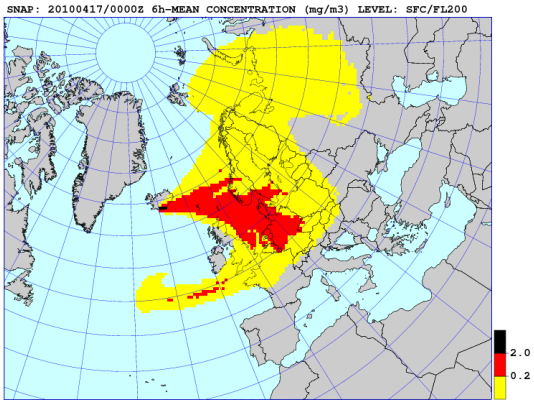
SNAP: 20100417/0000Z 6h-MEAN CONCENTRATION (mg/m3) LEVEL: SFC/FL200
2.0
0.2

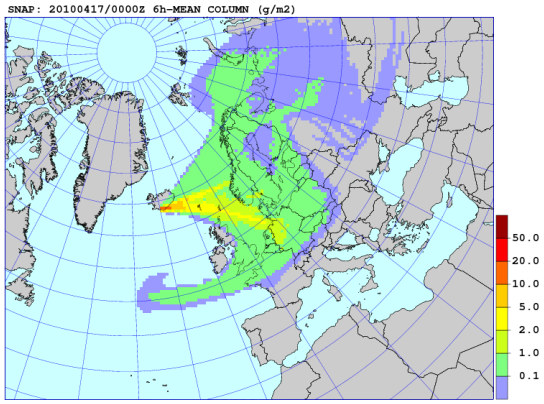
SNAP: 20100417/0000Z 6h-MEAN COLUMN (g/m2)
50.0
20.0
10.0
5.0
2.0
1.0
0.1

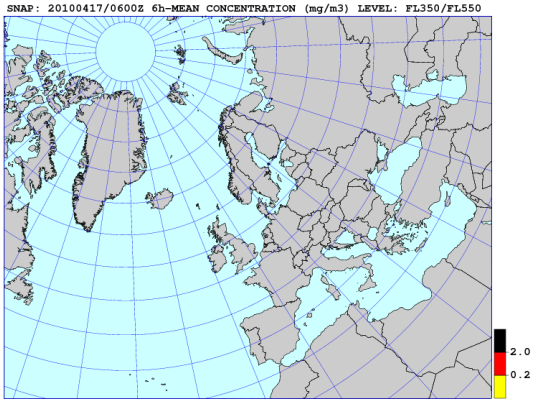
SNAP: 20100417/0600Z 6h-MEAN CONCENTRATION (mg/m3) LEVEL: FL350/FL550
2.0
0.2

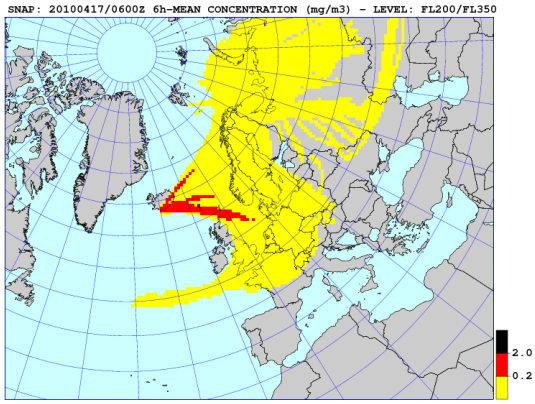
SNAP: 20100417/0600Z 6h-MEAN CONCENTRATION (mg/m3) - LEVEL: FL200/FL350
2.0
0.2

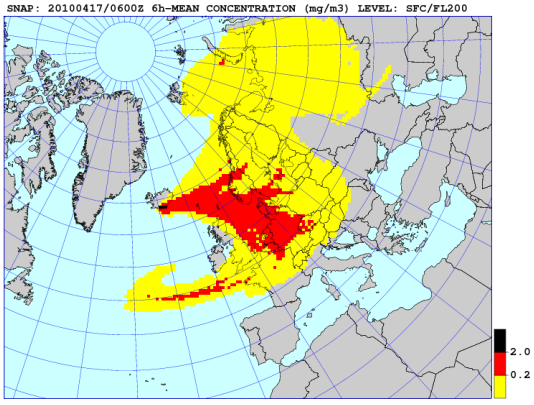
SNAP: 20100417/0600Z 6h-MEAN CONCENTRATION (mg/m3) LEVEL: SFC/FL200
2.0
0.2

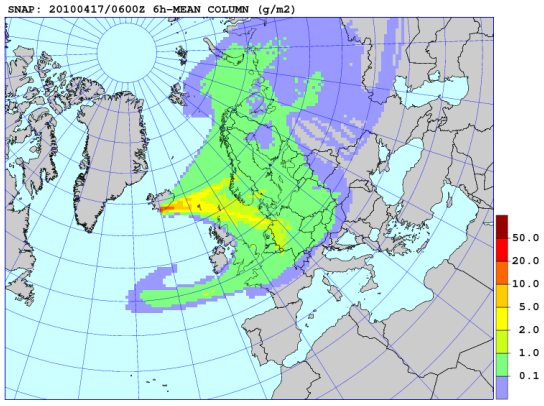
SNAP: 20100417/0600Z 6h-MEAN COLUMN (g/m2)
50.0
20.0
10.0
5.0
2.0
1.0
0.1

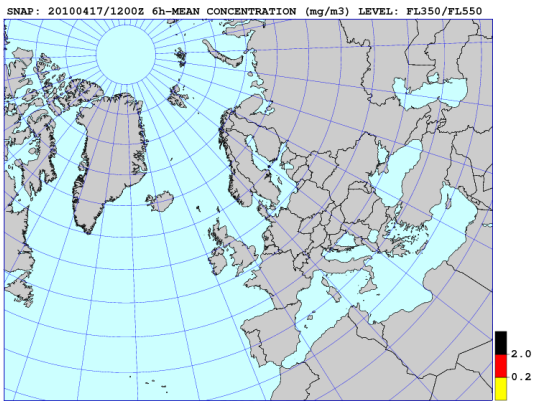
SNAP: 20100417/1200Z 6h-MEAN CONCENTRATION (mg/m3) LEVEL: FL350/FL550
2.0
0.2

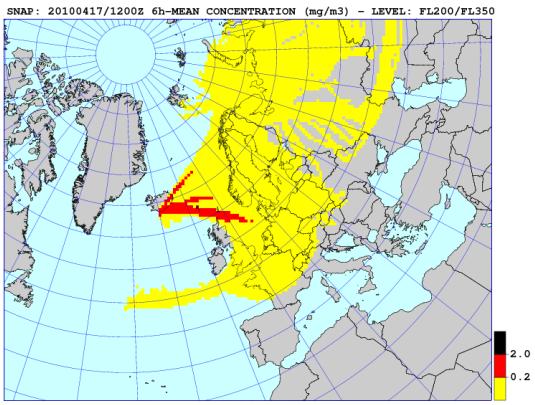
SNAP: 20100417/1200Z 6h-MEAN CONCENTRATION (mg/m3) - LEVEL: FL200/FL350
2.0
0.2

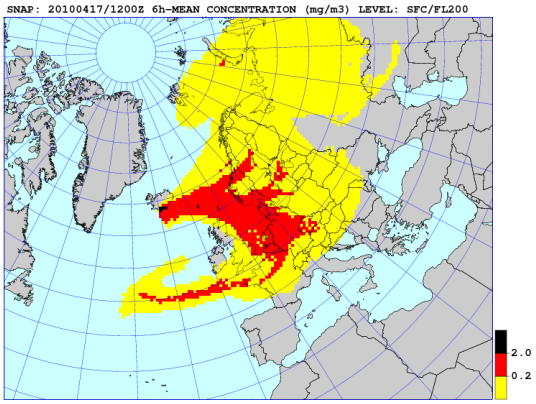
SNAP: 20100417/1200Z 6h-MEAN CONCENTRATION (mg/m3) LEVEL: SFC/FL200
2.0
0.2

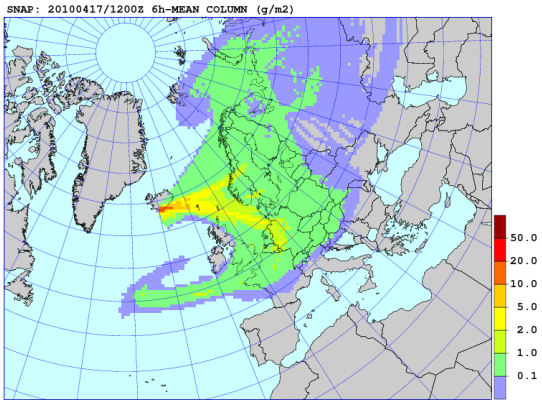
SNAP: 20100417/1200Z 6h-MEAN COLUMN (g/m2)
50.0
20.0
10.0
5.0
2.0
1.0
0.1

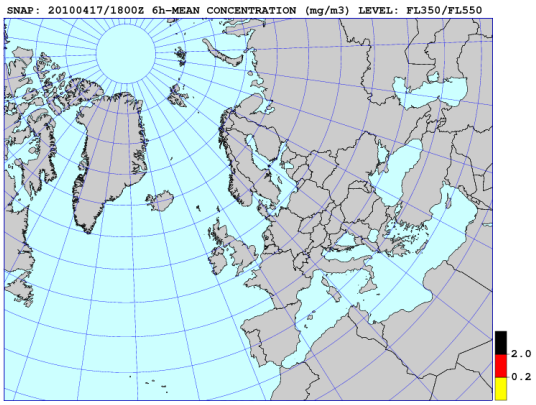
SNAP: 20100417/1800Z 6h-MEAN CONCENTRATION (mg/m3) LEVEL: FL350/FL550
2.0
0.2

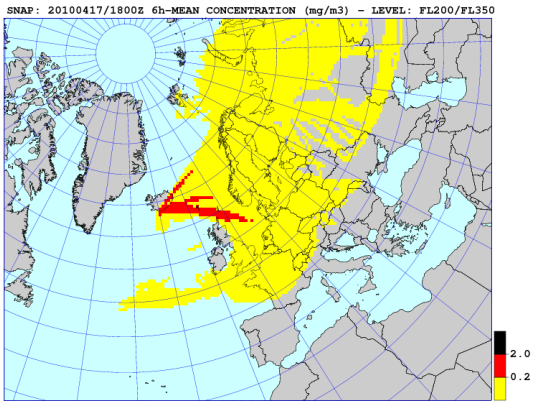
SNAP: 20100417/1800Z 6h-MEAN CONCENTRATION (mg/m3) - LEVEL: FL200/FL350
2.0
0.2

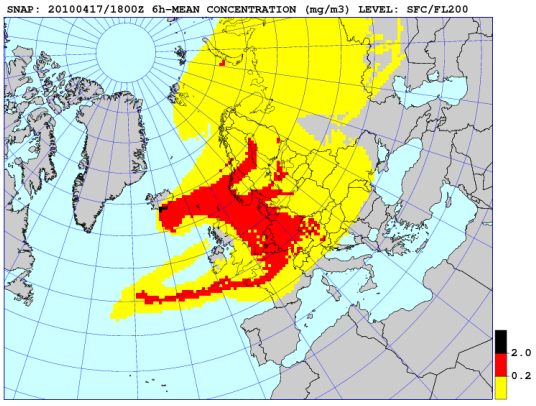
SNAP: 20100417/1800Z 6h-MEAN CONCENTRATION (mg/m3) LEVEL: SFC/FL200
2.0
0.2

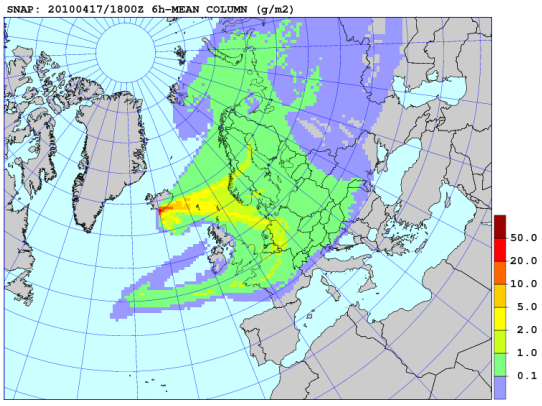
SNAP: 20100417/1800Z 6h-MEAN COLUMN (g/m2)
50.0
20.0
10.0
5.0
2.0
1.0
0.1

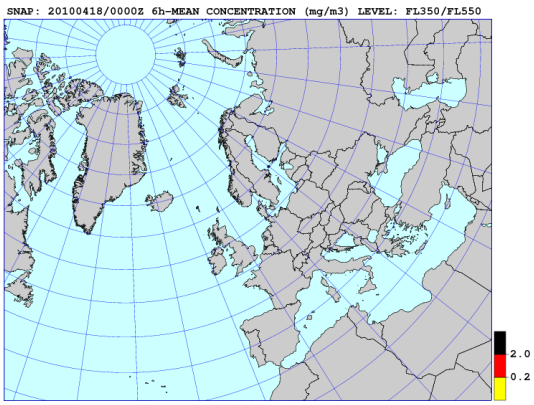
SNAP: 20100418/0000Z 6h-MEAN CONCENTRATION (mg/m3) LEVEL: FL350/FL550
2.0
0.2

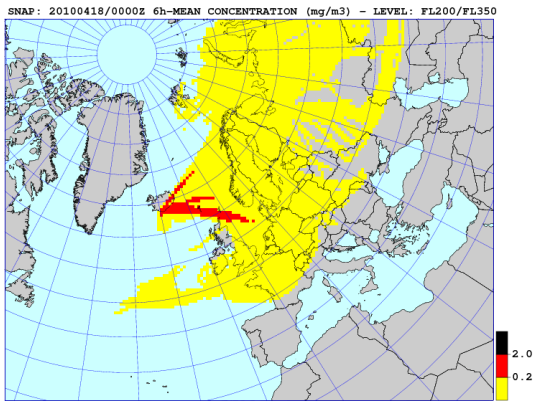
SNAP: 20100418/0000Z 6h-MEAN CONCENTRATION (mg/m3) - LEVEL: FL200/FL350
2.0
0.2

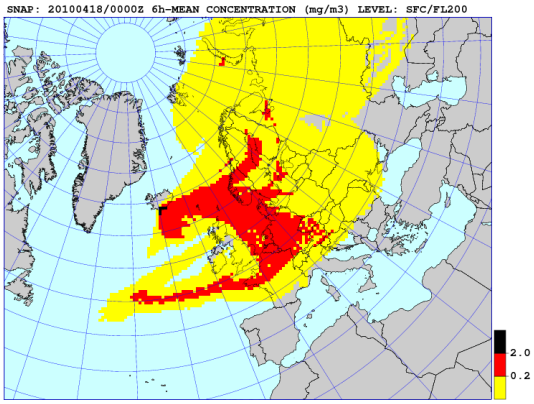
SNAP: 20100418/0000Z 6h-MEAN CONCENTRATION (mg/m3) LEVEL: SFC/FL200
2.0
0.2

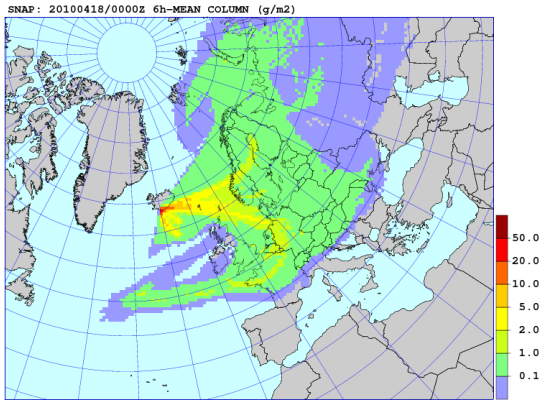
SNAP: 20100418/0000Z 6h-MEAN COLUMN (g/m2)
50.0
20.0
10.0
5.0
2.0
1.0
0.1

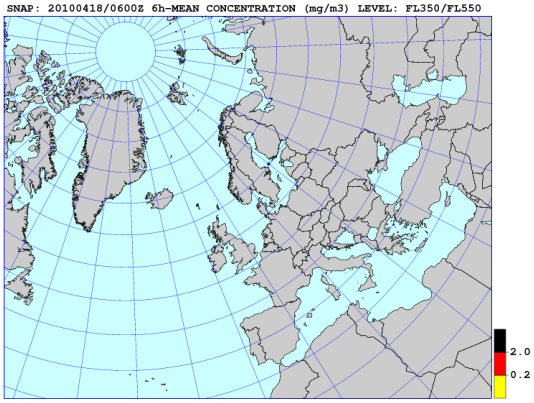
SNAP: 20100418/0600Z 6h-MEAN CONCENTRATION (mg/m3) LEVEL: FL350/FL550
2.0
0.2

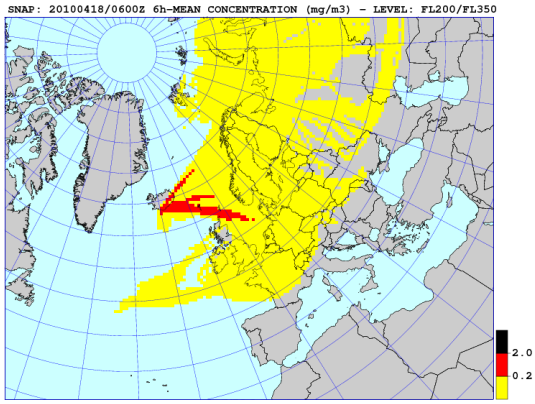
SNAP: 20100418/0600Z 6h-MEAN CONCENTRATION (mg/m3) - LEVEL: FL200/FL350
2.0
0.2

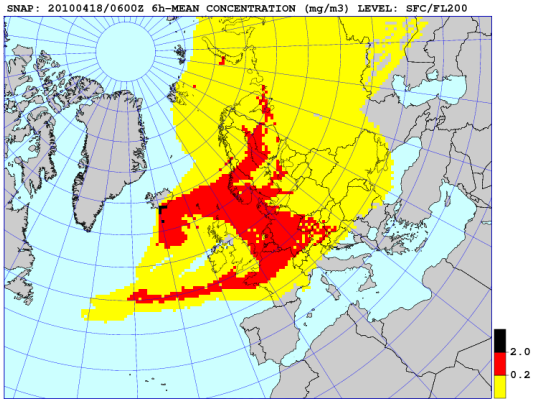
SNAP: 20100418/0600Z 6h-MEAN CONCENTRATION (mg/m3) LEVEL: SFC/FL200
2.0
0.2

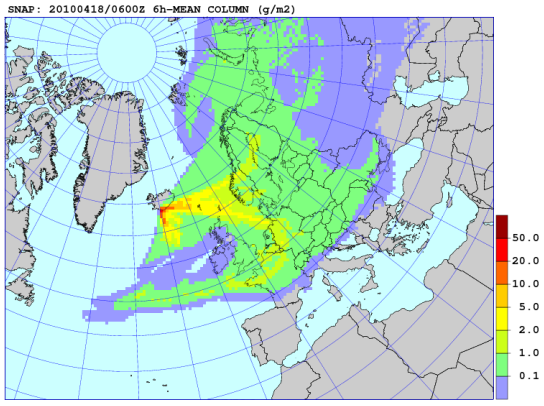
SNAP: 20100418/0600Z 6h-MEAN COLUMN (g/m2)
50.0
20.0
10.0
5.0
2.0
1.0
0.1

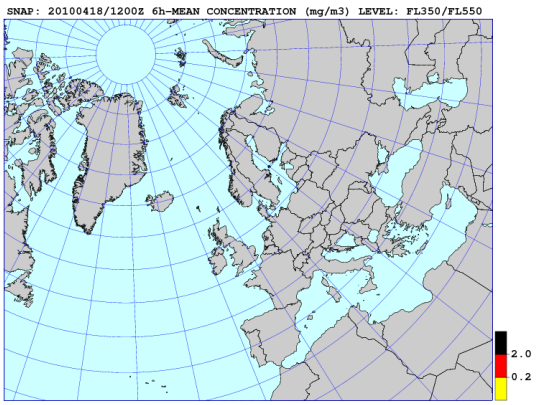
SNAP: 20100418/1200Z 6h-MEAN CONCENTRATION (mg/m3) LEVEL: FL350/FL550
2.0
0.2

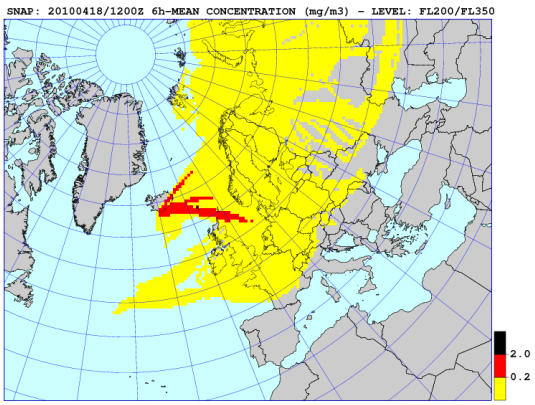
SNAP: 20100418/1200Z 6h-MEAN CONCENTRATION (mg/m3) - LEVEL: FL200/FL350
2.0
0.2

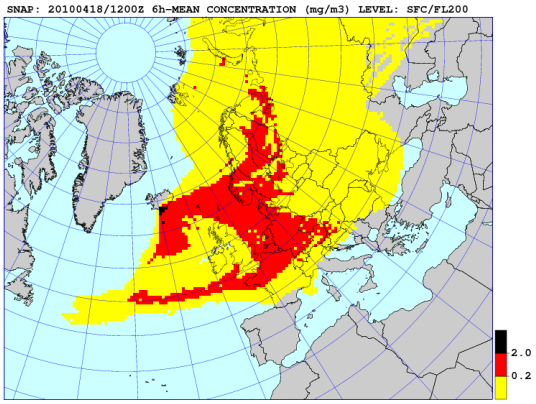
SNAP: 20100418/1200Z 6h-MEAN CONCENTRATION (mg/m3) LEVEL: SFC/FL200
2.0
0.2

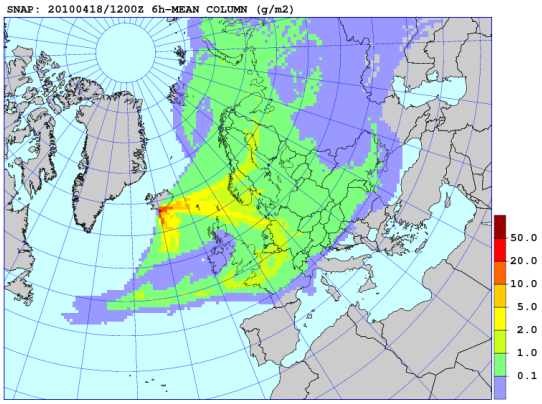
SNAP: 20100418/1200Z 6h-MEAN COLUMN (g/m2)
50.0
20.0
10.0
5.0
2.0
1.0
0.1

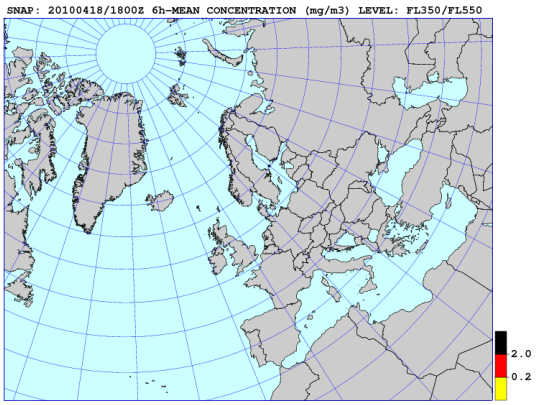
SNAP: 20100418/1800Z 6h-MEAN CONCENTRATION (mg/m3) LEVEL: FL350/FL550
2.0
0.2

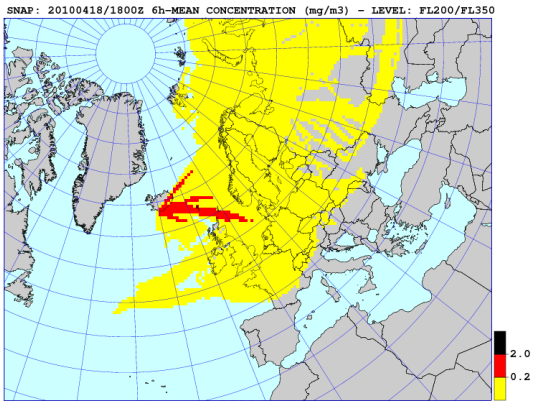
SNAP: 20100418/1800Z 6h-MEAN CONCENTRATION (mg/m3) - LEVEL: FL200/FL350
2.0
0.2

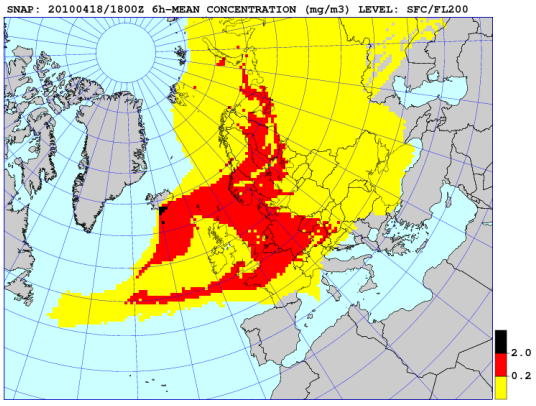
SNAP: 20100418/1800Z 6h-MEAN CONCENTRATION (mg/m3) LEVEL: SFC/FL200
2.0
0.2

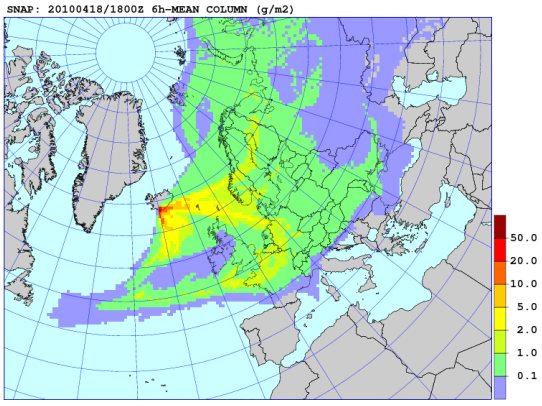
SNAP: 20100418/1800Z 6h-MEAN COLUMN (g/m2)
50.0
20.0
10.0
5.0
2.0
1.0
0.1

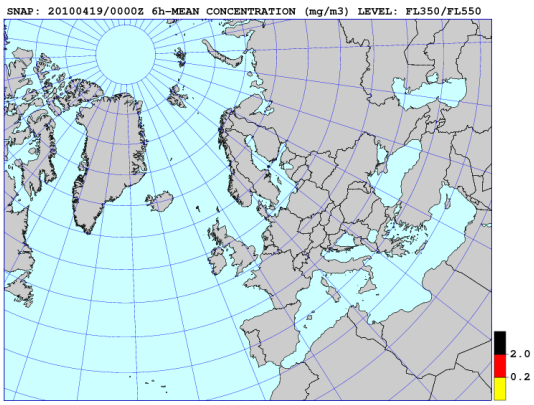
SNAP: 20100419/0000Z 6h-MEAN CONCENTRATION (mg/m3) LEVEL: FL350/FL550
2.0
0.2

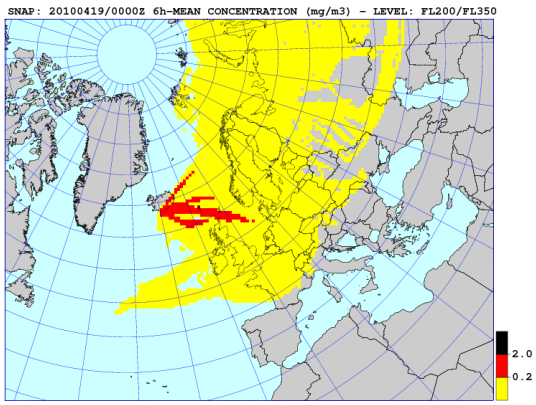
SNAP: 20100419/0000Z 6h-MEAN CONCENTRATION (mg/m3) - LEVEL: FL200/FL350
2.0
0.2

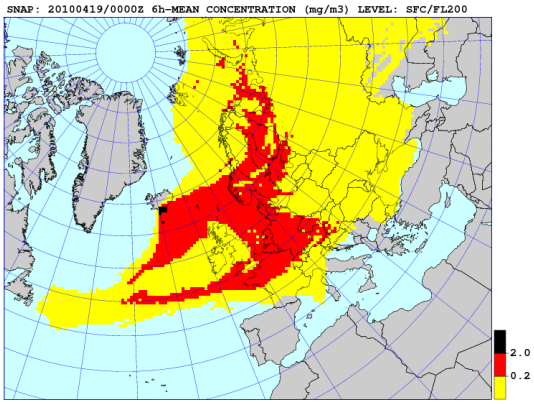
SNAP: 20100419/0000Z 6h-MEAN CONCENTRATION (mg/m3) LEVEL: SFC/FL200
2.0
0.2

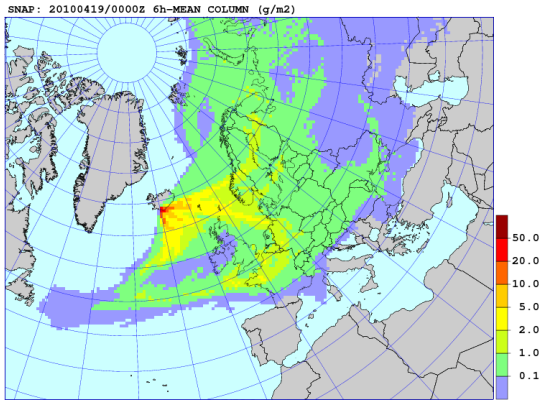
SNAP: 20100419/0000Z 6h-MEAN COLUMN (g/m2)
50.0
20.0
10.0
5.0
2.0
1.0
0.1

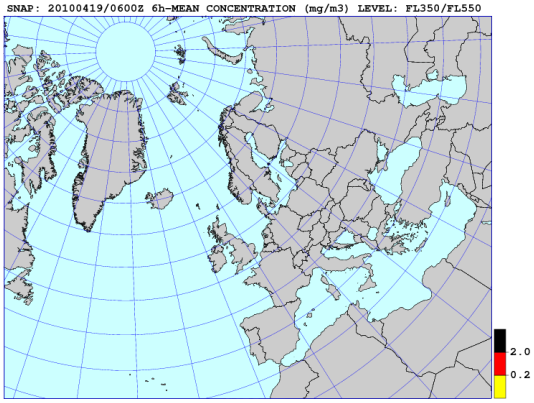
SNAP: 20100419/0600Z 6h-MEAN CONCENTRATION (mg/m3) LEVEL: FL350/FL550
2.0
0.2

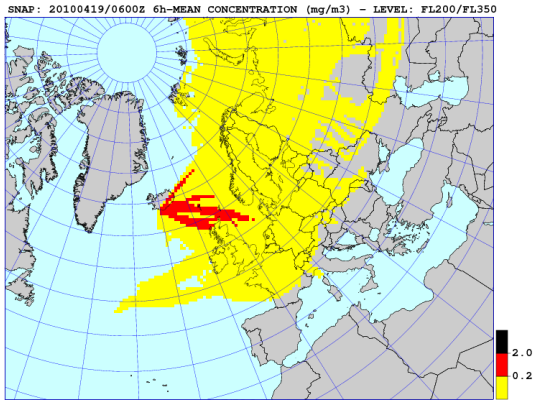
SNAP: 20100419/0600Z 6h-MEAN CONCENTRATION (mg/m3) - LEVEL: FL200/FL350
2.0
0.2

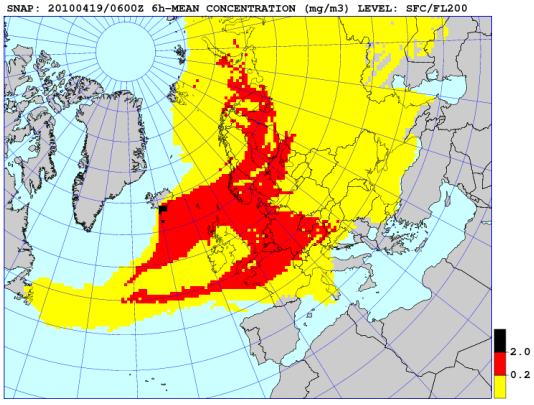
SNAP: 20100419/0600Z 6h-MEAN CONCENTRATION (mg/m3) LEVEL: SFC/FL200
2.0
0.2

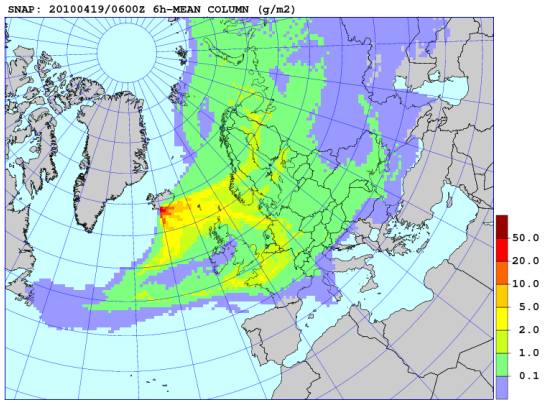
SNAP: 20100419/0600Z 6h-MEAN COLUMN (g/m2)
50.0
20.0
10.0
5.0
2.0
1.0
0.1

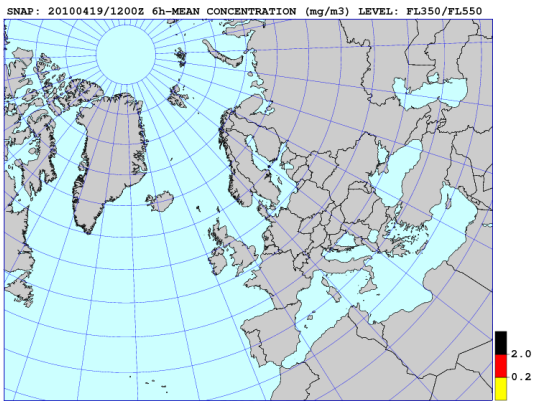
SNAP: 20100419/1200Z 6h-MEAN CONCENTRATION (mg/m3) LEVEL: FL350/FL550
2.0
0.2

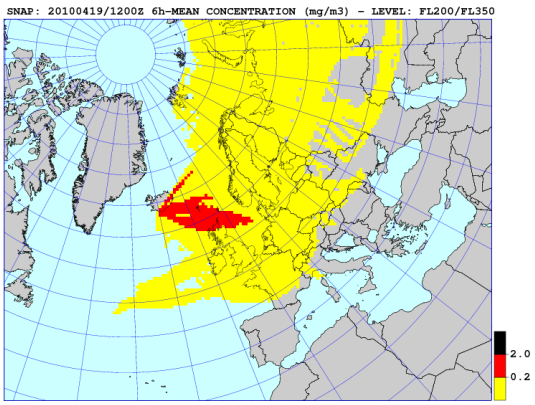
SNAP: 20100419/1200Z 6h-MEAN CONCENTRATION (mg/m3) - LEVEL: FL200/FL350
2.0
0.2

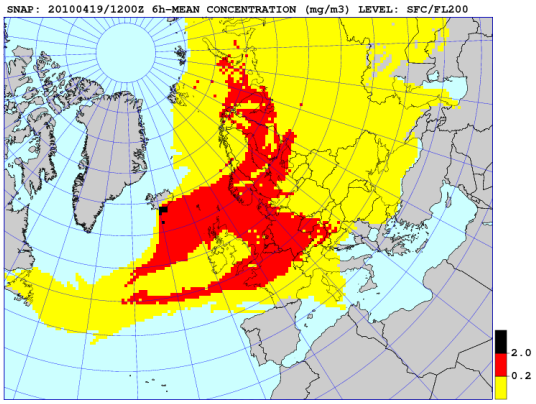
SNAP: 20100419/1200Z 6h-MEAN CONCENTRATION (mg/m3) LEVEL: SFC/FL200
2.0
0.2

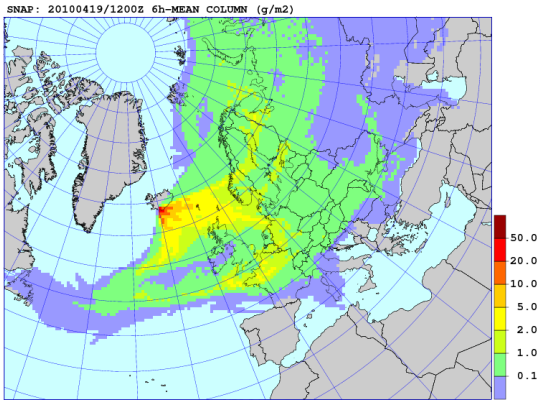
SNAP: 20100419/1200Z 6h-MEAN COLUMN (g/m2)
50.0
20.0
10.0
5.0
2.0
1.0
0.1

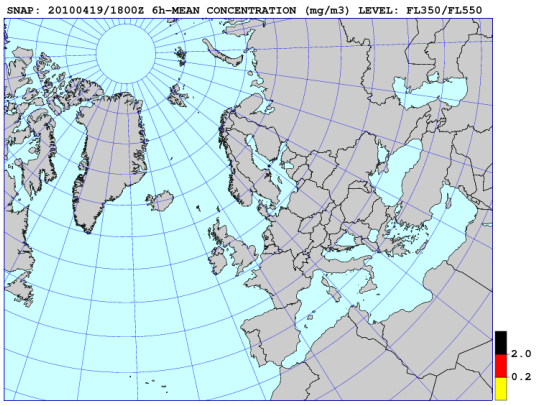
SNAP: 20100419/1800Z 6h-MEAN CONCENTRATION (mg/m3) LEVEL: FL350/FL550
2.0
0.2

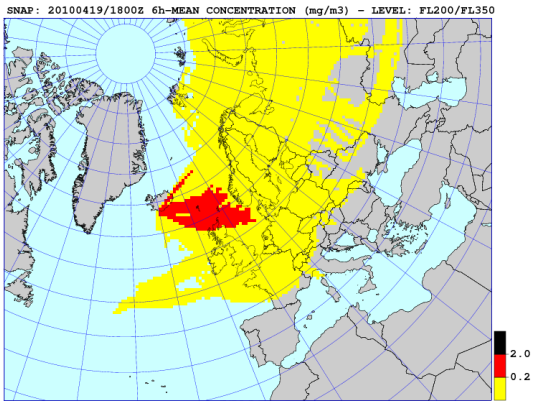
SNAP: 20100419/1800Z 6h-MEAN CONCENTRATION (mg/m3) - LEVEL: FL200/FL350
2.0
0.2

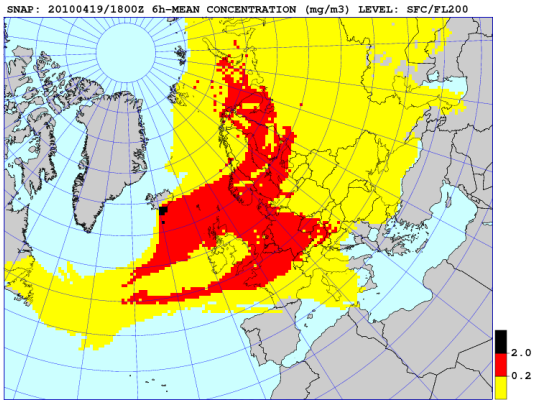
SNAP: 20100419/1800Z 6h-MEAN CONCENTRATION (mg/m3) LEVEL: SFC/FL200
2.0
0.2

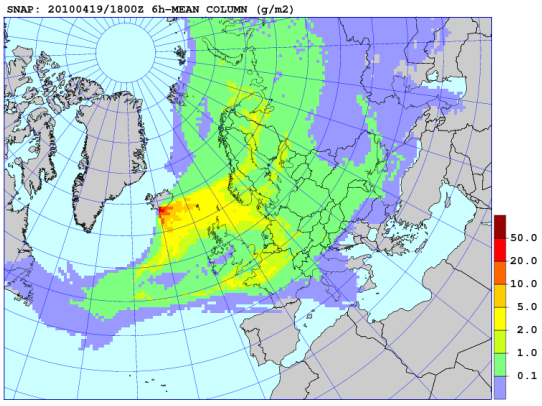
SNAP: 20100419/1800Z 6h-MEAN COLUMN (g/m2)
50.0
20.0
10.0
5.0
2.0
1.0
0.1

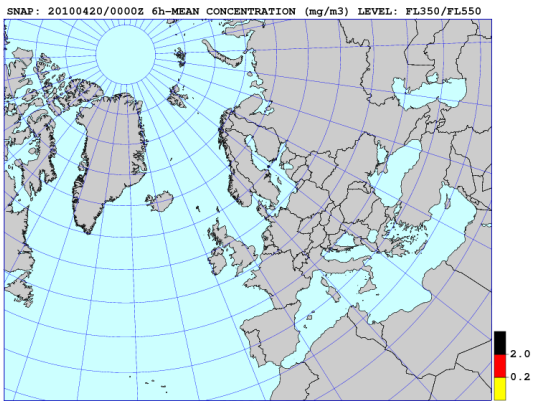
SNAP: 20100420/0000Z 6h-MEAN CONCENTRATION (mg/m3) LEVEL: FL350/FL550
2.0
0.2

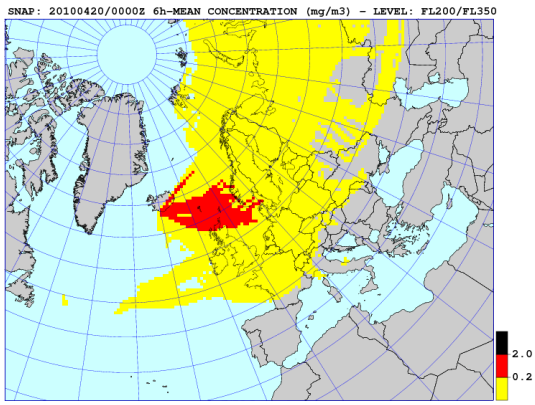
SNAP: 20100420/0000Z 6h-MEAN CONCENTRATION (mg/m3) - LEVEL: FL200/FL350
2.0
0.2

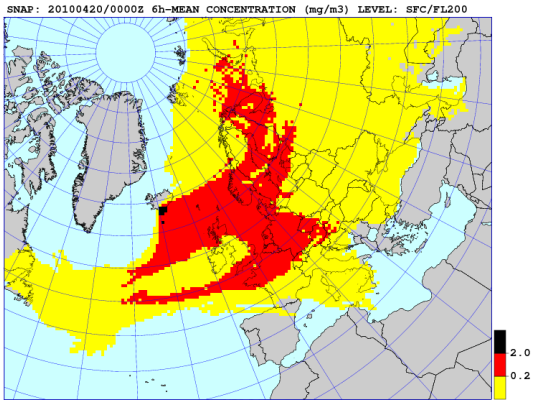
SNAP: 20100420/0000Z 6h-MEAN CONCENTRATION (mg/m3) LEVEL: SFC/FL200
2.0
0.2

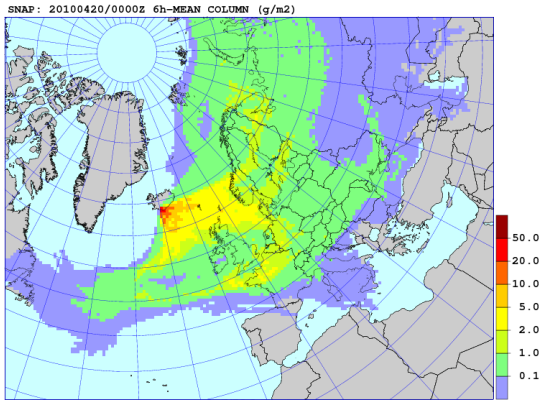
SNAP: 20100420/0000Z 6h-MEAN COLUMN (g/m2)
50.0
20.0
10.0
5.0
2.0
1.0
0.1

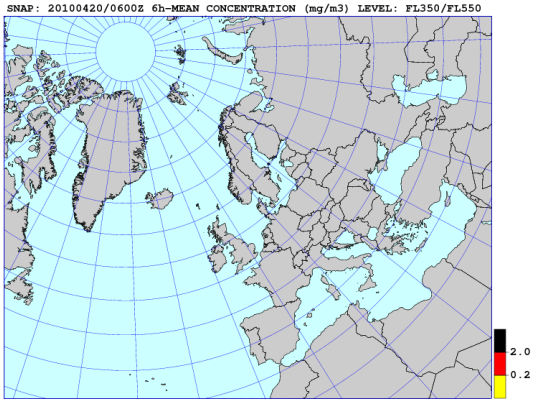
SNAP: 20100420/0600Z 6h-MEAN CONCENTRATION (mg/m3) LEVEL: FL350/FL550
2.0
0.2

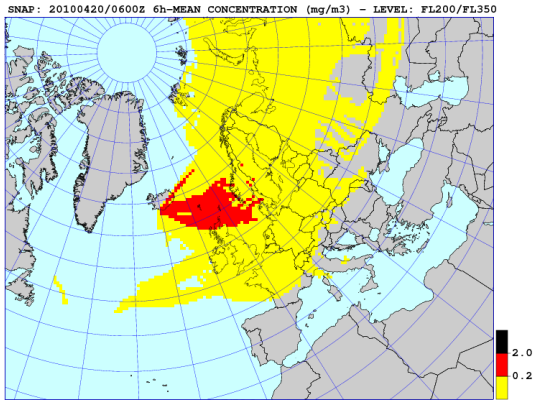
SNAP: 20100420/0600Z 6h-MEAN CONCENTRATION (mg/m3) - LEVEL: FL200/FL350
2.0
0.2

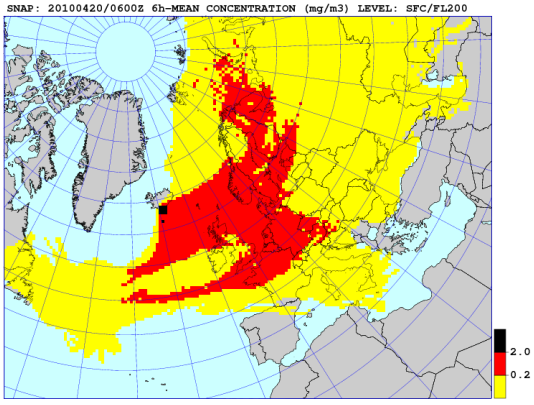
SNAP: 20100420/0600Z 6h-MEAN CONCENTRATION (mg/m3) LEVEL: SFC/FL200
2.0
0.2

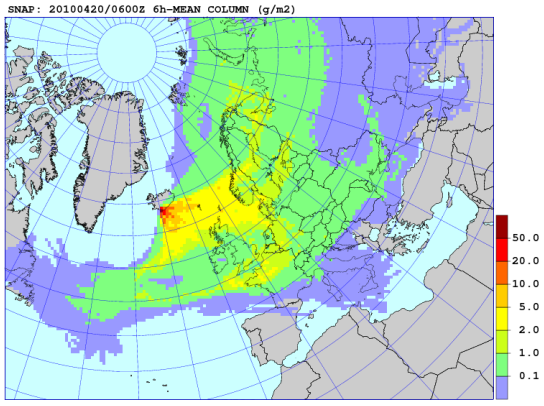
SNAP: 20100420/0600Z 6h-MEAN COLUMN (g/m2)
50.0
20.0
10.0
5.0
2.0
1.0
0.1

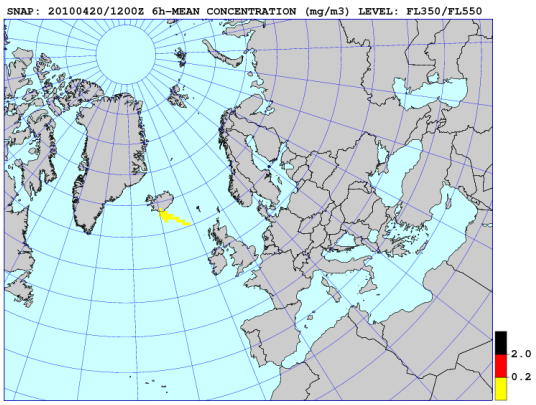
SNAP: 20100420/1200Z 6h-MEAN CONCENTRATION (mg/m3) LEVEL: FL350/FL550
2.0
0.2

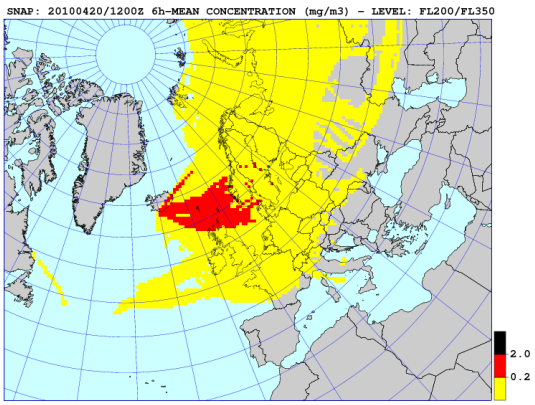
SNAP: 20100420/1200Z 6h-MEAN CONCENTRATION (mg/m3) - LEVEL: FL200/FL350
2.0
0.2

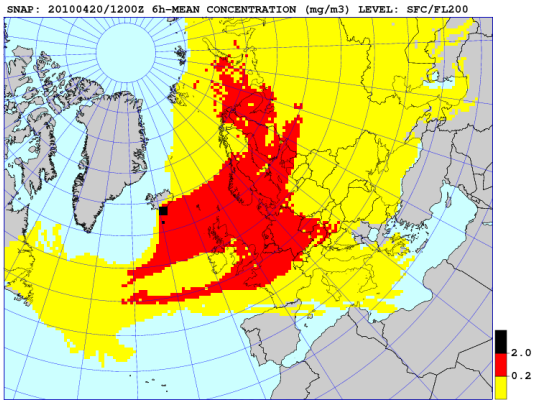
SNAP: 20100420/1200Z 6h-MEAN CONCENTRATION (mg/m3) LEVEL: SFC/FL200
2.0
0.2

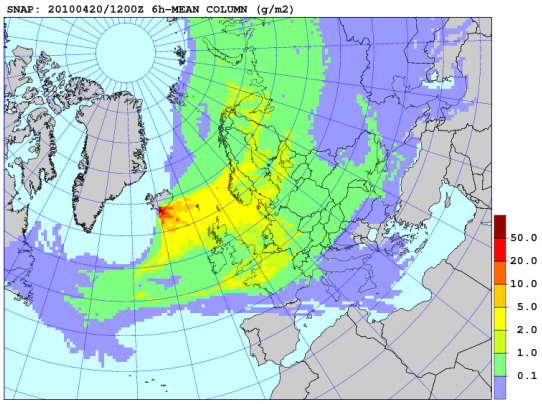
SNAP: 20100420/1200Z 6h-MEAN COLUMN (g/m2)
50.0
20.0
10.0
5.0
2.0
1.0
0.1

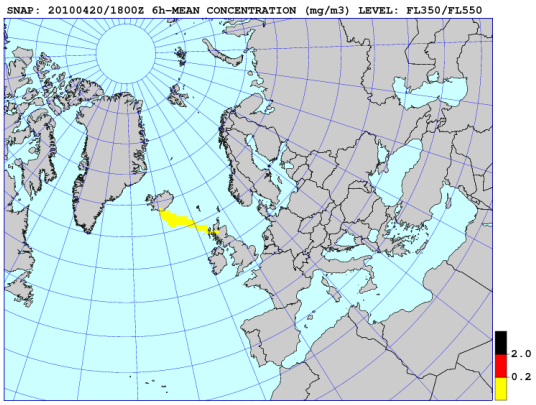
SNAP: 20100420/1800Z 6h-MEAN CONCENTRATION (mg/m3) LEVEL: FL350/FL550
2.0
0.2

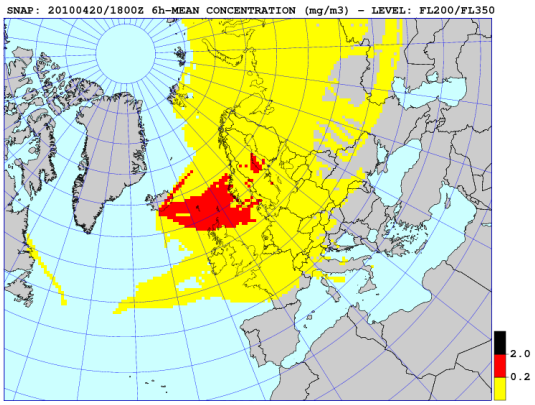
SNAP: 20100420/1800Z 6h-MEAN CONCENTRATION (mg/m3) - LEVEL: FL200/FL350
2.0
0.2

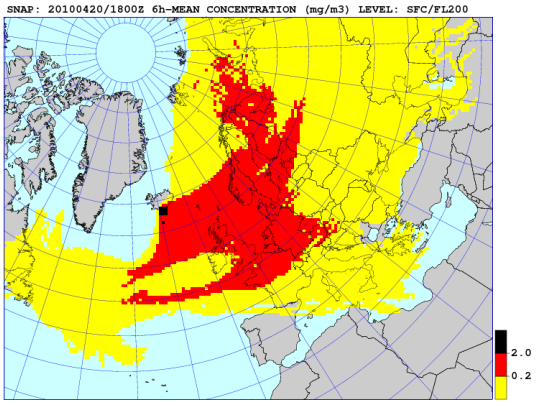
SNAP: 20100420/1800Z 6h-MEAN CONCENTRATION (mg/m3) LEVEL: SFC/FL200
2.0
0.2

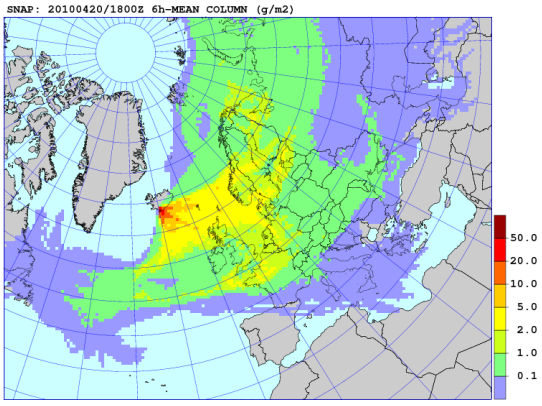
SNAP: 20100420/1800Z 6h-MEAN COLUMN (g/m2)
50.0
20.0
10.0
5.0
2.0
1.0
0.1

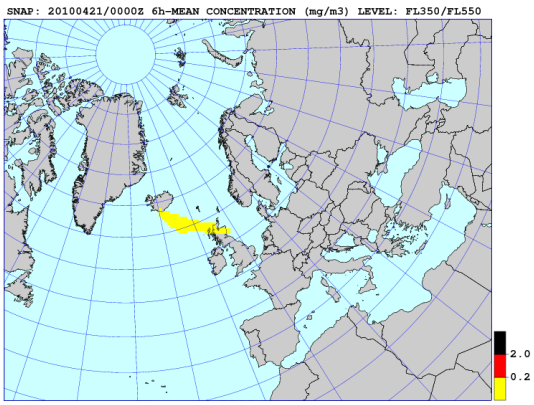
SNAP: 20100421/0000Z 6h-MEAN CONCENTRATION (mg/m3) LEVEL: FL350/FL550
2.0
0.2

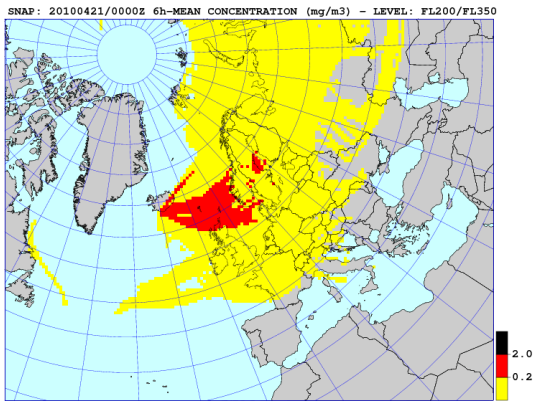
SNAP: 20100421/0000Z 6h-MEAN CONCENTRATION (mg/m3) - LEVEL: FL200/FL350
2.0
0.2

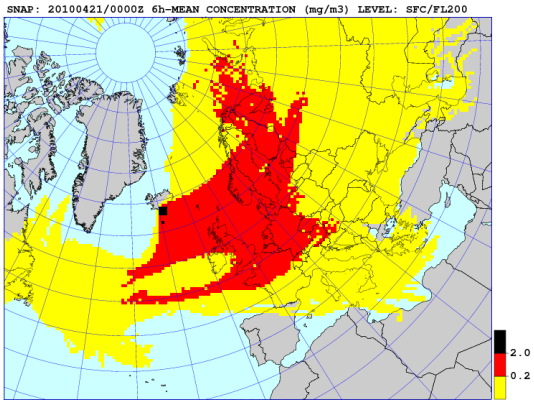
SNAP: 20100421/0000Z 6h-MEAN CONCENTRATION (mg/m3) LEVEL: SFC/FL200
2.0
0.2

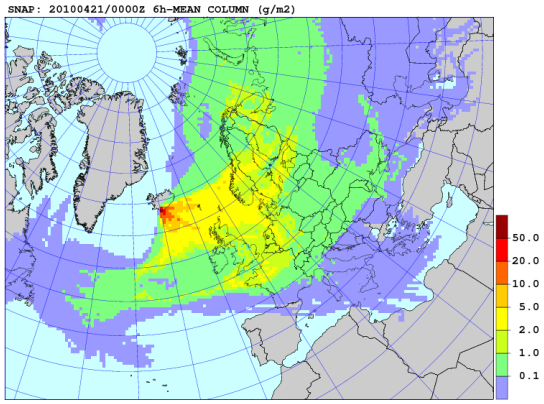
SNAP: 20100421/0000Z 6h-MEAN COLUMN (g/m2)
50.0
20.0
10.0
5.0
2.0
1.0
0.1

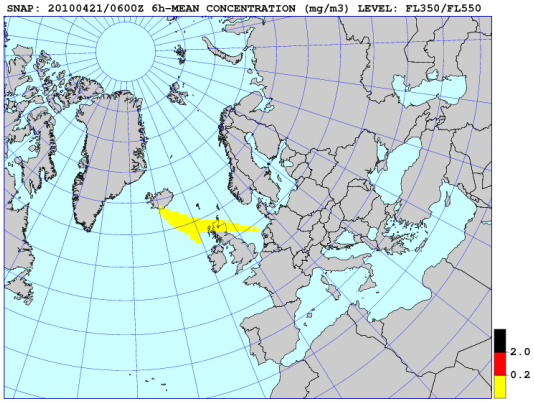
SNAP: 20100421/0600Z 6h-MEAN CONCENTRATION (mg/m3) LEVEL: FL350/FL550
2.0
0.2

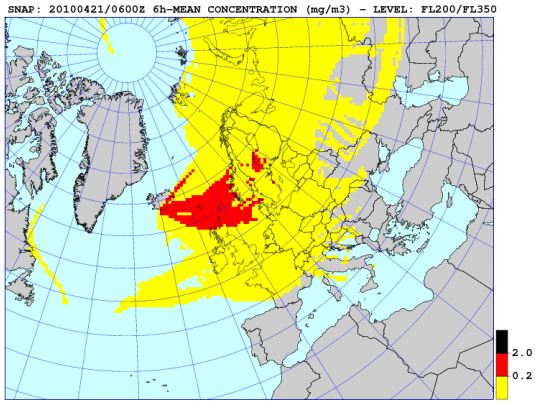
SNAP: 20100421/0600Z 6h-MEAN CONCENTRATION (mg/m3) - LEVEL: FL200/FL350
2.0
0.2

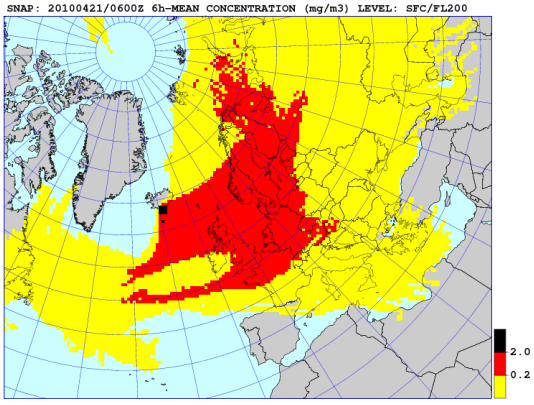
SNAP: 20100421/0600Z 6h-MEAN CONCENTRATION (mg/m3) LEVEL: SFC/FL200
2.0
0.2

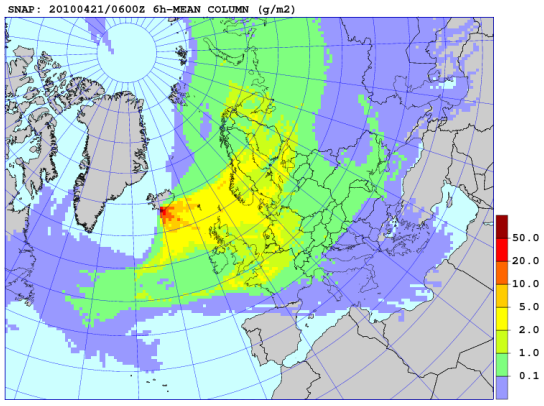
SNAP: 20100421/0600Z 6h-MEAN COLUMN (g/m2)
50.0
20.0
10.0
5.0
2.0
1.0
0.1

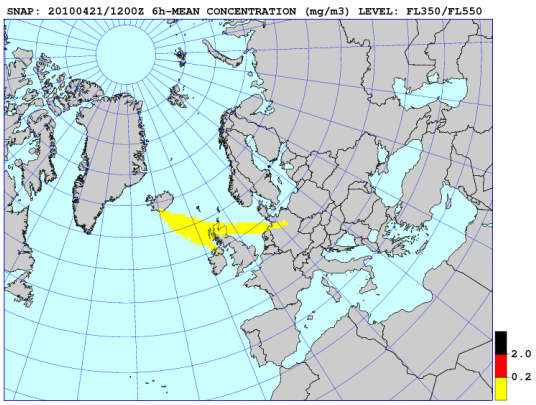
SNAP: 20100421/1200Z 6h-MEAN CONCENTRATION (mg/m3) LEVEL: FL350/FL550
2.0
0.2

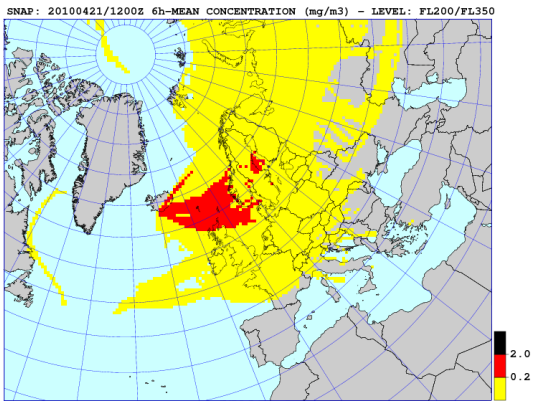
SNAP: 20100421/1200Z 6h-MEAN CONCENTRATION (mg/m3) - LEVEL: FL200/FL350
2.0
0.2

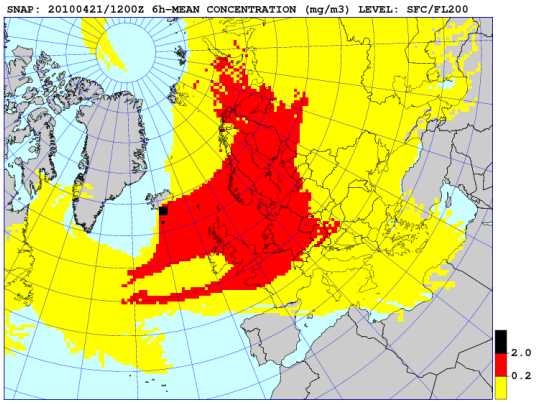
SNAP: 20100421/1200Z 6h-MEAN CONCENTRATION (mg/m3) LEVEL: SFC/FL200
2.0
0.2

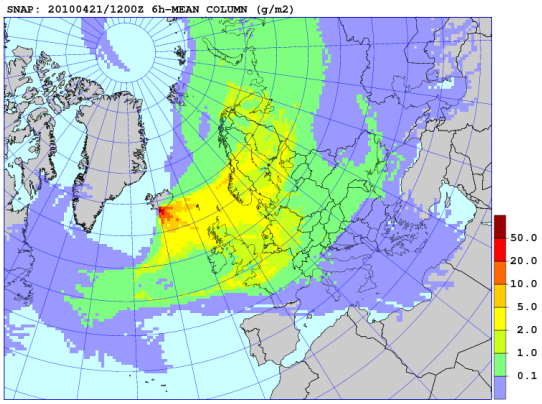
SNAP: 20100421/1200Z 6h-MEAN COLUMN (g/m2)
50.0
20.0
10.0
5.0
2.0
1.0
0.1

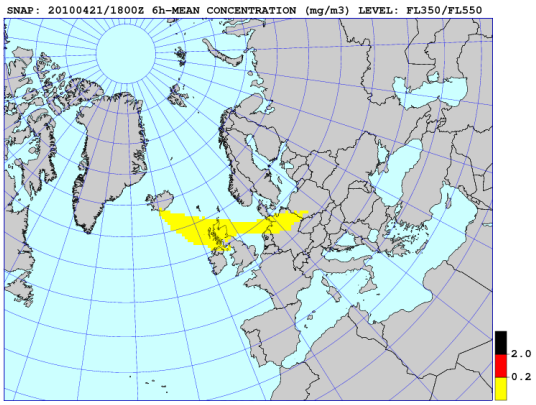
SNAP: 20100421/1800Z 6h-MEAN CONCENTRATION (mg/m3) LEVEL: FL350/FL550
2.0
0.2

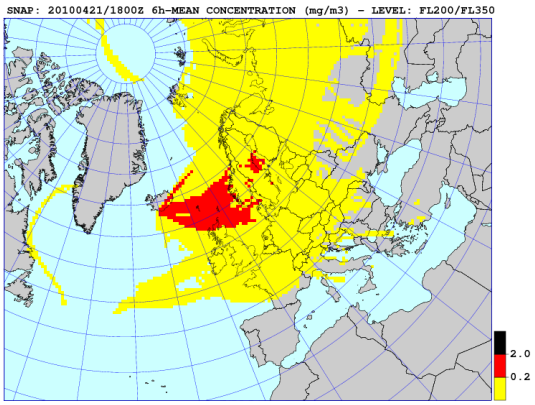
SNAP: 20100421/1800Z 6h-MEAN CONCENTRATION (mg/m3) - LEVEL: FL200/FL350
2.0
0.2

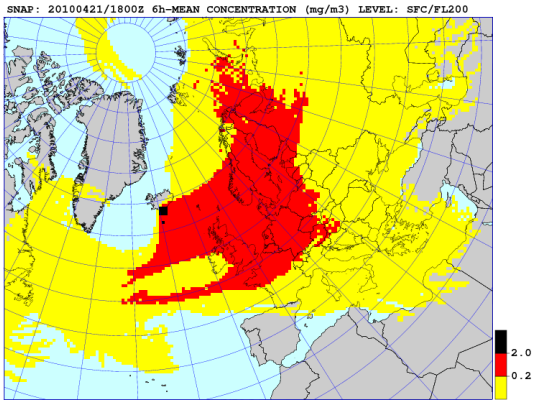
SNAP: 20100421/1800Z 6h-MEAN CONCENTRATION (mg/m3) LEVEL: SFC/FL200
2.0
0.2

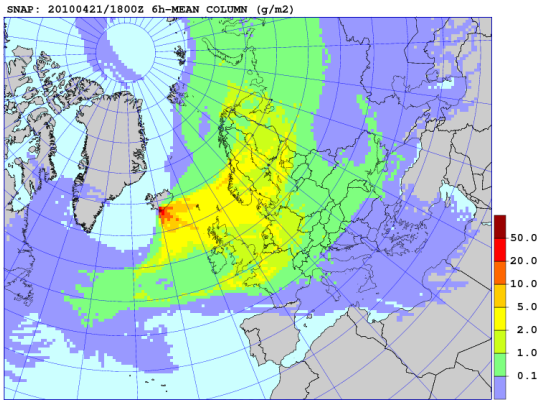
SNAP: 20100421/1800Z 6h-MEAN COLUMN (g/m2)
50.0
20.0
10.0
5.0
2.0
1.0
0.1

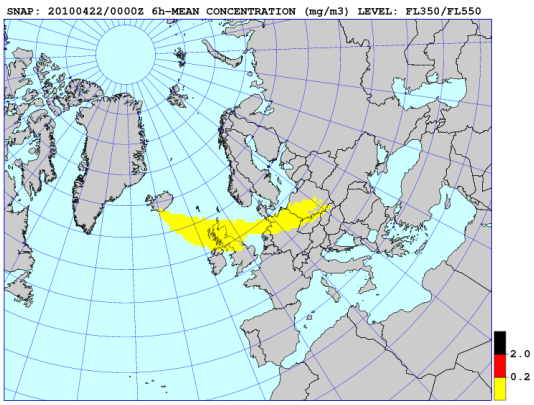
SNAP: 20100422/0000Z 6h-MEAN CONCENTRATION (mg/m3) LEVEL: FL350/FL550
2.0
0.2

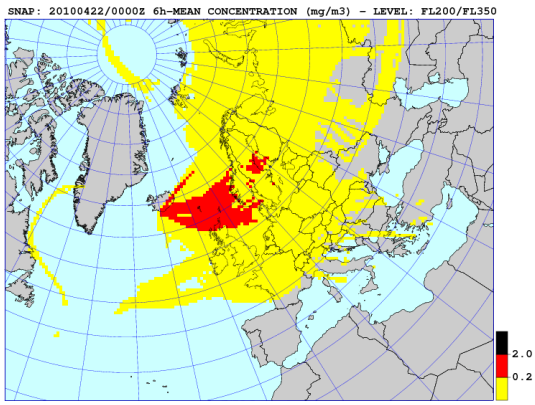
SNAP: 20100422/0000Z 6h-MEAN CONCENTRATION (mg/m3) - LEVEL: FL200/FL350
2.0
0.2

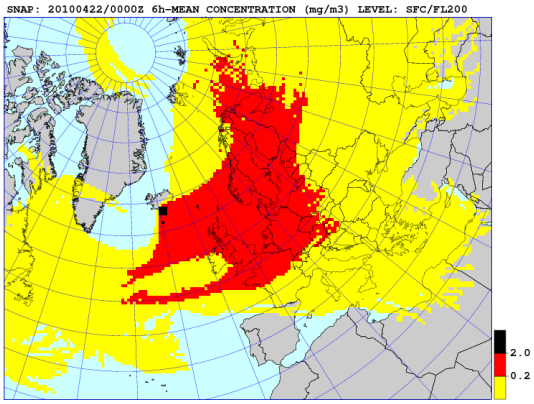
SNAP: 20100422/0000Z 6h-MEAN CONCENTRATION (mg/m3) LEVEL: SFC/FL200
2.0
0.2

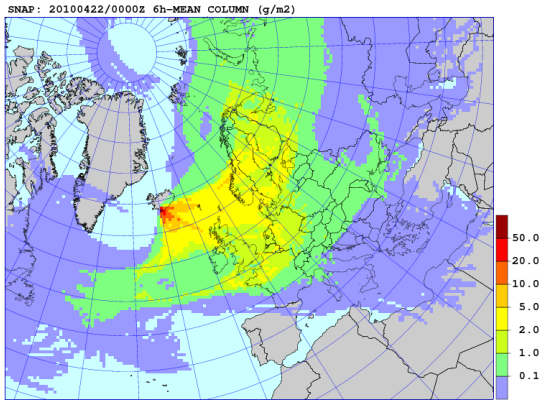
SNAP: 20100422/0000Z 6h-MEAN COLUMN (g/m2)
50.0
20.0
10.0
5.0
2.0
1.0
0.1

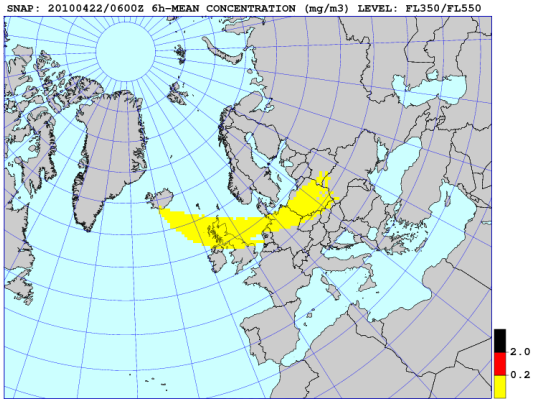
SNAP: 20100422/0600Z 6h-MEAN CONCENTRATION (mg/m3) LEVEL: FL350/FL550
2.0
0.2

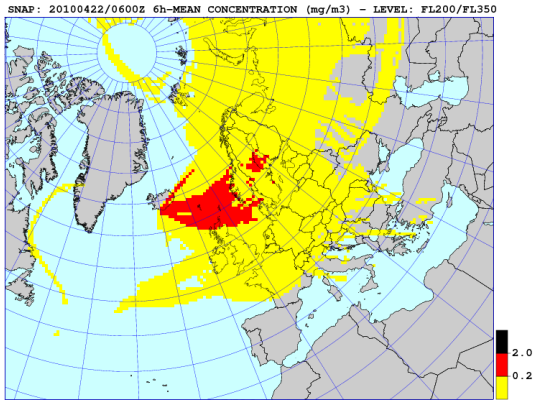
SNAP: 20100422/0600Z 6h-MEAN CONCENTRATION (mg/m3) - LEVEL: FL200/FL350
2.0
0.2

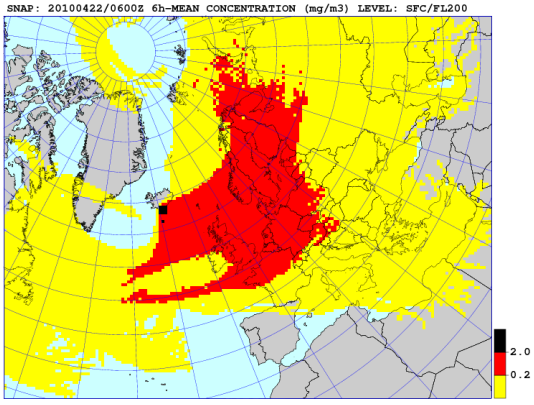
SNAP: 20100422/0600Z 6h-MEAN CONCENTRATION (mg/m3) LEVEL: SFC/FL200
2.0
0.2

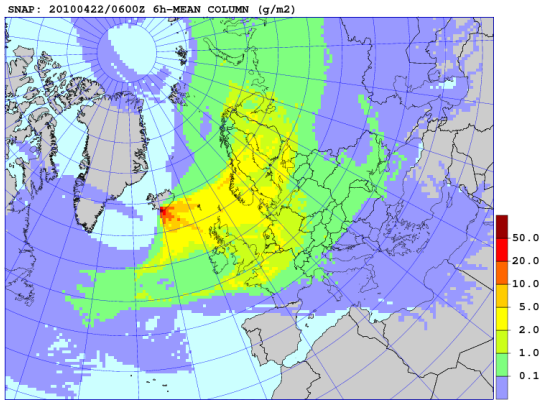
SNAP: 20100422/0600Z 6h-MEAN COLUMN (g/m2)
50.0
20.0
10.0
5.0
2.0
1.0
0.1

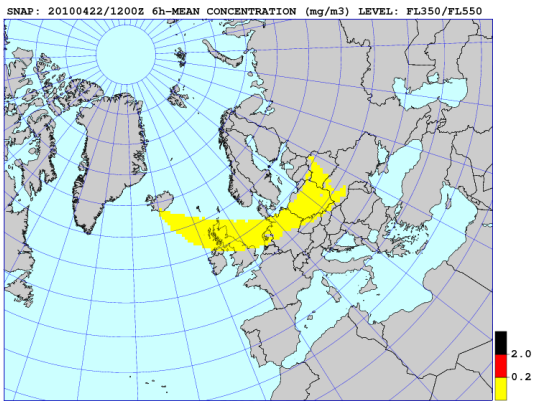
SNAP: 20100422/1200Z 6h-MEAN CONCENTRATION (mg/m3) LEVEL: FL350/FL550
2.0
0.2

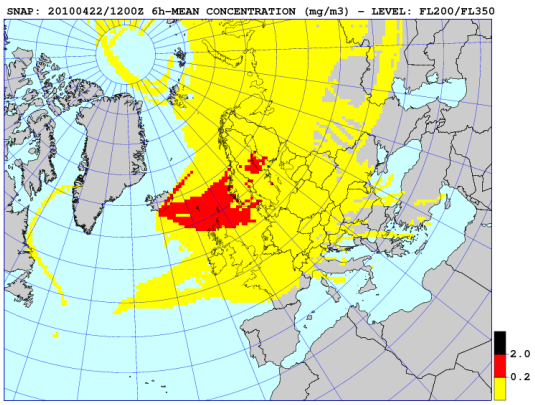
SNAP: 20100422/1200Z 6h-MEAN CONCENTRATION (mg/m3) - LEVEL: FL200/FL350
2.0
0.2

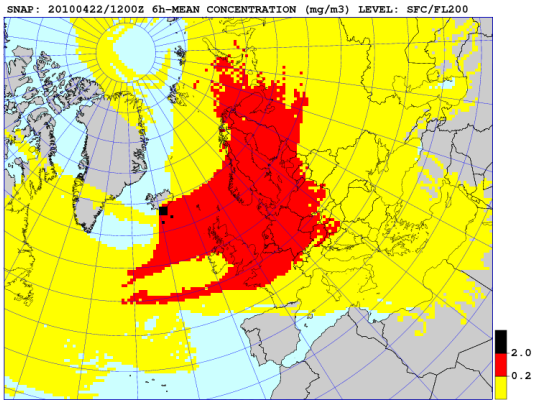
SNAP: 20100422/1200Z 6h-MEAN CONCENTRATION (mg/m3) LEVEL: SFC/FL200
2.0
0.2

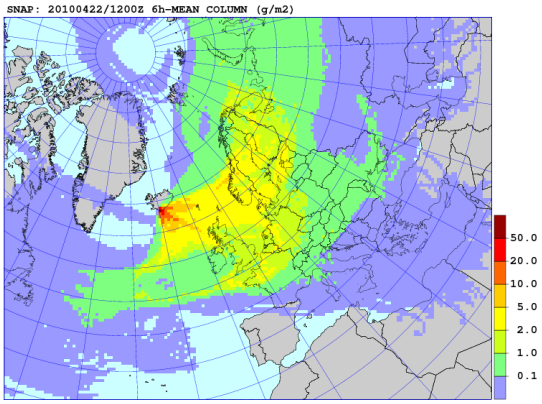
SNAP: 20100422/1200Z 6h-MEAN COLUMN (g/m2)
50.0
20.0
10.0
5.0
2.0
1.0
0.1

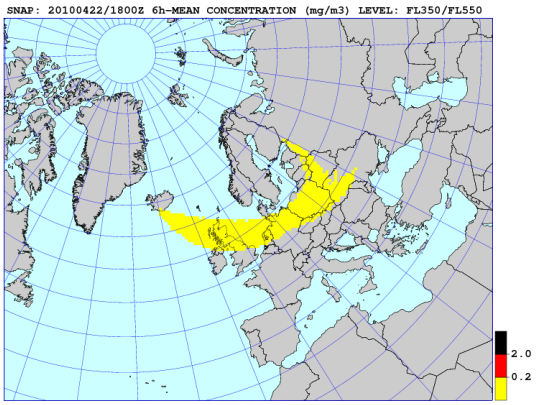
SNAP: 20100422/1800Z 6h-MEAN CONCENTRATION (mg/m3) LEVEL: FL350/FL550
2.0
0.2

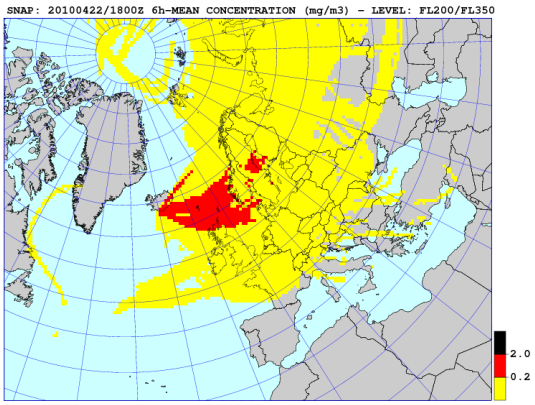
SNAP: 20100422/1800Z 6h-MEAN CONCENTRATION (mg/m3) - LEVEL: FL200/FL350
2.0
0.2

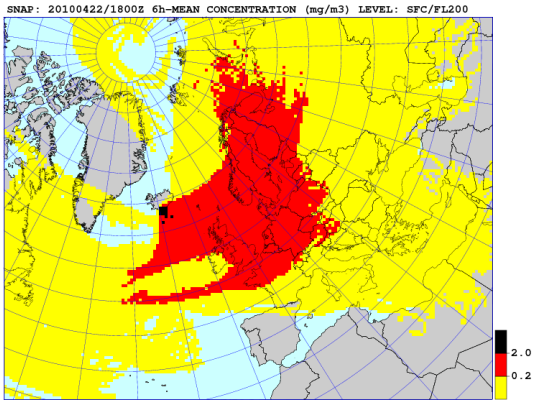
SNAP: 20100422/1800Z 6h-MEAN CONCENTRATION (mg/m3) LEVEL: SFC/FL200
2.0
0.2

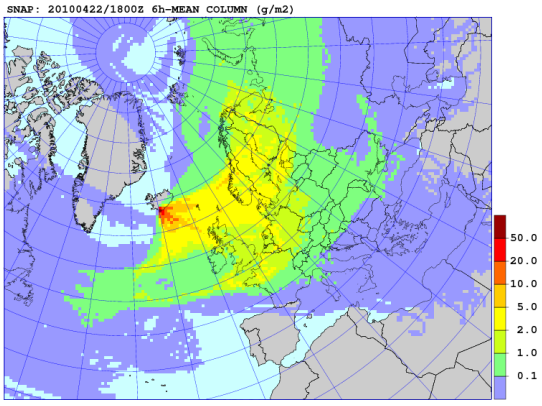
SNAP: 20100422/1800Z 6h-MEAN COLUMN (g/m2)
50.0
20.0
10.0
5.0
2.0
1.0
0.1

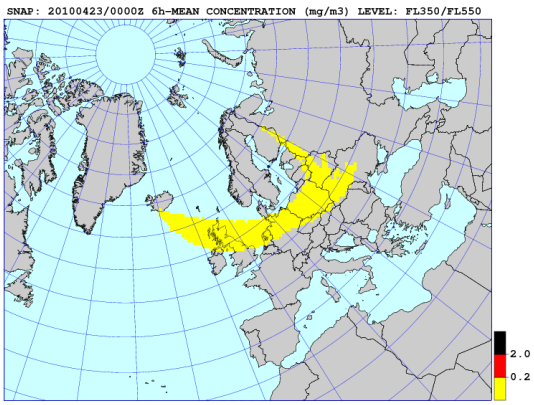
SNAP: 20100423/0000Z 6h-MEAN CONCENTRATION (mg/m3) LEVEL: FL350/FL550
2.0
0.2

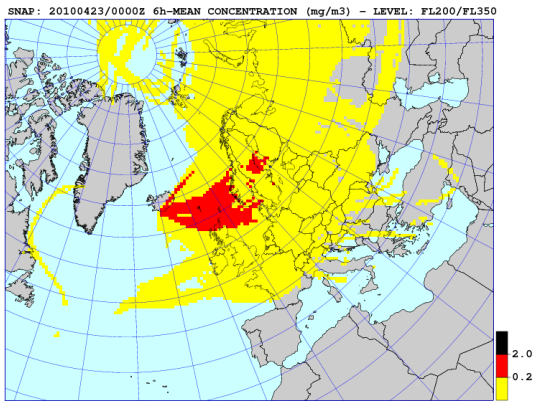
SNAP: 20100423/0000Z 6h-MEAN CONCENTRATION (mg/m3) - LEVEL: FL200/FL350
2.0
0.2

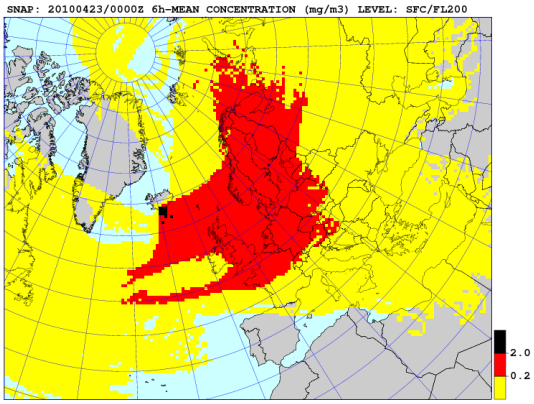
SNAP: 20100423/0000Z 6h-MEAN CONCENTRATION (mg/m3) LEVEL: SFC/FL200
2.0
0.2

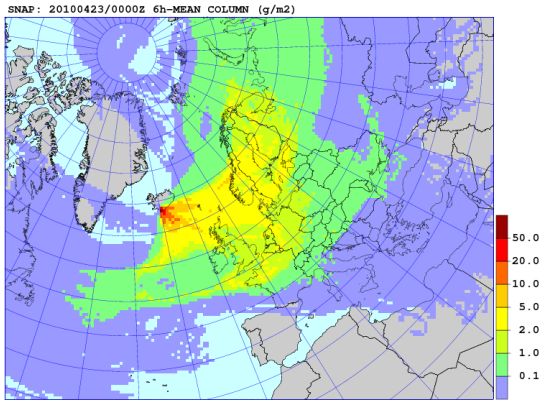
SNAP: 20100423/0000Z 6h-MEAN COLUMN (g/m2)
50.0
20.0
10.0
5.0
2.0
1.0
0.1

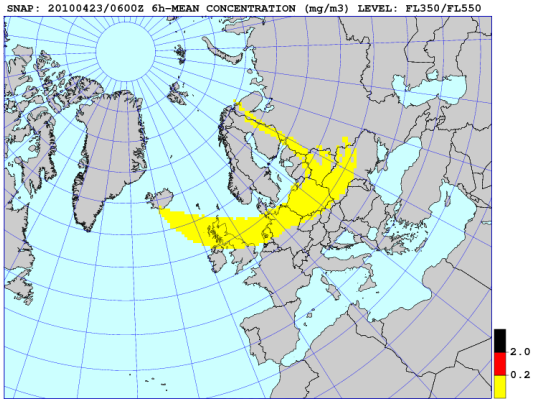
SNAP: 20100423/0600Z 6h-MEAN CONCENTRATION (mg/m3) LEVEL: FL350/FL550
2.0
0.2

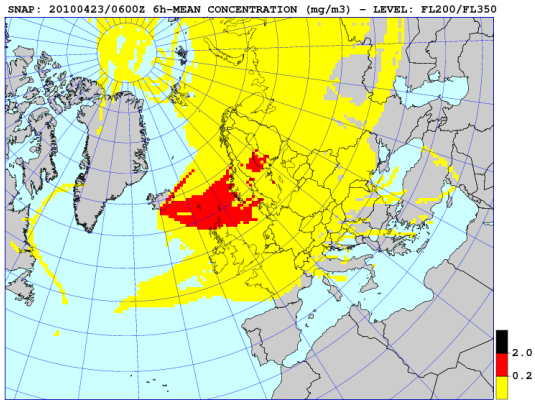
SNAP: 20100423/0600Z 6h-MEAN CONCENTRATION (mg/m3) - LEVEL: FL200/FL350
2.0
0.2

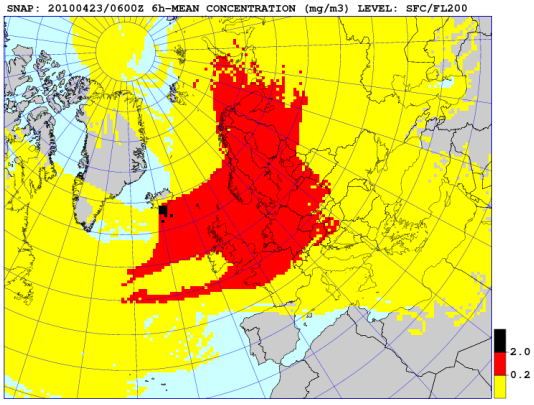
SNAP: 20100423/0600Z 6h-MEAN CONCENTRATION (mg/m3) LEVEL: SFC/FL200
2.0
0.2

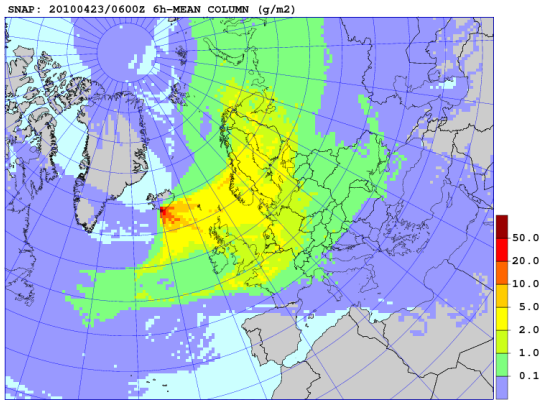
SNAP: 20100423/0600Z 6h-MEAN COLUMN (g/m2)
50.0
20.0
10.0
5.0
2.0
1.0
0.1

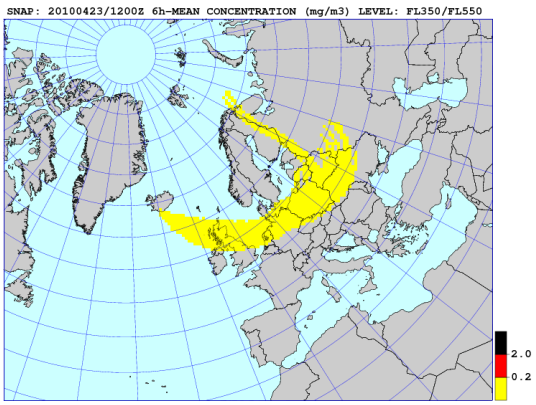
SNAP: 20100423/1200Z 6h-MEAN CONCENTRATION (mg/m3) LEVEL: FL350/FL550
2.0
0.2

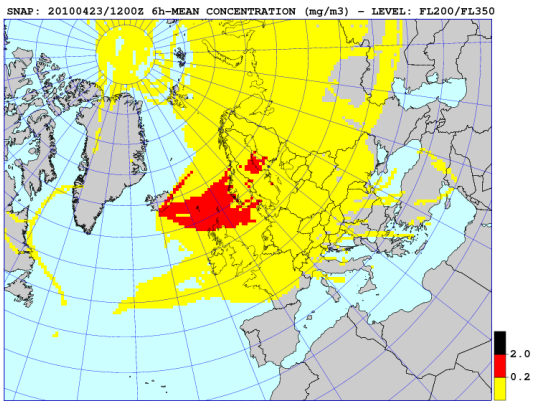
SNAP: 20100423/1200Z 6h-MEAN CONCENTRATION (mg/m3) - LEVEL: FL200/FL350
2.0
0.2

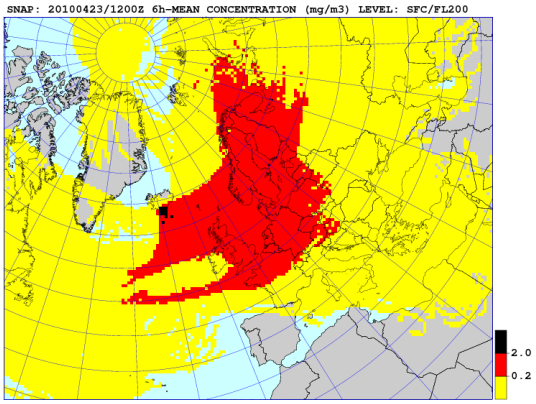
SNAP: 20100423/1200Z 6h-MEAN CONCENTRATION (mg/m3) LEVEL: SFC/FL200
2.0
0.2

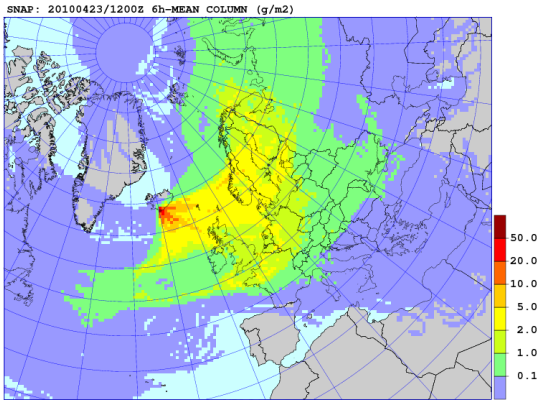
SNAP: 20100423/1200Z 6h-MEAN COLUMN (g/m2)
50.0
20.0
10.0
5.0
2.0
1.0
0.1

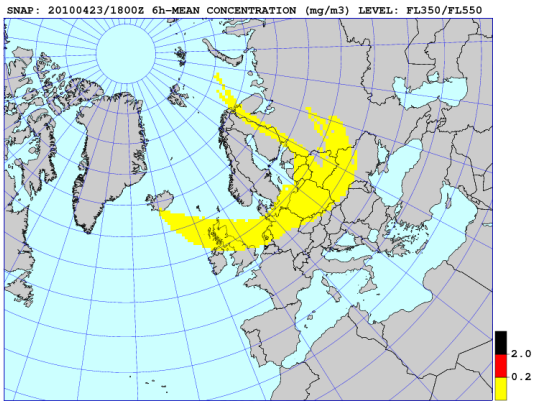
SNAP: 20100423/1800Z 6h-MEAN CONCENTRATION (mg/m3) LEVEL: FL350/FL550
2.0
0.2

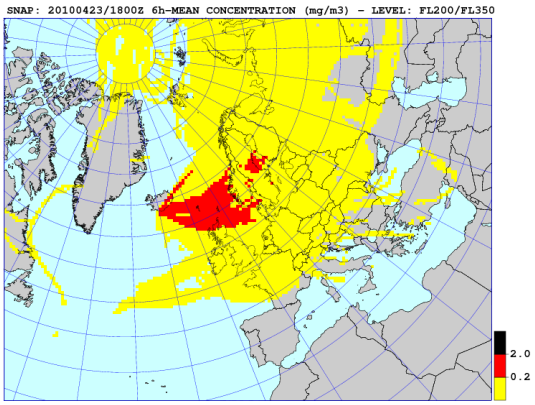
SNAP: 20100423/1800Z 6h-MEAN CONCENTRATION (mg/m3) - LEVEL: FL200/FL350
2.0
0.2

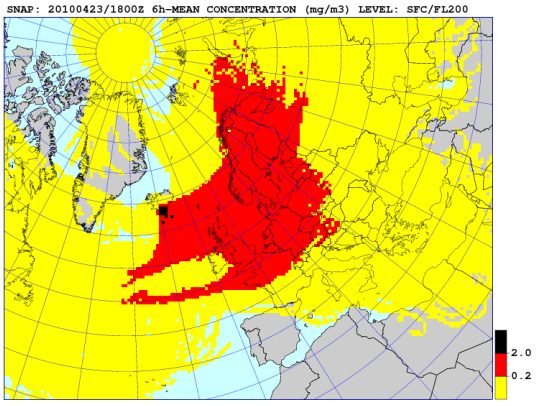
SNAP: 20100423/1800Z 6h-MEAN CONCENTRATION (mg/m3) LEVEL: SFC/FL200
2.0
0.2

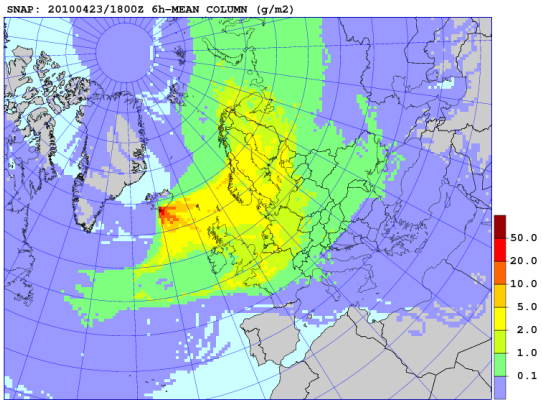
SNAP: 20100423/1800Z 6h-MEAN COLUMN (g/m2)
50.0
20.0
10.0
5.0
2.0
1.0
0.1

SNAP: 20100424/0000Z 6h-MEAN CONCENTRATION (mg/m3) LEVEL: FL350/FL550

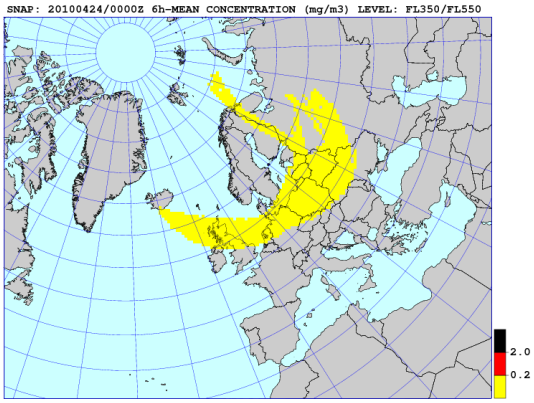

SNAP: 20100424/0000Z 6h-MEAN CONCENTRATION (mg/m3) - LEVEL: FL200/FL350

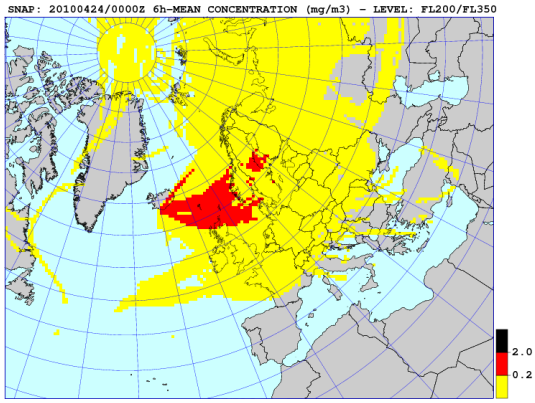

SNAP: 20100424/0000Z 6h-MEAN CONCENTRATION (mg/m3) LEVEL: SFC/FL200

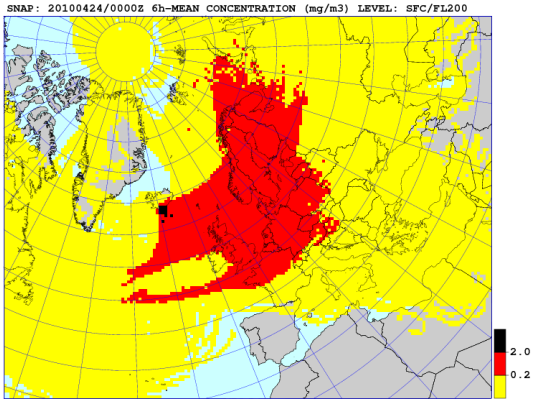

SNAP: 20100424/0000Z 6h-MEAN COLUMN (g/m2)

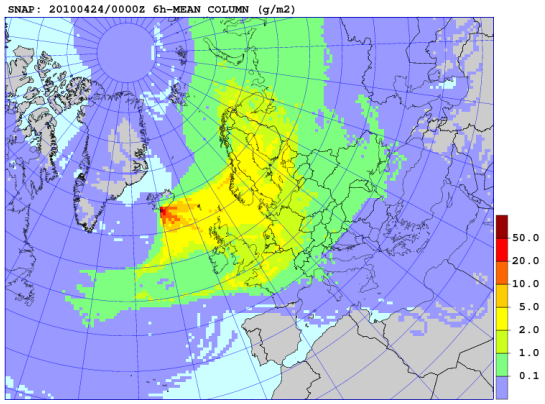

SNAP: 20100424/0600Z 6h-MEAN CONCENTRATION (mg/m3) LEVEL: FL350/FL550

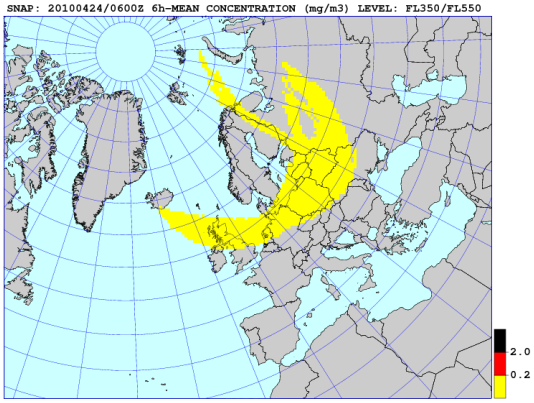

SNAP: 20100424/0600Z 6h-MEAN CONCENTRATION (mg/m3) - LEVEL: FL200/FL350

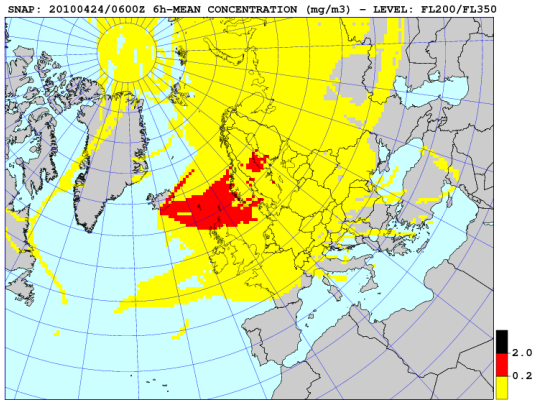

SNAP: 20100424/0600Z 6h-MEAN CONCENTRATION (mg/m3) LEVEL: SFC/FL200

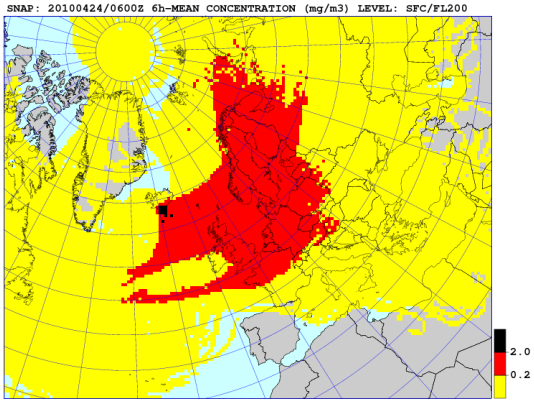

SNAP: 20100424/0600Z 6h-MEAN COLUMN (g/m2)